**Universidade de Lisboa**

**Faculdade de Medicina da Universidade de Lisboa**


# Neuroprotective Strategies for Transient Focal Cerebral Ischemia – An Experimental Model

**Bernardo Oliveira Ratilal**

**Doutoramento em Medicina**

**Neurocirurgia**

**2014**

**Universidade de Lisboa**

**Faculdade de Medicina da Universidade de Lisboa**

# Neuroprotective Strategies for Transient Focal Cerebral Ischemia – An Experimental Model

[Estratégias Neuroprotectores na Isquemia Cerebral Focal Transitória – Modelo Experimental]

**Bernardo Oliveira Ratilal**

Tese orientada pela Prof.ª Doutora Cristina Sampaio

e co-orientada pelos Prof. Doutor João Lobo Antunes

e Prof. Doutor Helder Mota-Filipe

**Doutoramento em Medicina**

**Neurocirurgia**

**A impressão desta dissertação foi aprovada pela Comissão Coordenadora do Conselho Científico da Faculdade de Medicina de Lisboa em reunião de 28 de Outubro de 2014**

**Todas as afirmações efetuadas no presente documento são da exclusiva responsabilidade do seu autor, não cabendo qualquer responsabilidade à Faculdade de Medicina da Universidade de Lisboa pelos conteúdos nele apresentados.**

**Dissertação de Doutoramento apresentada à Faculdade de Medicina da Universidade de Lisboa para obtenção do grau de Doutor em Medicina (Neurocirurgia)**

# ACKNOWLEDGMENTS

I want to express my gratitude to Prof. Doutora Cristina Sampaio and Prof. Doutor João Lobo Antunes for their wise orientations and impartial opinions during this research. I am also grateful to Prof. Doutor Helder Mota-Filipe for his unconditional support, which included designing and providing physical and material conditions for this preclinical investigation. I acknowledge Prof. Doutora Anna Planas and her group for their help and advice during the setting up of the animal model. I also must extend my gratitude to Prof. Doutor Bruno Sepodes and Prof. Doutor João Rocha for their valuable work and cooperation. I appreciate Prof. Doutora Adelaide Fernandes and Prof. Doutor Rui Pinto for collecting and analyzing some of the data. Finally, I am indebted to my clinical colleagues and also friends, Dr. Carlos Vara Luiz and Dr. Nuno Reis, for keeping me motivated and enthusiastic about my experiments.

# DISCLOSURE

I, Bernardo Ratilal, on behalf of all coworkers involved in this research, declare no actual or potential conflict of interest, including any financial support or financial interest in drugs described in it.

# ABSTRACT

**Object:** The aim of this research was to explore the effects of single pretreatment dose of potential neuroprotective drugs in a focal cerebral ischemia-reperfusion (I-R) model.

**Methods:** After the setting up and establisment of the selected animal model, forty-two Wistar male adult rats were subjected to right middle cerebral artery (MCA) intraluminal occlusion for 60 minutes, under continuously cortical perfusion monitoring. Rats were randomly divided into three groups: control (saline), recombinant human erythropoietin (rhEPO, 1.000 IU/kg)-treated and 4-benzyl-2-methyl-1,2,4-thiadiazolidine-3,5-dione (TDZD-8, 5 mg/kg) -treated. Saline or drugs were administered 10 minutes before the onset of ischemia. At 24-hour reperfusion, animals were examined for neurological deficits, blood samples were collected and animals euthanized. The following parameters were blindly evaluated: brain infarct volume, ipsilateral hemispheric edema, neuron specific enolase (NSE) plasma levels, parenchyma histology, Fluoro-Jade positive neurons, p-Akt and total Akt expression, and p-Akt-positive nuclei.

**Results:** Data demonstrated that for rhEPO-treated group severity of neurological deficits ($p<0.001$), brain edema ($p<0.001$), and NSE plasma levels ($p<0.001$) were significantly reduced when compared to control group. Infarct volume and counting number of degenerating neurons in the interest area were similar between these groups, however, perivascular edema was less marked following treatment. No variations on the expression or localization of p-Akt were seen. TDZD-8-treated group compared to control group had: reduced infarct volume ($p<0.001$) and hemispheric edema ($p<0.001$), diminished number of dying neurons ($p<0.001$), decreased serum rise of NSE ($p<0.001$), and improved neurological performance ($p<0.001$). Fewer signs of perivascular edema and increased p-Akt nucleus translocation ($p<0.05$) were found.

**Conclusions:** Results suggest that TDZD-8 has neuroprotective effects due to a complex and mixed synergic interaction between direct neuronal GSK-3β inhibition and Akt modulation, but further research is required before this drug may become clinically available. Additionally, it is presented first evidence that prophylactic rhEPO administration at the considered dose, which has its safety profile well-described in humans, reduced brain edema

and preserved the neuronal pool of the penumbra area following I-R-injury. These benefits appear to be the result of an indirect effect in brain swelling as a consequence of diminished blood-brain barrier disruption and not due to a direct rhEPO neuronal action in the infarct area. Erythropoietin is a potential therapy to prevent neuronal injury induced by intraoperative transient artery occlusion. A translational study is supported and a summary protocol for a putative clinical trial is proposed.

**Keywords:** erythropoietin; intracranial aneurysm; ischemia reperfusion injury; neuroprotective agents; TDZD-8; transient clipping.

# RESUMO

**Objectivo:** A interrupção transitória do fluxo sanguíneo de artérias cerebrais em doentes submetidos a cirurgia de aneurismas intracranianos é, por vezes, inevitável, podendo resultar em lesões de isquemia cerebral. O período de tempo de oclusão tolerado, sem repercussão neurológica, é difícil de prever e muito variável. Nestes doentes, o uso de fármacos neuroprotetores seria desejável. Esta investigação teve como objectivo avaliar compostos com potencial efeito cerebroprotetor, passíveis de serem utilizados profilaticamente em situações com necessidade de oclusão transitória de artérias cerebrais. Respeitando as recomendações para ensaios em animais e tendo em conta uma aproximação à realidade clínica, procedeu-se a um modelo animal de isquemia-reperfusão (I-R) cerebral focal. Na sequência de uma revisão da literatura, foram selecionados dois compostos: eritropoietina humana recombinante (rhEPO) e 4-benzil-2-metil-1,2,4-thiadiazolidina-3,5-diona (TDZD-8).

A eritropoietina é uma hormona bem estudada, com propriedades anti-apoptóticas neuronais, de preservação da integridade da barreira hemato-encefálica (BHE), de promoção do aporte de oxigénio e de neurogénese após lesão cerebral. Em altas doses, o seu efeito neuroprotetor foi demonstrado em modelos de I-R cerebral focal.

O TDZD-8, recentemente descrito, é um inibidor da cinase 3β da sintase do glicogénio (GSK-3β) que atravessa a BHE com propriedades anti-inflamatórias e protetoras de órgãos e tecidos perante agressão. Os ensaios clínicos aparentam um perfil de eficácia/segurança favorável e poderá ser aprovado a médio prazo para uso humano no tratamento da diabetes *mellitus* e de determinadas doenças neurológicas.

**Métodos:** Após o desenvolvimento e a validação de um modelo de I-R cerebral focal no rato, foram avaliados de forma independente os efeitos de doses únicas de TDZD-8 e de rhEPO. Quarenta e dois ratos Wistar machos adultos foram submetidos a 60 minutos de isquemia da artéria cerebral media (ACM) direita sob monitorização contínua do fluxo sanguíneo cerebral com uma microsonda Doppler. Os animais foram distribuídos aleatoriamente por 3 grupos: grupo controlo (soro fisiológico), grupo tratamento TDZD-8 (5 mg/kg) e grupo tratamento rhEPO (1.000 UI/kg). As administrações dos compostos foram feitas por via endovenosa, 10 minutos antes da indução da isquemia. Resumidamente, a técnica consistiu na introdução de um filamento de nylon 4-0 com a ponta revestida por silicone na artéria carótida externa, de

forma retrógrada até à bifurcação da artéria carótida primitiva e posterior progressão pela artéria carótida interna até à sua bifurcação, ocluindo a ACM. A interrupção do fluxo sanguíneo na ACM era objetivada pela monitorização Doppler por uma queda abrupta para valores inferiores a 30% do valor basal. Após 60 minutos de isquemia, procedeu-se à remoção cuidadosa do filamento, restabelecendo-se a circulação na ACM. Às 24 horas de reperfusão, foi avaliada a condição neurológica e os animais submetidos a eutanásia para análise dos seguintes parâmetros: volume de infarto cerebral, edema hemisférico ipsilateral, níveis plasmáticos da enolase específica do neurónio (EEN), histologia do parênquima cerebral, quantificação dos neurónios positivos para Fluoro-Jade, expressão dos p-Akt e Akt total por Western Blot e quantificação dos núcleos positivos para p-Akt por imunohistoquímica.

**Resultados:** Os resultados demonstraram que o grupo tratamento com rhEPO, quando comparado com o grupo controlo, apresentou uma redução significativa do grau de incapacidade neurológica ($p<0.001$), do edema cerebral ($p<0.001$) e dos níveis plasmáticos da EEN ($p<0.001$). Apesar de histologicamente se verificar uma menor acentuação do edema perivascular, o volume do infarto cerebral, a contagem de neurónios positivos para Fluoro-Jade e a expressão e localização do p-Akt mostrou-se idêntica nos 2 grupos.
O tratamento com TDZD-8 reduziu a extensão da lesão cerebral, o número de neurónios apoptóticos/degenerados ($p<0.001$), evitou a subida dos níveis plasmáticos da EEN ($p<0.001$) e melhorou significativamente a condição neurológica dos ratos às 24 horas de reperfusão ($p<0.001$). O grupo tratado com TDZD-8 apresentou reduções de 48% no volume do infarto cerebral ($p<0.001$) e de 59% no edema hemisférico ($p<0.001$) comparativamente com o grupo controlo. Ainda, no grupo tratado com TDZD-8, verificou-se menor acentuação de edema perivascular na área isquémica e embora os níveis de expressão de Akt total e p-Akt não tenham sofrido alterações significativas, verificou-se translocação nuclear do p-Akt ($p<0.05$).

**Conclusões:** A maioria dos estudos pré-clínicos referentes a fármacos neuroprotetores são desenhados para doentes com acidentes vasculares cerebrais em evolução. A subpopulação de doentes neurocirúrgicos submetidos a clipagem transitória de artérias cerebrais carece de investigação específica. Os resultados deste trabalho demonstram que a administração de TDZD-8 antes da indução de um período transitório de isquemia cerebral pode ter efeitos neuroprotetores que resultam de uma interação sinérgica entre a inibição da GSK-3β e a

modulação da via Akt, pois apesar da expressão do p-Akt total não se ter alterado, a sua translocação nuclear sugere a ativação desta via. Efetivamente, esta via tem sido descrita e implicada como uma das principais promotoras da sobrevivência celular após lesão neuronal. O TDZD-8 é um composto muito investigado em vários campos da medicina sendo um fármaco promissor como protetor do sistema nervoso central. Para um completo esclarecimento dos seus mecanismos de ação na I-R, são necessários estudos complementares. Adicionalmente, demonstrou-se, no modelo animal, que a administração profilática de rhEPO numa dose única e com perfil de segurança bem conhecido no humano, 1.000 UI/kg, preserva o *pool* neuronal funcional da área de penumbra e diminui o edema cerebral associado à lesão induzida pela I-R. Surpreendentemente, ao contrário de estudos anteriores, a ausência da ativação da via Akt/GSK-3β sugere que os efeitos da administração de rhEPO não foram resultado de uma ação neuronal direta. Apenas uma pequena fracção da rhEPO administrada por via sistémica atravessa a BHE, pelo que a dose relativamente baixa de rhEPO utilizada neste estudo quando comparada com as doses utilizadas em ensaios anteriores, poderá ser a explicação. A preservação da integridade da BHE e a consequente diminuição do edema e lesão cerebral secundária parecem constituir o mecanismo base deste efeito protetor. Concluiu-se que a rhEPO, clinicamente disponível e acessível, é uma potencial terapêutica para prevenir lesão cerebral induzida pela oclusão intraoperatória transitória de artérias cerebrais. Os resultados deste trabalho suportam a realização de um estudo translacional, pelo que se propõe um protocolo resumido para um ensaio clínico.

**Palavras-chave:** aneurisma intracraniano; clipagem transitória; eritropoietina; lesão de isquemia-reperfusão; fármacos neuroprotetores; TDZD-8.

# ABBREVIATIONS

| | |
|---|---|
| **AA** | Arachidonic acid |
| **ACA** | Anterior communicating artery |
| **AEPO** | Asialo-erythropoietin |
| **Akt** | Protein kinase B |
| **AMPA** | α-amino-3-hydroxy-5-methyl-4-propionate |
| **ANOVA** | Analysis of variance between groups |
| **ASICs** | Acid-sensing ion channels |
| **ATP** | Adenosine triphosphate |
| **BAD** | Bcl-2-associated death promoter |
| **BAX** | Bcl-2-associated X protein |
| **BBB** | Blood-brain barrier |
| **Bcl-2** | B-cell lymphoma 2 |
| **BDNF** | Brain-derived neurotrophic factor |
| **BSA** | Bovine serum albumin |
| **CBF** | Cerebral blood flow |
| **CCA** | Common carotid artery |
| **CEPO** | Carbamylated erythropoietin |
| **CHILI** | Controlled Hypothermia in Large Infarction |
| **COAST** | Cooling in Acute Stroke Trial |
| **COOL-AID** | Cooling for Acute Ischaemic Brain Damage |
| **CREB** | cAMP response element-binding protein |
| **CSD** | Cortical spreading depolarizations |
| **DAPI** | 4,6-diamidino-2-phenylindole |
| **ECA** | External carotid artery |
| **EEG** | Electroencephalogram |
| **eNOS** | Endothelial nitric oxide synthase |
| **EPO** | Erythropoietin |
| **EPOR** | Erythropoietin receptor |
| **EuroHYP** | European Stroke Research Network for Hypothermia |
| **GABA** | γ-aminobutyric acid |
| **GSK** | Glycogen synthase kinase |
| **H&E** | Hematoxilin & Eosin |
| **HIF-1** | Hypoxia inducible factor 1 |
| **HSF-1** | Heat shock factor-1 |
| **I-R** | Ischemia-reperfusion |
| **IA** | Intracranial aneurysm |
| **ICA** | Internal carotid artery |
| **ICTuS** | Intravascular Cooling in the Treatment of Stroke |
| **IGF-1** | Insulin-like growth factor 1 |
| **IHAST** | Intraoperative Hypothermia Aneurysm Surgery Trial |
| **IL** | Interleukin |

| | |
|---|---|
| **InfV** | Infarct volume |
| **IP** | Intraperitoneal |
| **IV** | Intravenous |
| **JAK2** | Janus-tyrosine kinase 2 |
| **LDF** | Laser-Doppler flowmetry |
| **LHV** | Left hemisphere volume |
| **MAPK** | Mitogen-activated protein kinase |
| **MCA** | Middle cerebral artery |
| **MCAO** | Middle cerebral artery occlusion |
| **MMP-9** | Matrix metallopeptidase-9 |
| **MRI** | Magnetic resonance imaging |
| **mRS** | Modified Ranking Scale |
| **NeuroEPO** | Nasal formulation of low-sialic acid erythropoietin |
| **NF-κB** | Nuclear factor-κB |
| **NIHSS** | National Institutes of Health Stroke Score |
| **NMDA** | N-methyl-d-aspartate |
| **NO** | Nitric oxide |
| **NOS** | Nitrous oxide synthase |
| **NSE** | Neuron specific enolase |
| **OA** | Occipital artery |
| **p-Akt** | Phosphorylated-Akt |
| **PBS** | Phosphate buffered saline |
| **PComA** | Posterior communicating artery |
| **PI3K** | Phosphoinositide 3-kinase |
| **PID** | Peri-infarct depolarization |
| **$PLA_2$** | Phospholipase $A_2$ |
| **PPA** | Pterygopalatine artery |
| **rhEPO** | Recombinant human erythropoietin |
| **RHV** | Right hemisphere volume |
| **RIPA** | Radioimmunoprecipitation assay |
| **ROS** | Reactive oxygen species |
| **SAH** | Subarachnoid hemorrhage |
| **SD** | Standard deviation |
| **SEM** | Standard error of the mean |
| **STA** | Superior tyroid artery |
| **STAIR** | Stroke Therapy Academic Industry Roundtable |
| **STAT5** | Signal transducer and activator of transcription 5 |
| **TCD** | Transcranial Doppler |
| **TDZD** | Thiadiazolidinone |
| **TDZD-8** | 4-benzyl-2-methyl-1,2,4-thiadiazolidine-3,5-dione |
| **TTC** | 2,3,5-triphenyltetrazolium chloride |
| **VEGF** | Vascular endothelial growth factor |

# FIGURE AND TABLE INDEX

## Figure Index

## Table Index

# GENERAL INDEX

# 1 BACKGROUND

## 1.1 Transient Focal Cerebral Ischemia for Cerebrovascular Procedures

Intracranial aneurysms (IAs) are acquired dilatations of intracranial arteries that are typically located at bifurcation sites along the Circle of Willis, which are areas prone to hemodynamic patterns that potentiate aneurysm development[1]. Histologically, thinned and dilated regions of the vascular wall that exhibit loss of the internal elastic lamina, thinning of the tunica media, and subsequent remodeling and degradation of extracellular matrix proteins throughout the vessel wall is observed. IAs affect around 3% of the general adult population and represent a major public health problem, in which a fraction will rupture and lead to subarachnoid hemorrhage (SAH) with possible devastating consequences[2]. The incidence of SAH due to IA rupture, depending on geography, varies from 6-10 in most populations to up to 21 cases per 100,000 person-years in Finland and Japan[3-5]. Typical symptoms include sudden onset of severe headache, nausea and, often, loss of consciousness. It is a serious neurosurgical emergency with poor prognosis; approximately 15% of patients die before admission and around 40% die in the hospital[6]. Only 25% of those who live past the first month recover completely, leaving many survivors requiring long-term care[7]. The key to minimizing the risk of rebleeding following aneurysmal rupture is to exclude the aneurysm from cerebral circulation. At present, this is achieved either by microsurgical clipping or endovascular coiling, although there has been much debate on the merits of each intervention.

IAs were first described in autopsy reports by Morgagni in 1761[8]. It was not until 1891, when Quinke introduced the lumbar puncture, that the diagnosis of SAH became possible in living patients[9]. The origin of both endovascular and surgical treatment of IAs goes back to 1927, when António Egas Moniz presented his newly developed technique of angiography in the *Société de Neurologie de Paris*[10]. This technique not only revolutionized the diagnostics of cerebral aneurysms but also had a key role in starting the development of IAs treatment. By 1931 Egas Moniz was able to perform a complete angiogram and brain aneurysms could be diagnosed in living humans. In that same year, Norman Dott became the first surgeon to perform an elective intracranial surgery for the treatment of a diagnosed IA by means of angiography, wrapping it with muscle[11]. A few years later, in 1937, Walter Dandy was the

first to treat an aneurysm by applying a silver clip (V-shaped) across the neck of an unruptured internal carotid artery aneurysm[12]. Modern era of IA surgery was launched in the sixties, when Lawrence Pool[13] pioneered the use of the operating binocular microscope and Mahmut Gazi Yasargil introduced the fundamental microsurgical approaches and techniques[14]. Meanwhile, in 1964, Luessenhop who used inflatable balloons to occlude aneurysm and arteriovenous malformations gave initial steps towards interventional neuroradiology[15]. Later on, Serbinenko pioneered the use of detachable balloons[16]. The introduction of microcatheters and microguidewires by Target Therapeutics Inc. (Fremont, CA, USA) in 1986 was a big step in endovascular therapy, but endovascular techniques gained definite importance with the development of electrolytically detachable platinum coils by Guglielmi and Viñuela in the nineties[17,18].

Neurovascular procedures requiring transient focal cerebral ischemia are mostly related to IAs. The use of elective transient artery occlusion in IA surgery was first described by Pool in 1961[19] and is now widely accepted amongst cerebrovascular surgeons. By reducing the pressure within the aneurysm, it became sometimes an essential approach for a safer dissection of the aneurysm neck, open of the aneurysm for thrombus removal, a definitive clip placement, and managing with an intraoperative rupture. Although a brief temporary interruption of arterial flow in virtually all intracranial vessels is safe, some circumstances may require more protracted time intervals of occlusion, which may threaten the viability of underperfused brain tissue. The period of stroke-free temporary occlusion varies considerably and depends on several clinical features, such as the degree, size, location and duration of the ischemia, presence and quantity of subarachnoid blood, timing of surgery, anatomical variability, reactivity of the circulation, patient's age, body temperature, genetic factors and other co-morbidities such as atherosclerosis[20-25]. The risk of using temporary clips is not, however, only limited to the transient interruption of focal cerebral blood flow (CBF). Kühnel found that arteries are particularly sensitive to microvascular trauma due to temporary clips, in which maximal histological changes were seen in the tunica media, and that greater microvascular trauma was caused by increased occlusion force rather than by increased clipping time[26]. It is possible that these structural endothelial and smooth muscle changes promote the formation of microemboli and have a role in aggravating vasospasm after aneurysmatic SAH, leading to higher morbidity and mortality[27]. Even though commercially

available temporary clips have lower occlusion force than definitive ones, specifically designed temporary clips with the minimum effective occlusion force would be desired[28]. This is a line of research that would deserve more investing. For instance, standard metal clips for temporary clipping may be cumbersome and difficult to place when the aneurysm ruptures. A different strategy for temporary arterial occlusion would be to position an unobtrusive remotely controlled occluding device in a parent artery and have it activated only if it turns out to be necessary. This would allow the surgeon to work under normal cerebral perfusion with the guarantee of a clean and immediate blood flow interruption if the situation arises. The use of remote-controlled occluders to limit transient vessel occlusion would be of interest as it could spare time spent on temporary clipping and thus, make aneurysm surgery safer.

For obvious reasons, randomized prospective studies to compare the outcome of cerebrovascular procedures with temporary occlusion and those without local circulatory arrest are not feasible. Most reports on the use of temporary arterial occlusion in humans have been retrospective analyses of case series in which the use or nonuse of temporary occlusion was based on the experience and judgment of the surgeon. Samson[29] reviewed 100 patients who underwent elective temporary arterial occlusion. Overall, 19% of patients demonstrated evidence of infarction in the vascular territories subjected to temporary arterial occlusion, with no registration of infarction attributed to temporary vessel occlusion of less than 14 minutes. Increased age (more than 61 years) and higher Hunt and Hess grades (III to IV) were associated with limited tolerability of temporary vessel occlusion. The authors stressed that regarding specific vascular territories undergoing temporary occlusion, the basilar and middle cerebral arteries appeared to be the most sensitive to ischemia-reperfusion (I-R) injury. The incidence of postoperative radiographic evidence of infarction was lower for internal carotid, anterior cerebral, and vertebral artery occlusion. Ferch[30] retrospectively analyzed 106 aneurysm patients and found that an overall rate of 17% of patients experienced symptomatic stroke and 26% showed radiological evidence of brain infarct attributable to temporary arterial occlusion. Stroke incidence was 12% in patients subjected to occlusion time periods of less than 10 minutes and 35% in patients with ischemic periods higher than 10 minutes. A longer duration of clip placement, older patient age, a poor clinical grade (Hunt and Hess Grades IV-V), early surgery, and the use of single prolonged clip placement rather than

repeated shorter episodes were associated with a higher risk of stroke.

Temporary focal ischemia covers a complex cascade of events with a continuum of potential outcomes ranging from no measurable effect to devastating neurological injury. The duration of temporary occlusion remains the most investigated factor in clinical series of patients undergoing temporary artery occlusion. For sure, the safety time of temporary clipping is not the same for all patients with cerebral aneurysms, but it is generally recommended that the duration of temporary occlusion be limited to less than 5 to 14 minutes whenever possible to avoid ischemic damage and neurologic complications, although there are several reports of patients with longer periods of occlusion without signs of neurological deficits[24,29,31-34]. Still, while numbers vary, a significant proportion of patients, up to 45%, undergoing clipping surgery with transient vessel occlusion may suffer from brain infarct[31]. Conflicting opinions exist regarding the mode of transient occlusion. Although repeated clip applications may led to formation of new microthrombi or detachment of already existing wall vessel thrombi, usually, brief repetitive clipping periods are preferred rather than a single episode of protracted ischemia[35-37].

While neurosurgeons are regularly using temporary arterial occlusion for the management of both routine and complex IAs, reducing the risks as much as possible is critical to this procedure. More specifically, effective neuroprotective drugs for these patients are essential for a safer surgery.

## 1.2 Cerebral Ischemia-Reperfusion Physiopathology

The brain has high-energy demands requiring a continuous supply of oxygen and its principal substrate, glucose. Blood flow cessation to the brain leads to disruption of the balance between energy generated by oxidative phosphorylation and energy needed for cell processes. The most immediate biochemical change in neurons affected by ischemia is a switch from aerobic to anaerobic metabolism. Insufficient oxygen inhibits the aerobic catabolism of pyruvate and promotes anaerobic glycolysis, leading to an accumulation of lactic acid and the consequential decrease in pH values. Ischemia triggers a series of interrelated events

culminating in cellular injury and death by affecting energy-dependent processes necessary for tissue cell survival (Figure 1.1). Each of the processes has a distinct time frame, some occurring over minutes, others over hours and days, causing injury to neurons, glia and endothelial cells.

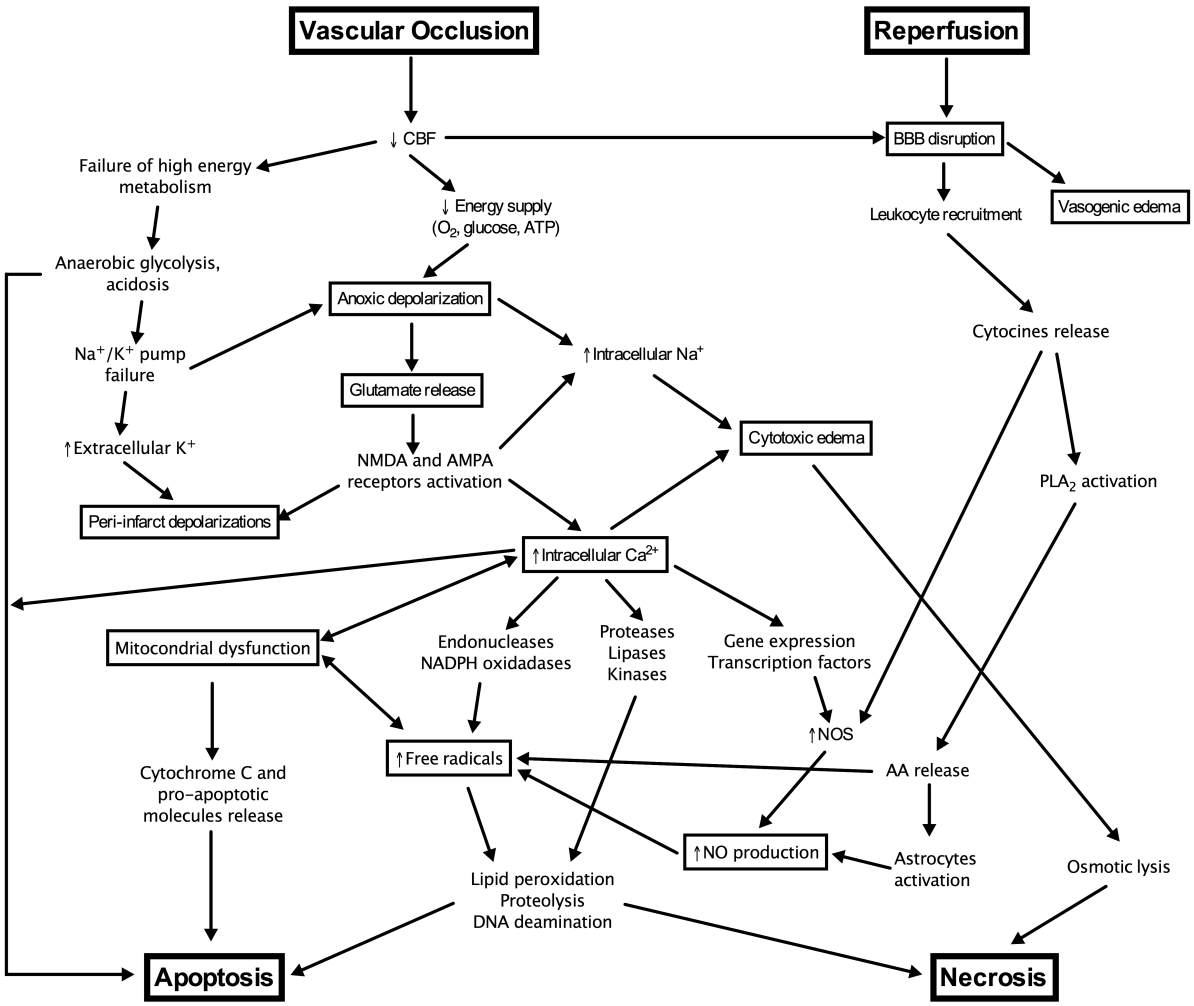


**Figure 1.1.** The cascade of biochemical events leading to cell death following cerebral ischemia and reperfusion. Reperfusion may also induce injury by enhancing BBB breakdown, inflammation and free radical production. *AA*, arachidonic acid; *ATP*, adenosine triphosphate; *BBB*, blood-brain barrier; *CBF*, cerebral blood flow; *NO*, nitric oxide; *NOS*, nitrous oxide synthase; *$PLA_2$*, Phospholipase $A_2$.

Cerebrovascular tissue undergoing ischemia has two layers: (a) inner core of the ischemic area, where blood flow is most severely restricted and necrosis of neuronal and supporting glial cells may occur within minutes; (b) periphery of the ischemic area (penumbra), supplied also by collaterals where blood flow can buffer the full effects of the stroke[38]. In the infarct core, where adenosine triphosphate (ATP) is severely depleted, necrosis may be the predominating form of cellular death, whereas in the penumbra, apoptosis, an energy-dependent programmed form of cell death, may be the predominant form of cell death. The penumbra area is characterized by the loss of action potential firing but maintenance of proper resting membrane potential and represents a functionally impaired but potentially salvageable area. On restoration of blood flow to the penumbra territory, normal function may return. If flow is not restored acutely, tissue originally in the penumbral region dies and the core infarct region evolves to encompass what was previously penumbral tissue[39].

During ischemia, unless perfusion is improved in a timely fashion or cells are made relatively more resistant to injury, the tissue at risk dies within minutes to a few hours[39]. Even a partial occlusion for a long enough period may cause harmful effects due to deterioration of ion gradient and by-products of anaerobic metabolism[40]. Experimental evidence shows that reperfusion triggers a set of unique, potentially pathologic events including, for example, increased prostaglandin synthesis, elevated production of second messengers, inflammation, and mitochondrial dysfunction, as indicated by elevated reactive oxygen species (ROS) and the opening of the mitochondrial permeability transition pore[41-43]. The paradox of reperfusion injury can be understood in terms of counter-adaptive changes occurring during cerebral ischemia that predispose tissues to cellular dysfunction, apoptosis, and necrosis during the reperfusion phase. Reperfusion may enhance inflammatory response, oxidative stress and blood-brain barrier (BBB) disruption that could increase secondary brain injury, including cerebral edema and hemorrhagic transformation[44].

Rapid energy depletion reflects very low energy reserves within the brain, a high metabolic rate, and an almost total reliance on glucose oxidation for energy production. Ischemia depletes ATP within minutes, in which the immediate consequence is the perturbation of electrochemical membrane gradients, leading to depolarization. The pathophysiology of

cerebral I-R is complex, and cell damage results from the interplay of ionic imbalance, excitotoxicity mechanisms, inflammatory pathways, oxidative stress, peri-infarct depolarizations (PIDs), apoptosis, and neuroprotection.

***Ionic imbalance***

The neuronal loss of calcium homeostasis is a hallmark of impending cell demise. Intracellular concentration of calcium is normally strictly regulated through control of ATP-dependent calcium channels and exquisite active sequestering systems, including endoplasmic reticulum, lysosomes and mitochondria[45]. Ischemia causes an increase in calcium intracellular concentrations from depolarization of voltage-gated channels, activation of ligand-gated channels, release of intracytoplasmic stores, and loss of ATP-dependent calcium extrusion pathways, particularly the $Na^+/Ca^{2+}$ exchanger[45,46]. Excessive calcium influx results in the activation of a multitude of enzymes including phospholipases and proteases, mediated through calcium serving as a secondary messenger for numerous downstream signaling pathways[47]. Activation of phospholipases and proteases causes membrane and protein degradation, decreasing cellular integrity and survival if no ATP is available for the re-synthesis of cellular constituents. Furthermore, endonucleases are also activated, potentiating cell death[48]. Calcium influx stimulates glutamate-mediated excitotoxicity as depolarization occurs and additional glutamate is released. In addition, activation of neuronal nitrous oxide synthase (NOS), phospholipase $A_2$, and other $Ca^{2+}$-dependent enzymes leads to production of nitric oxide (NO), arachidonic acid metabolites, and superoxide, which act as additional triggers of cell death[47,49]. Other channels and ion pumps activated during ischemia have also been implicated in the ionic imbalance such as acid-sensing ion channels (ASICs), volume-regulated anion channels, and transient receptor potential channels[50-53]. The former, ASICs, are stimulated within the pH range commonly found in ischemic brain tissue, thus explaining the well-established link between acidosis, one of the hallmark neurochemical elements of the anaerobic metabolism of ischemia, and worsening of ischemic outcome in animals and humans.

***Excitotoxicity mechanisms***

Glutamate is a major excitatory neurotransmitter in the mammalian brain and key mediator of communication, plasticity, growth and differentiation, The concentration of this neurotransmitter is usually maintained across the plasma membrane by sodium-dependent glutamate transporters located on pre- and postsynaptic membranes and, under normal homeostatic conditions, glutamate is rapidly cleared from the synapse via presynaptic and astrocyte uptake. During ischemia, membrane depolarization and intracellular accumulation of sodium lead to a reversal of glutamate transporters and allow glutamate to exit cells along its concentration gradient[54]. Also, breakdown of astrocytic functions results in impaired cell glutamate uptake[55]. The resulting glutamate concentration increase in the synapse results in prolonged and sustained stimulation of N-methyl-d-aspartate (NMDA) and α-amino-3-hydroxy-5-methyl-4-propionate (AMPA) ionotropic receptors subtypes that further enhance the influx of calcium, sodium, water and, therefore, cytotoxic edema[56].

***Peri-infarct depolarizations***

Besides excitotoxic events at the molecular and cellular level, the overwhelming release of glutamate and ionic imbalance negatively impact the evolution of ischemic injury at the tissue level. For instance, PIDs are spontaneous waves of electrochemical activity that propagate through the cortex following focal stroke. PIDs are triggered by high levels of extracellular glutamate and potassium and characterized by slowly propagating massive, high-energy consuming depolarization of neurons and astrocytes along with drastic disruption of ionic gradients[57]. Recurrent PIDs in the penumbra are associated with increased ischemic injury. The resulting infarct expansion is probably due to mismatch between high metabolic demand to support membrane repolarization and marginal tissue perfusion due to constrained penumbral blood flow. Electrophysiological and imaging data demonstrated cortical spreading depolarizations (CSD) in patients with ischemic stroke or with ruptured IAs and has been correlated with infarct maturation, vasospasm and delayed ischemic neurologic deficit following aneurysmal subarachnoid hemorrhage[57-59]. CSD has been shown to induce tone alterations in vessels, causing a physiological hemodynamic response of transient hyperperfusion in healthy tissue and an inverse hemodynamic response hypoperfusion in tissue at risk for progressive damage, which may enhance cortical spreading ischemia[58].

***Oxidative stress***

The brain is highly susceptible to free radical mediated insult due to its high lipid content and its limited antioxidant defenses[60]. Oxidative stress in cerebral I-R, induced by the production of ROS, can be attributed largely to mitochondrial dysfunction[41-43]. In I-R, excessive ROS results in a range of harmful events as endogenous scavenging systems may have been compromised by ischemia, therefore, inducing cell membrane disruption through phospholipid fatty acids peroxidation[61]. ROS block mitochondrial respiration by inhibiting enzymes involved in the electron transport chain and facilitate mitochondrial transition pore formation, which causes increased release of mitochondrial membrane constituents, in particularly apoptosis-related proteins[62]. Additionally, ROS may also cause damage to other fundamental cellular components such as nucleic acid or gene repair systems, leading to subsequent cell death by necrotic or apoptotic mode. It may activate various cell signaling pathways that are proposed to be involved in regulating cell survival/death, such as p38, c-Jun N-terminal kinases, p53, extracellular signal-regulated kinases 1/2, Akt (protein kinase B) pathway and the nuclear factor-κB (NF-κB)[63]. Nitric oxide is a vasodilator generated by endothelial NOS to increase local CBF during ischemia. The relatively low levels of NO produced by endothelial NOS are neuroprotective, whereas high levels of NO produced by macrophage NOS and induced NOS during ischemia may exacerbate or contribute to injury. High concentration of NO combines with superoxide to produce peroxynitrite, which is a potent oxidant[64]. Following reperfusion, as reoxygenation provides an excess supply of substrate for oxidation, there is even increased production of superoxide, NO and peroxynitrite[64,65]. These radicals activate matrix metalloproteases, which degrade collagen and laminins in the basal lamina resulting in disruption of the integrity of the vascular wall and increased BBB permeability[66]. ROS and reactive nitrogen species produced in mitochondria are involved in the release of cytochrome C and further pro-apoptotic proteins[67]. Oxidative and nitrative stress are simultaneously powerful mediators of ischemic injury and responsible for recruitment and migration of neutrophils and other leukocytes to the cerebral vasculature. Enzyme-release from these cells further increase basal lamina degradation and vascular permeability during reperfusion. These events can lead to parenchymal hemorrhage, vasogenic brain edema and neutrophil infiltration into the brain[68].

***Inflammatory pathway/Apoptosis***

The inflammatory response to vascular occlusion is immediately initiated within the vessel and results in activation of complement, platelets, and endothelium[69]. Sequential expression of adhesion molecules, results first in neutrophil and later in monocyte adhesion to the endothelial wall. Within the vasculature, activated leukocytes contribute to vessel occlusion both directly and by releasing proinflammatory cytokines, proteases, and ROS, which injure the endothelial surface, leading to thrombus formation, vasospasm, and worsening ischemia[69]. Inflammatory mediators contribute to breakdown of the BBB, further promoting the infiltration of leukocytes into the brain. The choreographed inflammatory response progresses for many days after ischemia, with multiple signals and targets triggering expression of novel proteins and secondary infarct expansion. In neurons, cerebral ischemia upregulates the expression of several apoptosis, cytoskeletal, and proinflammatory genes, including transcription factors, heat shock proteins, cytokines, chemokines and adhesion molecules. The complex network of kinases involved in cell response to I-R includes glycogen synthase kinase-3β (GSK-3β), which plays a critical role in the promotion of apoptosis in neurons. GSK-3β kinase and its inhibition to suppress cell death will be a subject of discussion in a later chapter. Ischemic damage causes an early response in gene expression of p53 and release of proapoptotic molecules cytochrome c and apoptosis-inducing factor from mitochondria. This leads to activation of caspases and other genes that potentiate cell death[70,71]. NF-kB has also its expression increased during in vivo ischemia and has been demonstrated to have a key role in the regulation of genes involved at multiple stages of immune responses, inflammation, dendritic cell maturation and lymphocyte activation by modulating the expression of tumor necrosis factor-α, interleukin-1β, interleukin-6, inducible NOS, cycloxygenase-2 and intercellular adhesion molecule-1[60]. In the periphery, NF-kB, was found to be expressed by activated macrophages, monocytes, lymphocytes, endothelial cells, fibroblasts, platelets, while in cerebral infarctions NF-kB has been seen to be induced in activated microglia and glial cells[72]. Similarly, numerous other metabolism-, cell communication- and signal transduction-related genes were found down-regulated at 6 hours after middle cerebral artery occlusion (MCAO)[73]. Remarkably, several phases of the neuroinflammatory response, including leukocyte infiltration, cytokine production and enzyme induction, significantly contribute to cause delayed I-R injury.

***BBB disruption***

Cerebral edema resulting from stroke is an important cause of death and disability. Acute hypoxia causes cytotoxic edema within minutes to hours, potentially reversible, which gives way to vasogenic edema with progression of infarction. Cytotoxic/cellular edema is characterized by swelling of all cellular elements of the brain, including neurons, glia, and endothelial cells, due to an inflow of water as a result of failure of ATP-dependent sodium and calcium pump. Particularly, focal ischemia followed by reperfusion leads to severe damage to the BBB integrity, allowing water and macromolecules to cross into brain tissue as early as 20 to 45 minutes following MCAO[74]. This detrimental vasogenic edema may reduce focal blood flow becoming a vicious cycle, accelerating brain damage[75]. The sustained increase in the intracranial pressure can cause persistent ischemia, irreversible brain damage, and ultimately, cerebral herniation and death.

***Neuroprotection mechanisms***

Ischemic cascade also activates various neuroprotective mechanisms against apoptotic and necrotic cell death. These include heat shock protein 70, pro-survival Bcl-2 pathway, phosphorylated-Akt (p-Akt), neurotrophin-3, interleukin-10 or granulocyte-colony stimulating factor[76-80]. Furthermore there is an unclear importance of autophagy in I-R, which is an energy-dependent process used by eukaryotes to degrade and recycle subcellular organelles. Autophagy has been implicated in the death process[81] but its role in ischemia may be cytoprotective, as demonstrated by some disease models[82]. As detailed, ischemia is mediated by highly redundant cellular, molecular, and physiological mechanisms involving neurons, astrocytes, and vascular cells. Upstream sensors have been implicated, including adenosine and its receptor, NMDA receptor, and the transcriptional regulator hypoxia inducible factor (HIF). HIF regulates a constellation of protective genes, including those whose protein products facilitate oxygen transport (erythropoietin), regulate glycolytic metabolism, and promote angiogenesis. The unexpected demonstration that a genetic deletion of HIF1$\alpha$ improves infarct volume after MCAO[83] leads, however, to the finding that a complex network of transcriptional activations of HIF target genes pathogenic mechanisms may be dependent on the degree of hypoxia[84]. During mild hypoxia, the transcriptional activations of HIF-inducible genes mainly promote cell survival by erythropoiesis, angiogenesis and anti-apoptosis. During severe hypoxia, HIF effects are represented by its participation in the

apoptotic process by increasing stability of tumor suppressor protein p53 and by inducing cell necrosis.

## 1.3 Intraoperative Cerebral Protection

Neuroprotection involves mechanisms and strategies to protect against neuronal injury or degeneration following acute disorders, such as stroke or trauma, or as a result of chronic neurodegenerative diseases. Specifically for cerebral hypoxia, it could be defined as any strategy, or combination of strategies, that antagonizes, interrupts, or delays the sequence of injurious biochemical and molecular events that, if left unchecked, would result in irreversible cerebral ischemic injury[85]. According to this classic definition, protection from injury is settled at the neuron itself and therefore, excludes therapeutic strategies that are directed primarily at the cerebral vasculature. The fact that all cell types participate in the complex pathophysiology of brain injury during ischemia, however, leads to the basis of the neurovascular unit model, providing a conceptual framework to integrate responses to an injury from all cell types, including neuronal, glial, and vascular cells[86,87]. Cell-to-cell interactions in the neurovascular unit form the basis for brain function. It is now clear that it is insufficient to approach brain function and dysfunction from a uniquely neuronal standpoint but whereas the intricate molecular pathways of cell death in the neuron have been dissected in detail, the mechanisms of how the entire neurovascular unit responds to I-R are not so clear. Moreover, how each cell type in the neurovascular unit might alter its response to ischemia in the context of different environments remains to be elucidated. The concept of neuroprotection, therefore, is shifting to the concept of cerebroprotection, in which the neurovascular unit takes advantage of the neuron[86]. The growing understanding that neuron protection solely and prevention of its death alone may not be enough, suggests that future therapeutic approaches should target multiple cell types in an attempt to protect their structural, functional integrity and reciprocal interactions.

Prevention of iatrogenic brain ischemia in the operating room during cerebrovascular procedures includes non-pharmacological and pharmacological strategies. Precluding or limiting the duration of a transient artery occlusion is the most direct and obvious strategy. As the duration of stroke-free period for temporary artery occlusion, as earlier stated, is highly

variable, intraoperative prediction of this time period for each particular patient is currently an important line of clinical research. The reports of use of electrophysiological monitoring such as electroencephalography, electrocorticography, multimodality and somatosensory evoked potentials monitoring to alter the course of the intraoperative management of IAs to minimize postoperative infarction are increasing[25,88-91]. Monitoring brain tissue oxygenation is also being investigated as a risk indicator of cerebral ischemia and post-operative infarction for aneurysm surgery[92,93]. Evidently, accomplishing vessel patency after aneurysmal clip placement is of higher importance, which is done with a meticulous surgical technique and could be confirmed with systems such as microvascular Doppler, fluorescent angiography with indocyanine green, ultrasonic flow probe or intraoperative angiography.

Nonpharmacological strategies may also include maintenance of CBF by adequate control of mean arterial pressure, normoglycemia, and adequate hemoglobin levels. Also, whenever a transient occlusion of a cerebral artery is considered necessary, induction of hypertension may increase collateral perfusion of the ischemic penumbra and hence, increase cerebral tolerance to transient ischemia[94]. While avoiding hyperthermia is critical and consensual, inducing hypothermia is controversial and has been matter of intense research. Hypothermia has shown significant efficacy in animal models of cerebral ischemia[95] and to be clinically feasible in surgical and acute stroke patients[96-98]. Still, hypothermia has failed to achieve effective neuroprotective effects in the clinical setting. The rationale of hypothermia was to protect the brain through a pleiotropic of effects within the neurovascular unit. It has been shown to reduce brain metabolism, glutamate release, ROS production, peri-infarct depolarizations, inflammatory markers, microglial activation, leukocyte infiltration, and BBB disruption[99]. Moreover, studies have shown that hypothermia suppresses apoptotic cell death, decreases mitochondrial release of cytochrome C and apoptosis-inducing factor and upregulates cell survival pathways[99]. Therefore, reducing the body core temperature illustrates, at least theoretically, the potential power of approaching stroke therapy using combinations of modalities that engage multiple cell types to enhance protection and recovery. However, several complications have been associated with hypothermia, including shivering, pneumonia, infections, hypotension, cardiac arrhythmias and an increase in intracranial pressure during the rewarming period. Kimme[98] evaluated the safety of intraoperative moderate hypothermia in 326 patients who underwent 359 aneurysm-clipping operations. No

significant difference in circulatory instability, coagulopathy, and infection was evident in comparison to previous studies. Pulmonary complications (ventilator dependency) were thought to be secondary to neurogenic pulmonary edema and could be ameliorated by rapid rewarming and early extubation. Efficacy outcomes were not evaluated. Other clinical trials were performed, namely the Intraoperative Hypothermia Aneursym Surgery Trial (IHAST)[100], Cooling for Acute Ischaemic Brain Damage (COOL-AID) studies, COOL-AID I (using surface cooling)[101], COOL-AID II (using endovascular cooling)[96] and the Intravenous thrombolysis plus hypothermia for acute treatment of ischemic stroke (ICTuS-L)[97]. All showed that mild therapeutic hypothermia for acute ischemic stroke or in the intraoperative setting is feasible but had no change in clinical outcome. Lately, enthusiasm regarding the use of intraoperative hypothermia has fallen out of favor as a neuroprotective adjunct[102-104], highlighting the need for the use of and research on cerebroprotective agents. Nevertheless, several other efficacy and safety clinical trials are ongoing: Cooling in Acute Stroke (COAST-II) trial, Controlled Hypothermia in Large Infarction (CHILI) trial, the European Stroke Research Network for Hypothermia (EuroHYP)-1 trial (protocols available at http://www.strokecenter.org), and The Intravascular Cooling in the Treatment of Stroke (ICTuS) trial[105].

The classic theory of pharmacological cerebral protection is based on the concept that by decreasing cerebral metabolic demand, the neuronal survival will improve during periods of inadequate CBF. Because barbiturates decrease cerebral metabolism, it was the first drug group to be considered as a potential cerebral protectant. It was demonstrated that barbiturates decreased cerebral metabolic activity in a dose-dependent manner, which produced progressive decrease in electroencephalogram (EEG) activity, reduction in the rate of ATP depletion, and protection from incomplete cerebral ischemia[106]. Therefore, with barbiturate treatment to an isoelectric EEG during ischemia, all metabolic energy is believed to be used for maintenance of basal cellular integrity. Accordingly, Nussmeier[107] confirmed that barbiturates only work during incomplete ischemia, that is when EEG activity is still present during the ischemic period, and that barbiturates decrease cerebral metabolism in a dose-dependent manner only until the EEG becomes isoelectric. One could expect similar effects in other anesthetics, such as etomidate, propofol or isoflurane, as they suppress neurotransmission. Lavine[33] has probably reported the best clinical evidence so far regarding

this issue, from a small retrospective analysis of 49 patients who underwent surgery for middle cerebral artery (MCA) aneurysms with transient vessel clipping. Thirty-eight patients received intravenous pentobarbital, etomidate, or propofol, whereas the remaining 11 inhaled isoflurane. Postoperative radiographic evidence of infarction was noted in 45% of patients receiving the inhaled agent as opposed to 16% of those who underwent intravenous anesthesia, suggesting a protective effect with their use during temporary intracranial vessel occlusion. Nevertheless, a secondary analysis of the large IHAS trial, which included 441 patients who underwent temporary clipping during cerebral aneurysm surgery, concluded that supplemental pharmacologic agents such as barbiturates did not improve 24-hour or 3-month neurologic outcomes[102].

Up to date, there is no strong evidence that any of the commonly used drugs for patients undergoing transient cerebral clipping have effective cerebroprotective properties.

## 1.4 Translation from bench to bedside

Within the past few years, a wide variety of pharmacologic agents have shown beneficial effects in reducing infarct volume in animal stroke models. Therapies evaluated have included calcium channel blockers, glutamate antagonists, γ-aminobutyric acid (GABA) agonists, NOS inhibitors/free radical scavengers, phospholipid precursor, NO signal-transduction down-regulator, leukocyte inhibitors, statins, hemodilution, and miscellaneous other agents. Translating these successes to the clinical sphere, however, has been complicated by inconsistent results and toxic side effects. In fact, over 1000 potential neuroprotective drugs have been tested in preclinical animal studies, in which around 100 progressed to clinical trials but, so far, none have proven efficacious for the human population[108].

The failed translation from bench to bedside of numerous drugs, however, has provided some important concerns for investigators to consider before designing a preclinical or considering a translational trial for a potential neuroprotective agent[109-111]:

(1) **Robust supportive preclinical data** – Preclinical data should include sample size calculation, inclusion/exclusion criteria, randomization, allocation concealment, blinded assessment of outcome, adequate acute and long-term outcome measures (histopathological and functional response), disclosure of relevant conflicts of interest, and data should be sent for publishing for review in a peer-reviewed journal;

(2) **Definition of the route of administration and effective dose**– Route of administration in preclinical trials should be feasible in real life. Also, there should be a target concentration, a tissue level of effect identified from animal studies, or a surrogate marker that, when the drug is given to humans, will give some indication of whether there is a reasonable prospect of achieving neuroprotection in human clinical trials. The translation of preclinically protective doses for clinical trials is frequently not possible to approximate because of dose-limiting toxicity in humans;

(3) **Consider time-window to treatment** – In animal models, the time of the stroke or ischemic onset is known precisely, whereas in humans this may not be the case. Clinical trials should not evaluate a time-window to treatment significantly longer than was justified by the preclinical findings;

(4) **Approach as possible preclinical condition to clinical setting** – An important reason for the failure of clinical trials to confirm positive results in animal studies may relate to the lack of direct linkage between the model and the clinical situation. For instance, if the mechanism of drug action suggests that reperfusion will be necessary for drug effect, clinical research should be linked to reperfusion as well.

By far, most preclinical and clinical studies aiming toward neuroprotection were designed for patients with ongoing stroke, in which the treatment drug was administered after the onset of ischemia, as clinical setting would demand. Neurosurgical patients, although fewer in number, have the advantage of having several of the important variables controlled in the operating room, including the physiological parameters and the timing of the administration of cerebroprotective drug(s), which could even be done at or before the onset of the induced cerebral ischemia. It is intuitive that these circumstances may better resemble preclinical conditions of cerebral I-R produced in the laboratory and raise chances of clinical success.

# 2 OBJECTIVES

Main objectives of this research were:

1. To set up and establish an intraluminal MCA I-R rat model suitable to investigate potential benefits of drugs as possible treatments against neuronal damage in surgical procedures that require transient cerebral artery occlusion;

2. To investigate the potential benefits of a single dose of 1.000 IU/kg intravenous (IV) recombinant human erythropoietin (rhEPO) in the implemented I-R animal model; additionally, if results support it, to elaborate a protocol to promote a translational clinical trial;

3. To investigate the potential benefits of a single dose of 5 mg/kg IV 4-benzyl-2-methyl-1,2,4-thiadiazolidine-3,5-dione (TDZD-8) in the implemented I-R animal model.

# 3 CEREBRAL ISCHEMIA-REPERFUSION ANIMAL MODEL

## 3.1 Background

Experimental animal models of cerebral ischemia, with or without reperfusion, are designed to allow investigators to recreate specific aspects of human brain ischemia to study pathophysiologic and neuroprotective mechanisms, as well as therapeutic responses under controlled conditions that cannot be done easily or at all in clinical patients.

Rodents are particularly useful for stroke research because their cerebrovascular anatomy and physiology closely resemble that of humans and are reasonably inexpensive compared to larger animals[112]. The small brain volume of the rat is well suited for different analytical procedures and there are several well-described and standardized functional outcomes for rats in experimental stroke, including behavioral, cognitive, and sensorimotor outcomes[113-117]. Measurement of the extent of cerebral infarction is easily accomplished by histological staining for tissue damage using 2,3,5-triphenyltetrazolium chloride (TTC), cresyl violet (Nissl stain) or hematoxylin and eosin (H&E).

Rodent models of cerebral ischemia can be classified as global or focal and as reversible or irreversible. Focal cerebral ischemia models are designed to induce ischemia by occlusion or blockage of major cerebral arteries, most commonly MCA. Middle cerebral artery occlusion can be proximal or distal, permanent or temporary, alone or combined with carotid artery occlusions (ipsi-, contra-, or bilateral). Occlusion methods include ligation with suture/clipping/electric cauterization, blood clot injection, photochemical thrombosis, stereotactic injection of endothelin-1, or intraluminal filament[118-122].

The Stroke Therapy Academic Industry Roundtable (STAIR)[109,110] provided recommendations with the goal of improving preclinical stroke therapy assessment and increasing the translational potential of experimental stroke treatments. The whole design of this research intended to follow these guidelines, in which preclinical studies should closely replicate the clinical environment to increase the likelihood of translational success. Accordingly, a reversible focal cerebral ischemia model using an intraluminal filament was

chosen, as this model is the one that best mimics the ischemia-reperfusion injury that occurs during intraoperative transient cerebral artery occlusion. Although this surgical model is demanding and has a learning curve, it does not require craniectomy or brain manipulation, and the resulting proximal MCAO produces a big infarction that involves both cortical and subcortical areas.

In this chapter, a description of the technique implemented in the Pharmacology & Translational Research Laboratory of the Faculdade de Farmácia da Universidade de Lisboa is done, followed by preliminary results that allowed establishment of the MCA I-R rat model. Assessments of drug experiments are described in subsequent chapters.

Animal care was followed in accordance with the recommendations of the European Convention for the Protection of Vertebrate Animals Used for Experimental and Other Scientific Purposes (Council Directive 2010/63/UE) and National Law 113/2013 (rules for protection of experimental animals). The Ethics Committee of Faculdade de Medicina da Universidade de Lisboa approved all animal procedures. All efforts were made to minimize animal suffering and to reduce the number of animals used.

## 3.2 Materials and Methods

### 3.2.1 *Middle Cerebral Artery Ischemia-Reperfusion Technique*

Adult Wistar male rats weighting between 280 to 350 g housed under diurnal light conditions with unlimited access to food and water were used.

Male animals were used on the assumption that pathophysiology and treatment outcome does not differ amongst gender and to reduce experimental variability caused by female hormone cycling. Rats were food deprived for a period of 12 hours prior to surgery.

The MCA I-R surgical procedure performed is essentially a noninvasive method of reversible MCAO by the use of an intraluminal suture, originally described by Koizumi[120], with some minor modifications (Figure 3.1).

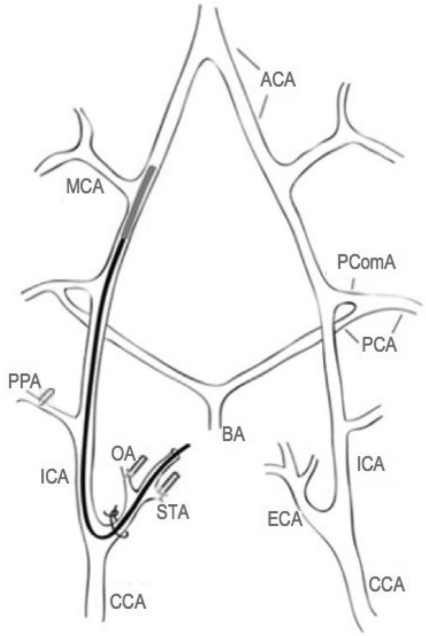


**Figure 3.1.** Diagram of the cranial circulatory system of the rat showing a silicone-coated intraluminal suture in place occluding the origin of the MCA. The OA and STA branches off of the left ECA have been ligated and a suture tie around the ECA stump holds the intraluminal thread in place. *ACA,* anterior communicating artery; *CCA,* common carotid artery; *ECA*, external carotid artery; *ICA*, internal carotid artery; *OA*, occipital artery; *PComA*, posterior communicating artery; *PPA*, pterygopalatine artery; *STA*, superior thyroid artery.

During the course of the experiments, general anesthesia was induced. Intraperitoneal (IP) pentobarbital administration (60 mg/kg) was used during experimental setting, and supplemented as required. Later, with the use of experimental drugs, ketamine (80 mg/kg) and xylazine (8 mg/kg) IP mixture was used to avoid potential neuroprotective effects of pentobarbital. Below, a step-by-step description for the surgical procedure is provided:

1. The anesthetized animal is placed on a pre-warmed thermoregulatory heating pad and a temperature probe is inserted about 2 to 3 cm into the rectum. Body temperature is displayed on the control unit's temperature monitor and maintained between 36.5ºC to 37,5ºC.
2. Artificial tear ointment is applied to both eyes to protect the corneas from drying.
3. The animal is positioned in ventral position and the skin and fur on the head is disinfected with 70% alcohol solution.

4. A midline head incision is done to expose the bregma, retractors put in place and a small burr hole is drilled 2 mm posterior to the bregma and 3.5 mm lateral to the midline down to dura-mater in the supply territory of the right MCA, where transient ischemia is to be done. A micro-Doppler holder probe is glued with cyanoacrylate to the bone and the Laser-Doppler probe put in place (Periflux System 4000, Probe 407, Perimed-Instruments, Stockholm, Sweden) (Figure 3.2, *A-D*). The skin incision is closed with a 2-0 silk suture.
5. The animal is then changed to supine position with a pad under the neck to slightly extend it to aid vessel exposure (Figure 3.2, *E*).
6. Skin and fur on the ventral cervical area is disinfected with 70% alcohol solution.
7. Under the operating microscope, a ventral midline neck incision is made and the superficial fascia dissected; the right sides of the sternohyoid muscle, which lies midline over the trachea, sternomastoid muscle laterally and digastric muscle superiorly, are blunt dissected and gently retracted to expose the right common carotid artery (CCA). The omohyoid muscle is retracted downwards with a silk line and retractors are positioned between the sternomastoid and sternohyoid muscles (Figure 3.2, *F-G*).
8. The CCA, external carotid artery (ECA) and internal carotid artery (ICA) are exposed and mobilized from the surrounding tissues to near the skull base. The vagus nerve (X nerve) is sharply dissected from the CCA and ICA (Figure 3.2, *H)*.
9. The occipital artery (OA), a branch of the ECA, is coagulated. Other branches of the ECA including superior thyroid (STA) and ascending pharyngeal arteries are cauterized (Figure 3.2, *I*). This allows greater ease in mobilizing the larger vessels.
10. Further dissection of the ICA identifies the glossopharyngeal nerve (IX nerve) near the origin of the pterygopalatine artery (PPA), which is ligated close to its origin with a McEnzie clip (Figure 3.2, *J*). At this point, the ICA is the only remaining branch of the CCA.
11. A 6-0 loose silk knot is left at the beginning of the ECA stump, near the bifurcation (Figure 3.2, *K*).
12. The ECA is further dissected, tied off as distally as possible with 6-0 silk suture and McEnzie surgical clip and then cut. The ECA terminal stump, about 5 mm long from the ECA-ICA bifurcation, is freed from surrounding tissue (Figure 3.2, *L-M*).

13. Microvascular clips are place on CCA and ICA and a small arteriotomy is made with spring scissors in the ECA stump, distal to the loose knot (Figure 3.2, *N*).
14. A 4-0 nylon silicone rubber-coated tip monofilament (Doccol Corporation, Sharon, MA, USA) is then gently inserted into the ECA stump towards the ICA. The loose silk suture around the ECA stump/intraluminal nylon filament is tightened to prevent bleeding (Figure 3.2, *O*).
15. Microvascular clips are removed from both the CCA and ICA and the filament is then slowly advanced about 19 to 21 mm from the fork. While advancing the filament, a slight resistance may be felt and laser-Doppler flowmetry (LDF) should confirm a sudden decrease to less than 30% of baseline values when the blunted tip of the filament has blocked the origin of the MCA and reached the proximal segment of the ACA (Figure 3.2, *P*-*Q*). At this point, the intraluminal filament is blocking the origin of the MCA, occluding all sources of blood flow from the ICA, ACA, and posterior communicating artery. About 7-10 mm length of the filament remains outside, to be withdrawn to allow reperfusion.
16. The timer is started and ischemia persists for 60 minutes, until the thread is withdrawn. The operational sequence for reestablishing the blood flow in the MCA is to slowly retract the intraluminal filament, loosen the silk knot, withdraw the filament and quickly apply a McEnzie clip to the stump of the ECA to block blood flow. LDF should confirm reperfusion.
17. The skin incision is closed with a continuous 2-0 silk suture, and the animal is placed in a clean cage. CBF values are measured throughout recovery period.
18. One milliliter of pre-warmed sterile saline is administered IP to provide hydration during recovery stage.

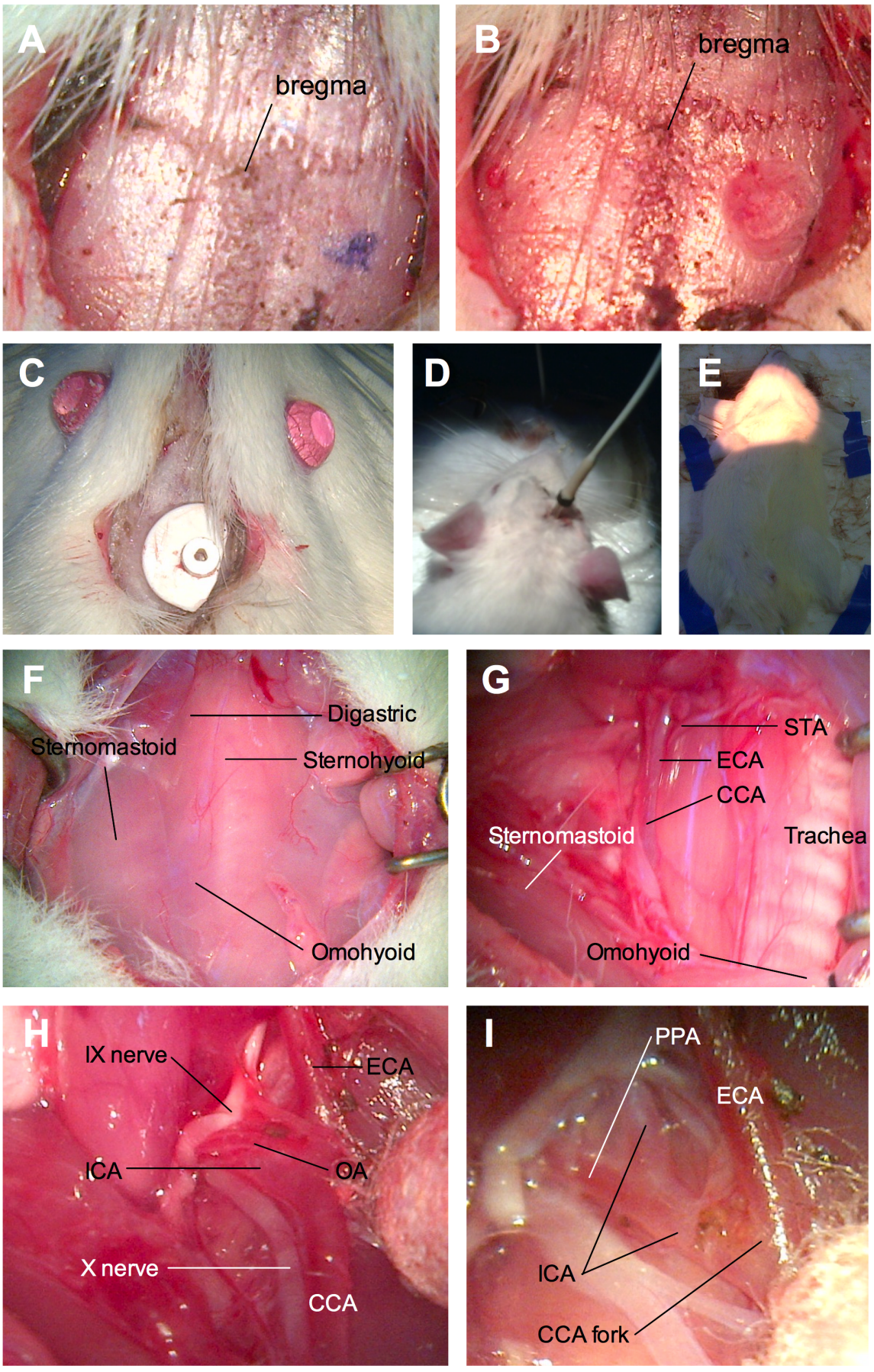
A
bregma
B
bregma
C
D
E
F
Digastric
Sternomastoid
Sternohyoid
Omohyoid
G
STA
ECA
CCA
Sternomastoid
Trachea
Omohyoid
H
IX nerve
ECA
ICA
OA
X nerve
CCA
I
PPA
ECA
ICA
CCA fork

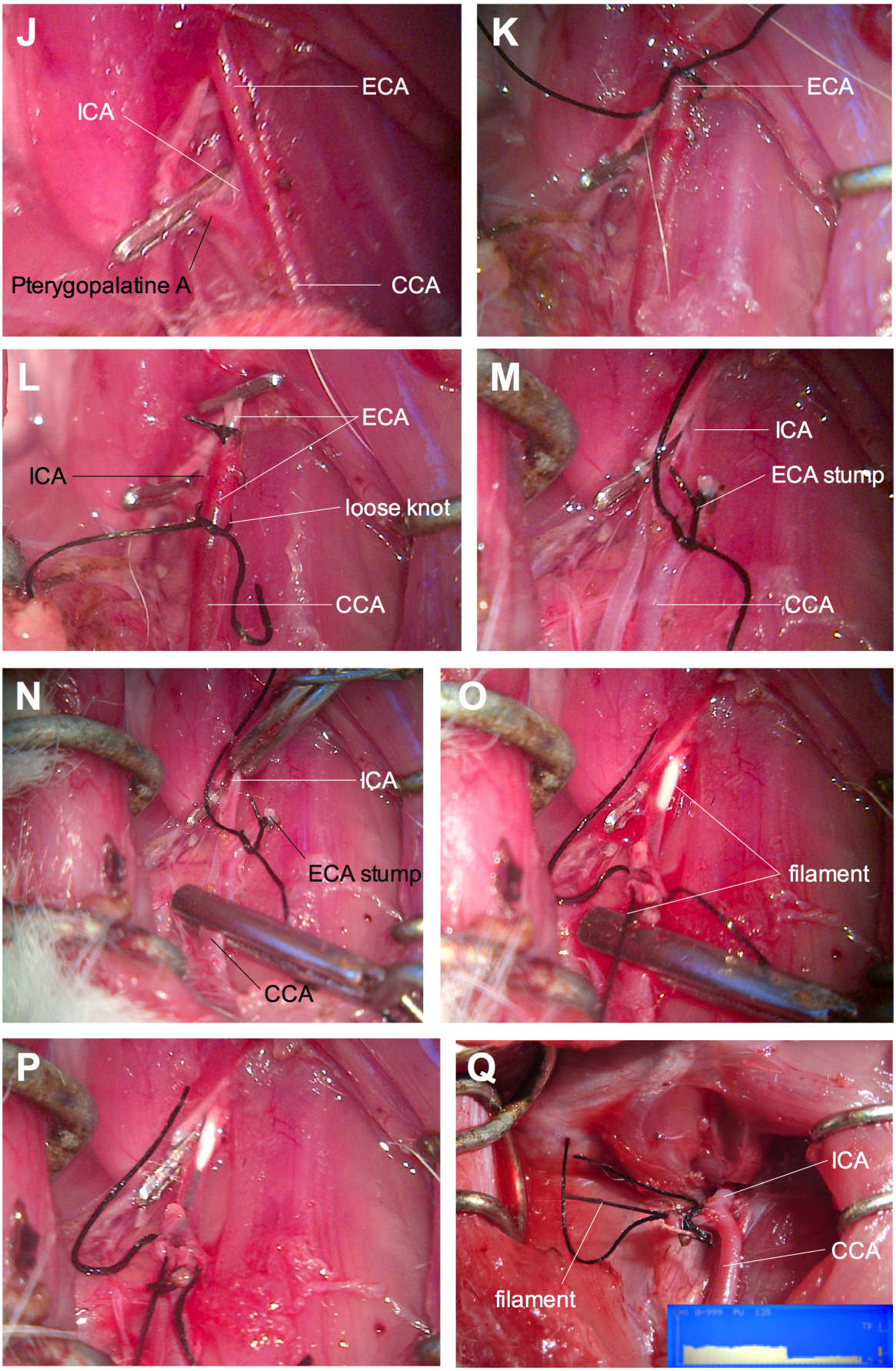
J
ECA
ICA
Pterygopalatine A
CCA
K
ECA
L
ECA
ICA
loose knot
CCA
M
ICA
ECA stump
CCA
N
ICA
ECA stump
CCA
O
filament
P
Q
ICA
CCA
filament

**Figure 3.2.** Step-by-step MCA I-R surgical technique. *A,* The bregma is located at the junction of the sagittal and coronal sutures. The blue dot located 2 mm posterior and 3.5 mm right lateral the bregma spots the point for drilling. *B,* 2 mm drill hole down to the dura-mater. *C,* Laser-Doppler probe holder glued to the bone. *D,* Laser-Doppler probe attachment to probe holder. *E,* Rat positioned in supine and limbs fixed. *F,* Skin incision and retraction to expose ventral cervical muscles. *G,* Retraction of cervical muscles to expose CCA, ECA, STA, trachea and vagus (X) nerve. *H,* STA and ascending pharyngeal artery exposed to diathermia and further dissection expose CCA fork, ICA, ECA, OA and glossopharyngeal (IX) nerve. *I*, OA cauterized and digastric muscle retracted to expose ICA and its collateral PPA. *J,* A McEnzie clip inserted to ligate the PPA. *K*, 6-0 silk loose knot left at the origin of the ECA. *L,* ECA ligated as distally as possible with the use of 6-0 silk knot and McEnzie clip. *M,* ECA cut and stump exposed. *N,* Transient microvascular clips applied on both CCA and ICA. *O,* A small ECA arteriotomy and 4-0 nylon monofilament insertion in the artery. The loose knot is tightened to prevent bleeding and the ICA clip removed. The white silicone rubber-coated tip can be seen inside the ICA. *P,* Removal of CCA clip. *Q,* The monofilament is carefully introduced until a drop in the baseline of the CBF is noticed (inner figure). *CCA,* common carotid artery; *ECA*, external carotid artery; *ICA*, internal carotid artery; *OA*, occipital artery; *PPA*, pterygopalatine artery; *STA*, superior thyroid artery.

Throughout recovery period, animals are left in a cage with full water and food access.

### *3.2.2 Cortical Blood Flow Measurements*

Cortical CBF was monitored by LDF (Periflux System 4000, Probe 407, Perimed-Instruments, Stockholm, Sweden) before, during occlusion, and within 1 hour of reperfusion. As previously explained, a small burr hole was drilled 2 mm posterior to the bregma and 3.5 mm lateral to the midline and the micro-Doppler probe positioned above the dura in a micro-holder glued to the bone. Probe placement allows the specific measuring of a small amount of tissue focused on the right MCA. Steady-state baseline values were recorded before occlusion, and the CBF measured during occlusion and reperfusion was expressed as a percentage of the baseline values (Figure 3.3).

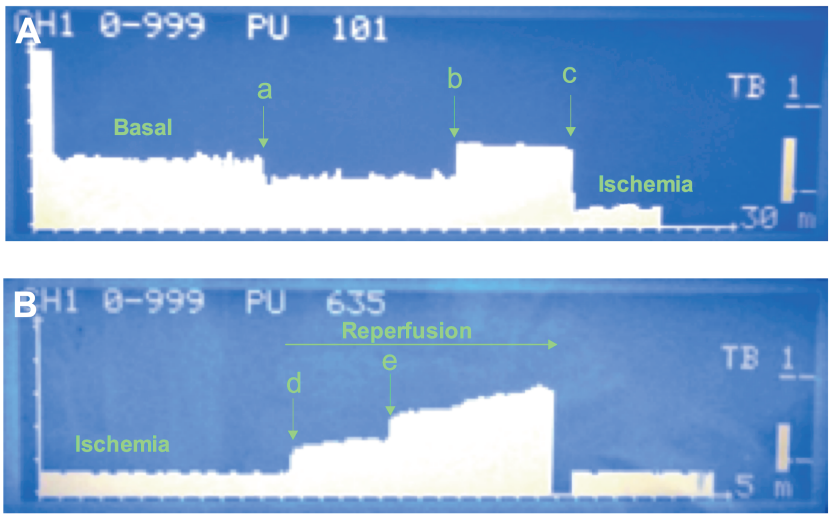


**Figure 3.3.** Representative images of CBF monitoring patterns during induction of ischemia and reperfusion phases of surgical procedure. *A*, CBF monitoring during MCAO. (a) clipping of CCA and ICA for ECA arteriotomy and filament intraluminal introduction, (b) clips removal for filament progressing, (c) sudden intraluminal MCAO with corresponding CBF value drop. *B*, CBF monitoring during MCA reperfusion. (d) filament retraction initiates reperfusion, (e) filament intraluminal removal from the ICA results in an additional slope in the CBF suggesting complete reperfusion.

Some CBF criteria indicate successful MCAO:

1. CBF decreases to less than 30% during period of intraluminal MCAO - baseline CBF is set at 100% before insertion of suture into ICA;
2. CBF remains at this low level during entire occlusion time;
3. CBF recovers to over 80% of baseline within 30 minutes of filament withdrawal.

Rats with CBF patterns suggesting subarachnoid hemorrhage, incomplete ischemia or incomplete reperfusion were excluded (Figure 3.4).

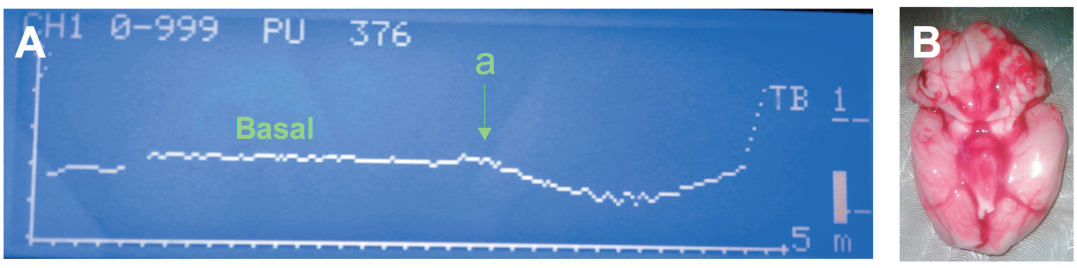


**Figure 3.4.** Subarachnoid hemorrhage. *A*, Representative CBF pattern suggesting SAH. (a) slow decrease on CBF while introducing the intraluminal thread through the ICA, in relation with its rupture and succeeding SAH. *B*, Brain with evidence of SAH.

### *3.2.3 Neurological Examination*

At 24-hour, a nine-point neurological scale (0=normal to 9=highest handicap) was implemented[115]. Four tests were performed in order to assess spontaneous activity, laterality in movement, resistance to left forepaw stretching and parachute reflex (Table 3.1). Scores obtained for each test were added to obtain the final neurological score.

**Table 3.1** *Scale neurological evaluation used at 24-hour into reperfusion*

| Neurological assessment | Item score |
|---|---|
| **A. Spontaneous activity** | **0-2** |
| *Moving/exploring* | *0* |
| *Moving without exploration* | *1* |
| *No displacement* | *2* |
| **B. Laterality in movement** | **0-3** |
| *Symmetrical* | *0* |
| *Left drifting when elevated by the tail* | *1* |
| *Spontaneous left drifting* | *2* |
| *Circling to the left* | *3* |
| **C. Resistance to left forepaw stretching** | **0-2** |
| *No stretching allowed* | *0* |
| *Stretching allowed* | *1* |
| *No resistance* | *2* |
| **D. Parachute reflex** | **0-2** |
| *Symmetrical* | *0* |
| *Asymmetrical* | *1* |
| *Contralateral forelimb retracted* | *2* |

### *3.2.4 Infarct Volume and Brain Edema Assessment*

At 24 hours into reperfusion, animals were euthanized with anesthetic overdose. The brains were removed, placed in a brain matrix (World Precision Instrument, Hertfordshire, UK) and sliced in 2-mm thick coronal sections, beginning 2 mm from the frontal pole and ending rostral to the corticocerebellar junction, resulting in 6 slices per animal (Figure 3.5, A-B).

The sections were then stained in 2% TTC (Sigma-Aldrich, St. Louis, MO, USA) saline solution for 10 minutes at 37°C in the dark. The staining action of TTC is based on the oxidation of TTC by intact mitochondrial dehydrogenase, which oxidizes the tetrazolium salts into formazan, a carmine red product. Accumulation of the red formazan stains the tissues red, and the intensity of the red color is proportional to the rate of respiration in those tissues[123]. Due to the absence of active dehydrogenase in the infarcted or necrotic tissue, it remains unstained. Therefore, this method can distinguish live (stained red) from infarct (unstained white) tissue. TTC stain demonstrates ischemic lesions that can be appreciated visually even without microscopic examination and enables assessment of lesion size with minimal tissue preparation (Figure 3.5, C-D). Quantitative measurements of infarct volume determined by this method have proven useful in determining the extent of brain injury in experimental stroke models and in assessing potential neuroprotective agents for cerebral ischemia. The brain sections were next fixed in 4% paraformaldehyde at 4°C overnight. The fixed brain tissue sections were then digitally scanned and analyzed with ImageJ software version 1.45 (Figure 3.5, E-F).

Total brain infarct volume was calculated by summing the infarct area of all brain slices (area of infarct in square millimeters x thickness [2 mm]). The amount of infarction was expressed both in absolute terms in cubic millimeters and as a percentage of contralateral hemisphere adjusted for brain edema, thereby avoiding the distortion caused by edema and surrounding white matter[124]. Therefore, a corrected infarct volume by computing the volume of the left and right hemispheres and applying the following formula was calculated, where LHV=total left hemisphere volume, RHV=total right hemisphere volume and InfV=measured infarct volume:

$$\text{Corrected infarct volume} = LHV - (RHV - InfV)$$

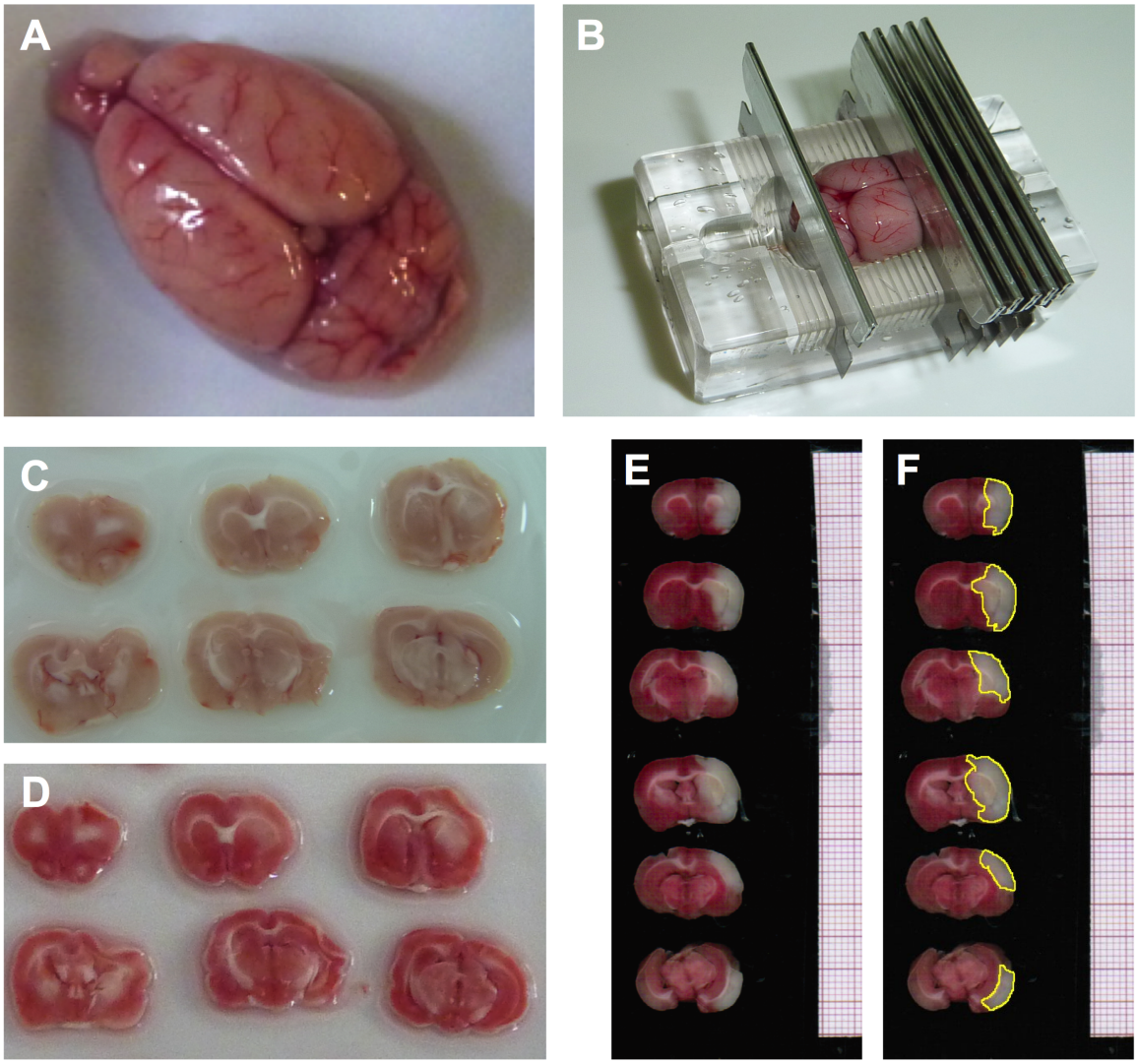


**Figure 3.5** Infarct and brain edema assessment technique. *A*, Brain removed from the cranium. *B*, Brain matrix for adult rat brains for standard 1 or 2 mm-coronal brain slicing. *C*, Representation of six coronal rat brain sections (24-hour reperfusion after 60-minute MCAO). *D*, Brain tissue slices are soaked in 2% TTC solution in a plastic dish for around 15 minutes. When tissue turns pinkish with white (unstained) regions, it is ready to fix. *E*, Representative image of scanned brain TTC-stained sections. *F*, Infarct area digitally demarcated for infarct and brain edema measurements.

The edema index, that is, the space-occupying effect was also calculated with the use of the equation described below and expressed as the percentage of volume increase of the injured hemisphere:

$$\text{Hemisphere edema index (\%)} = \frac{\text{RHV - LHV}}{\text{LHV}} \cdot 100$$

For each single experiment, a data extraction form was filled (Figure 3.6)

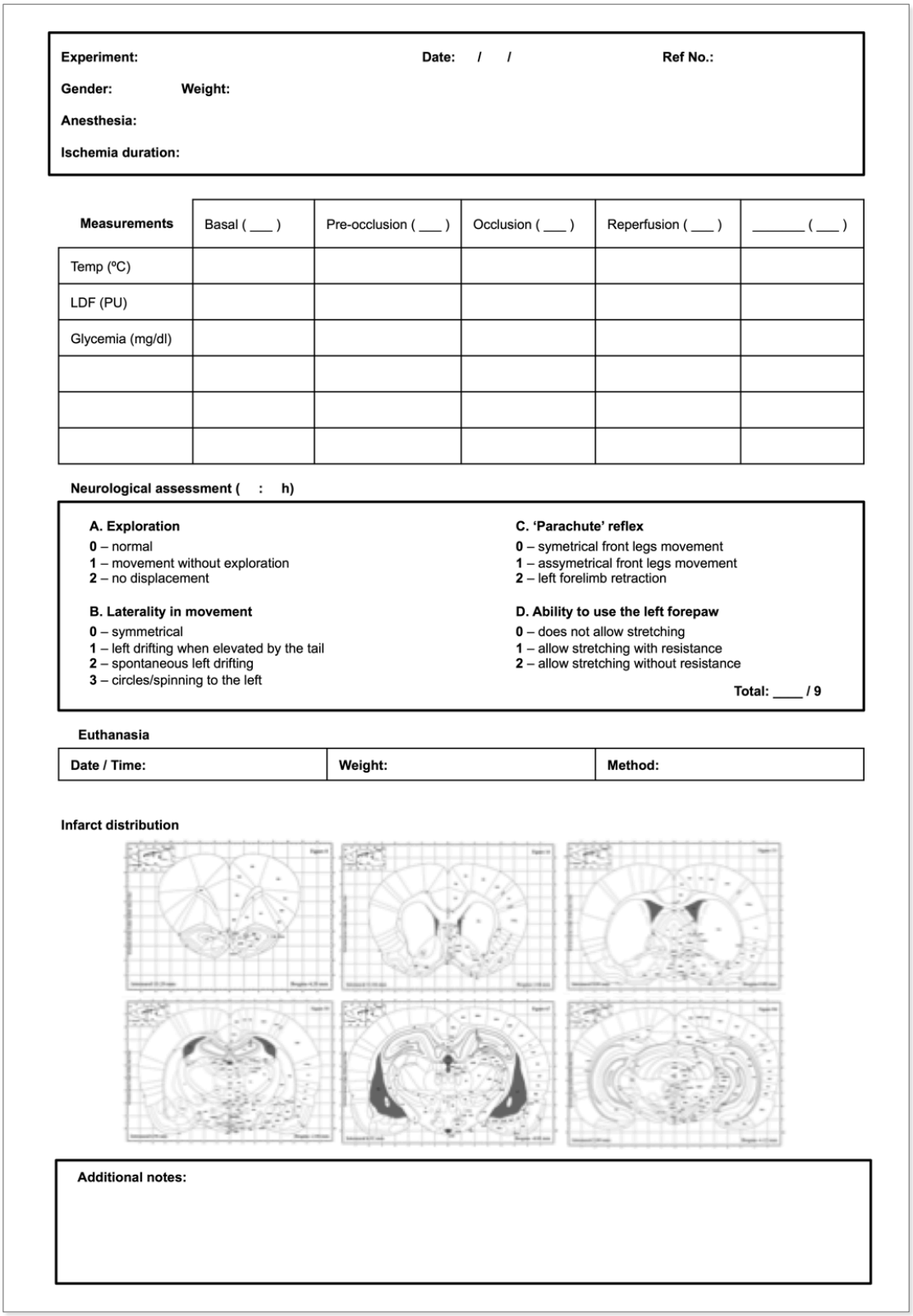

**Experiment:** **Date:** / / **Ref No.:**

**Gender:** **Weight:**

**Anesthesia:**

**Ischemia duration:**

| **Measurements** | Basal ( ___ ) | Pre-occlusion ( ___ ) | Occlusion ( ___ ) | Reperfusion ( ___ ) | _____ ( ___ ) |
|---|---|---|---|---|---|
| Temp (ºC) | | | | | |
| LDF (PU) | | | | | |
| Glycemia (mg/dl) | | | | | |
| | | | | | |
| | | | | | |
| | | | | | |

**Neurological assessment ( : h)**

**A. Exploration**
**0** – normal
**1** – movement without exploration
**2** – no displacement

**B. Laterality in movement**
**0** – symmetrical
**1** – left drifting when elevated by the tail
**2** – spontaneous left drifting
**3** – circles/spinning to the left

**C. 'Parachute' reflex**
**0** – symetrical front legs movement
**1** – assymetrical front legs movement
**2** – left forelimb retraction

**D. Ability to use the left forepaw**
**0** – does not allow stretching
**1** – allow stretching with resistance
**2** – allow stretching without resistance

**Total: ____ / 9**

**Euthanasia**

| **Date / Time:** | **Weight:** | **Method:** |
|---|---|---|

**Infarct distribution**

**Additional notes:**

**Figure 3.6** Data extraction form.

### *3.2.5 Statistical Analysis*

Statistical analysis was performed using GraphPad Prism software version 6.0. Parametric data were analyzed using Student's *t*-test for single comparisons between groups and non-parametric data (neurologic scores) were subjected to the two-tailed Mann-Whitney test, unless stated. Data are presented as mean±standard error of the mean (SEM) for *n* observations, where *n* represents the number of animals studied. A *p* value of less than or equal to 0.05 was the threshold considered to be a statistically significant difference or association.

## 3.3 Results

In order to assess the validity of the model, three groups with consecutive rats were performed: sham group, I-R 60' group (60-minute ischemia followed by 24-hour reperfusion), and I-R 90' (90-minute ischemia followed by 24 hour reperfusion).

From the thirteen consecutive rats anesthetized with pentobarbital undergoing transient MCA ischemia of 60 minutes, I-R 60' group, 8 rats were included in the analysis. The reasons for exclusion of 5 individuals were: evidence of subarachnoid hemorrhage (2), incomplete reperfusion according to LDF criteria (2), and unexplained mortality at 24-hour reperfusion (1). Table 3.2 details main endpoint results for this group. Overall mortality was 7,7%.

**Table 3.2** *I-R 60' group main endpoint results (n=8)*

| | Mean | SEM | Minimum | Maximum |
|---|---|---|---|---|
| **Neurological grade** | 6,38 | 0.32 | 5 | 8 |
| **Infarct volume ($mm^3$)** | 202,9 | 18,3 | 151,7 | 293,3 |
| **Infarct proportion (%)** | 24,6 | 3,1 | 16,2 | 40,9 |
| **Brain edema (%)** | 8,09 | 1,39 | 2,07 | 12,20 |
| **Initial weight (g)** | 322 | 7,3 | 298 | 350 |
| **Final weight (g)** | 285 | 7,0 | 262 | 312 |
| **Weight loss (%)** | 11,5 | 0,55 | 9,1 | 14,2 |

*SEM,* standard error of the mean.

Ten consecutive rats anesthetized with pentobarbital undergoing transient MCA ischemia of 90 minutes, I-R 90' group, were then performed. Three individuals were excluded due to: mortality at 24 hours (2) and incomplete reperfusion according to LDF criteria (1). Table 3.3 details main endpoint results for I-R 90' group. Overall mortality was 20%.

**Table 3.3** *I-R 90' group main endpoint results (n=7)*

| | Mean | SEM | Minimum | Maximum |
|---|---|---|---|---|
| **Neurological grade** | 7,14 | 0.46 | 5 | 9 |
| **Infarct volume ($mm^3$)** | 216,9 | 10,2 | 181,3 | 245,9 |
| **Infarct proportion (%)** | 27,3 | 1,4 | 22,2 | 31,4 |
| **Brain edema (%)** | 7,52 | 0,82 | 4,90 | 9,92 |
| **Initial weight (g)** | 313 | 7,2 | 282 | 343 |
| **Final weight (g)** | 275 | 7,9 | 244 | 312 |
| **Weight loss (%)** | 12,3 | 0,78 | 9,0 | 15,5 |

*SEM,* standard error of the mean.

A group of three sham rats anesthetized with pentobarbital was also constituted, in which the entire surgical procedure as with I-R was performed except for the filament introduction. No exclusions were necessary. Table 3.4 details main endpoint results for this group. The 3 animals in the sham group presented no evidence of brain infarct and measured edema was insignificant. There was no mortality in this group.

**Table 3.4** *Sham group main endpoint results (n=3)*

| | Mean | SEM | Minimum | Maximum |
|---|---|---|---|---|
| **Neurological grade** | 0,33 | 0,33 | 0 | 1 |
| **Infarct volume ($mm^3$)** | 0 | 0 | 0 | 0 |
| **Infarct proportion (%)** | 0 | 0 | 0 | 0 |
| **Brain edema (%)** | 0,09 | 0,46 | -0,74 | 0,86 |
| **Initial weight (g)** | 301 | 4,0 | 294 | 308 |
| **Final weight (g)** | 269 | 2,9 | 263 | 272 |
| **Weight loss (%)** | 10,7 | 0,70 | 9,6 | 12,0 |

*SEM*, standard error of the mean.

Simple comparisons between the groups were performed to assess the internal validity of the model. Comparison between pre-operative weight, at 24-hour, and percentage of weight loss were made with no differences between groups (Figure 3.7).

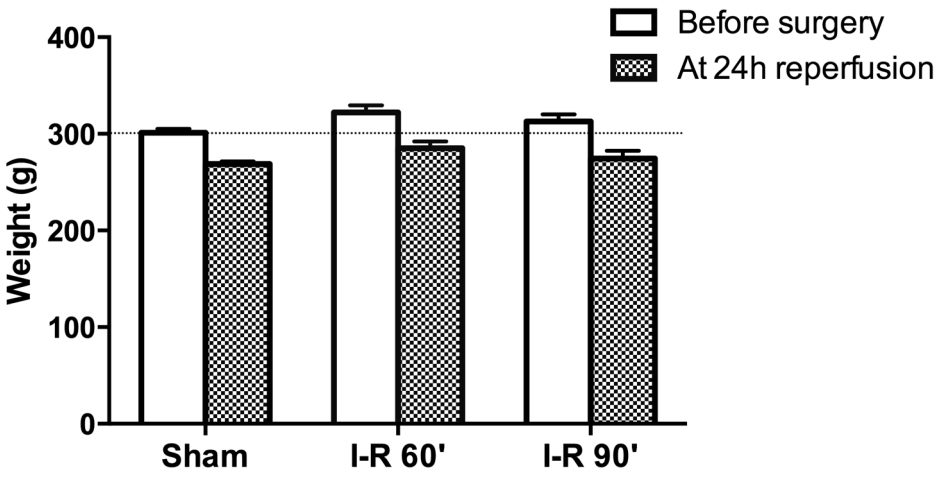


**Figure 3.7** Bar graph comparing the weight before surgery and at 24-hour reperfusion for each group. No significant differences between initial and final weights were found between the three groups. Data represent the mean±SEM, 2-way ANOVA.

Infarct volume was significantly smaller in I-R 60' compared to IR 90' group (24,62±3,08 compared to 27,30±1,35, p=0.044) (Figs. 3.8 and 3.9).

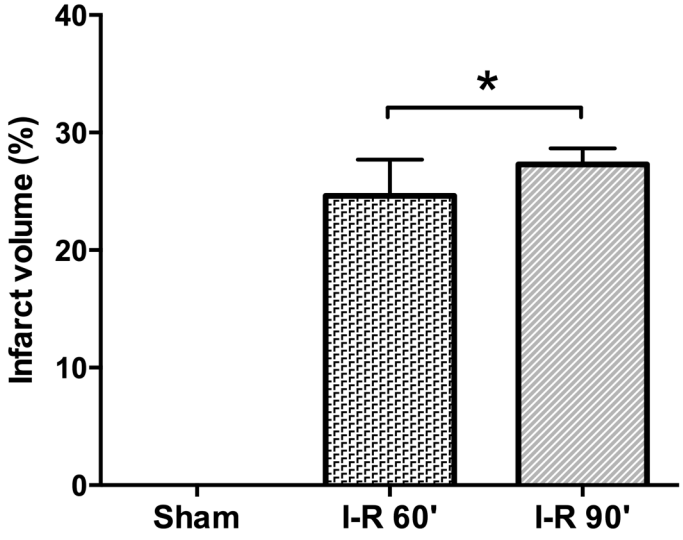


**Figure 3.8** Bar graph comparing total infarct volume between groups. Infarct volumes are presented as percentages of the total contralateral hemisphere volume. Data represent the mean±SEM *$p$<0.05, Student's $t$-test.

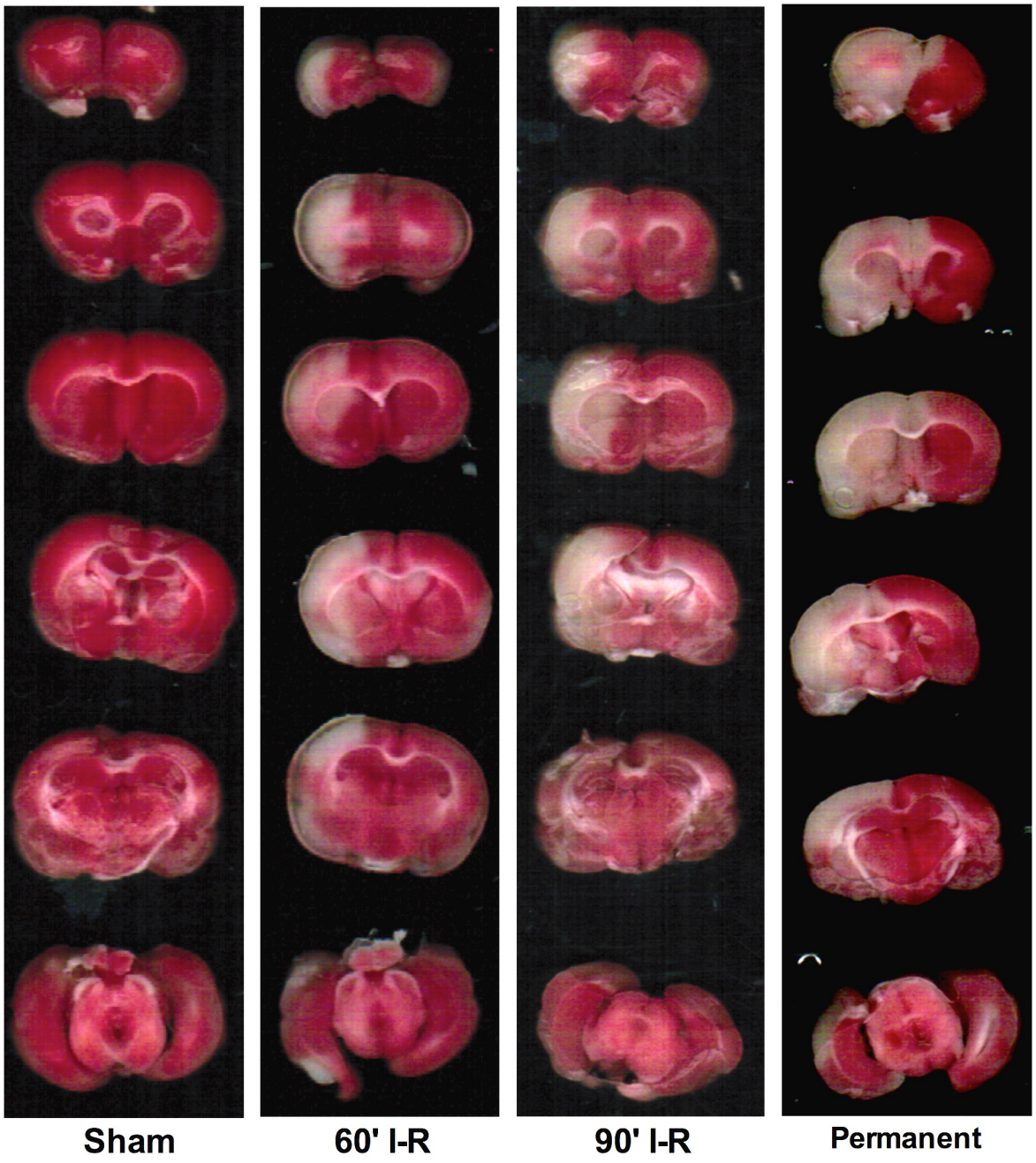


**Figure 3.9** Representative images of TTC-stained coronal brain sections of sham, 60' I-R, 90' I-R and permanent ischemia rats.

Nissl bodies-stained sections were performed in a pilot-study rat brain submitted to MCA I-R of 60 minutes followed by 24-hour reperfusion to compare neuronal population between hemispheres (Figure 3.10).

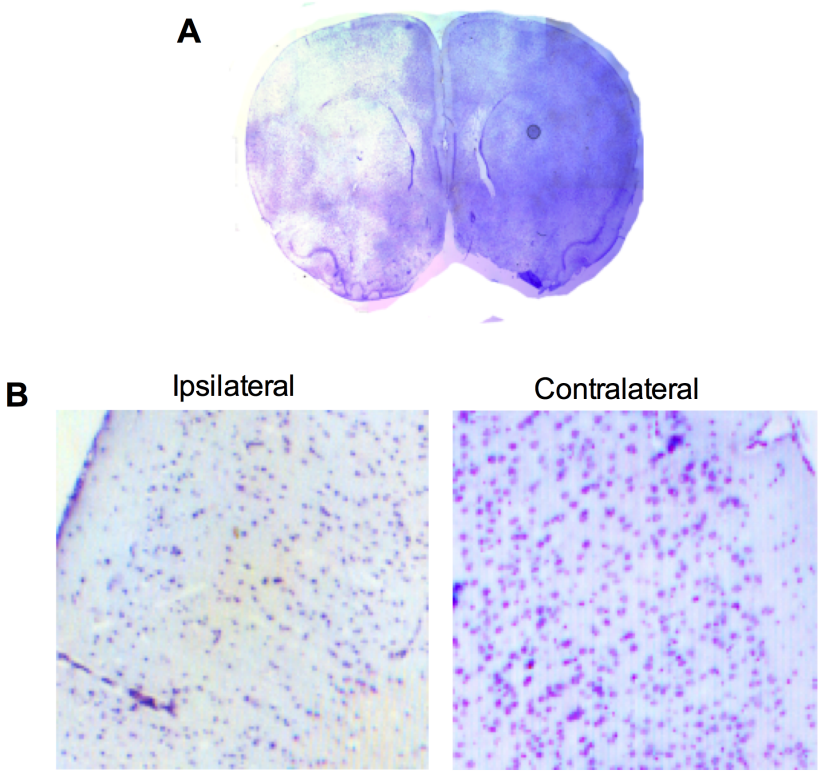


**Figure 3.10.** Photomicrographs Nissl bodies stain brain sections of I-R 60' pilot-study rat. *A*, Whole brain section images. *B*, Cerebrovascular changes in the infarct area of ipsilateral compared to contralateral hemisphere: ipsilateral ischemic area reveals predominance of dead or dying neurons as shown by the lower number of neurons and their picnotic nucleus.

Hemispheric edema was non-significant between ischemic groups (8,09±1,39 in I-R 60' group compared to 7,52±0,82 I-R 90' group) (Figure 3.11).

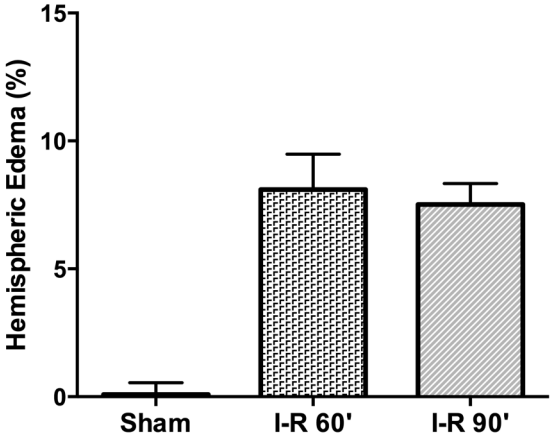


**Figure 3.11** Bar graph depicting the percentage of hemispheric edema for each group. No significant differences were found between I-R 60' and I-R 90' groups. Data represent the mean±SEM

Neurologic assessment showed no difference between 60-minute or 90-minute MCA ischemia groups (Figure 3.12).

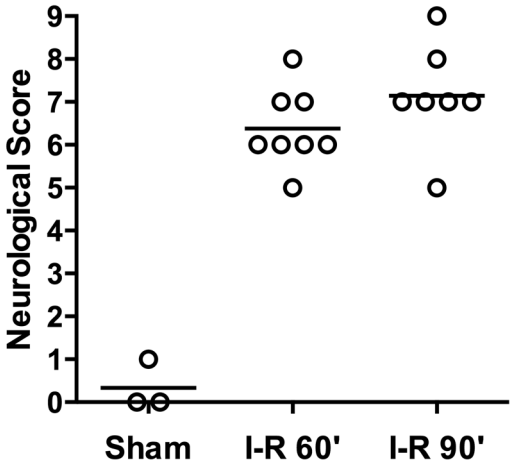


**Figure 3.12** Scatter plot showing the 9-point neurologic score results at 24 hours for each group. Open circles indicate values for individual animals. Horizontal bars indicate group median values. No significant differences were found between two ischemic groups, Mann-Whitney test.

## 3.4 Discussion and Conclusions

There is evidence that not only duration of ischemia influences infarct volume in this animal model, but also the differences in animal strain, size, cerebrovascular anatomy, temperature, anesthesia, duration of reperfusion, and type of suture.

Our protocol for using Wistar rats in a focal cerebral MCA ischemia followed by 24-hour reperfusion was mainly based on two assumptions:

- Wistar rats are preferred by some to Sprague-Dawley due to their higher susceptibility to infarction and reperfusion injury after MCAO[125]. Wistar strain also exhibits better survival rates after transient MCAO[126].
- Reglodi studied the evolution of infarct size at 4, 8, 12, 24, 48, and 72 hours after MCAO and found: infarct size gradually increased; individual response to the ischemic injury was very different during the first 12 hours; infarct volume peaked at 24 hours; and no significant difference could be demonstrated between the infarct sizes after 24, 48, or 72 hours[127].

Several anesthetics have been used. Pentobarbital has been shown to have protective characteristics in cerebral I-R rodent models[128]. Also, volatile anesthetics appear to temporally reduce ischemic cerebral injury during the early stage of reperfusion and, for example, isoflurane was reported to provide protection against transient focal ischemia[129]. During the setting up and establishment of the model we used pentobarbital (60 mg/kg) IP. In the following phase of this research, however, we have changed to a ketamine (80 mg/kg) and xilazine (8 mg/kg) mixture IP which, for legal issues, was initially not available and required the National Authority of Medicines and Health Products' authorization.

Traditionally, intraluminal sutures used to occlude the MCA are prepared by flame-rounding a 3- or 4-0 nylon suture tip. This procedure produce sutures with varying tip diameters and thus, requires several attempts at occlusion before finding a suture that matches the vessel diameter of a given rat. After some discouraging experiments with these flame-rounded filaments, it was decided to use commercially prepared silicon-coated 4-0 nylon filaments (Doccol Corporation, MA, USA) as it raised the success rate by providing better occlusion without increasing SAH.

Clearly, the experience of the researcher is a key factor. For instance, factors such as duration of surgery, adequate dissection and retraction of tissues, sparing blood losses, and perception of resistance to the thread's progress are highly dependent on training and directly related to the outcome. From the beginning, we have persistently searched for measures to reduce heterogeneity of groups: defining inclusion and exclusion criteria (gender, weight, LDF patterns, evidence of SAH), strictly controlling the body temperature, performing a fine step-by-step surgical technique, using a similar filament in all animals and standardizing endpoint evaluations.

Consistency and predictability of results are far more important than absolute values of infarct volume. Nevertheless, the following table is a non-exhaustive results review from several research groups for infarct volumes in adult untreated male Wistar rats evaluated with TTC at 24-hour reperfusion, after transient intraluminal MCA ischemia (Table 3.5).

**Table 3.5** *Previously published infarct volumes at 24-hour reperfusion after intraluminal transient MCAO among untreated rats. Data is presented as mean±SD, unless SEM stated*

| Author | Body weight (g)* | Anesthesia | Suture size | MCAO (min) | Infarct volume# |
|---|---|---|---|---|---|
| **Calloni 2010**[130] | 423±42 | Halotane | 5-0 | 90 | 162.9±110.8 |
| | 439+-46 | | | 120 | 259.3±125.1 |
| **Mouw 2002**[131] | 250-330 | Halotane | 4-0 | 180 | 134.6±108.9 |
| **Alkayed 1998**[132] | 255-360 | Halotane | 4-0 | 120 | 25.7%±6.8%, SEM |
| **Johnson 1998**[133] | 260-310 | Halotane | 3-0 + poly-L-lysine | 180 | 22.8%+-2.8%, SEM |
| **Hayashi 1998**[134] | 250-280 | Pentobarbital | 4-0 + silicone | 90 | 33.2%±4.2% |
| **Present study** | 322±21 | Pentobarbital | 4-0 + silicone | 60 | 202.9±51.8<br>24.6%±3.1%, SEM<br>24.6%±8.7% |
| | 313±19 | | | 90 | 216.8±27.0<br>27.3%±1.4%, SEM<br>27.3%±3.6% |

*SD*, standard deviation; *SEM*, standard error of the mean; *MCAO*, middle cerebral artery occlusion
* mean±SD and/or minimum-maximum, as described by original authors
# mean±SD ($mm^3$) and/or percentage total volume of ipsilateral hemisphere, as described by original authors

Despite difficulty in comparing endpoints between different research groups, as there are different variables to consider, overall, results from the present study, including deviations, are in accordance with the previous ones, that lead us to conclude the establishment of the model was accomplished.

The following figure summarizes the timeline for the acute phase of experiments detailed in next chapters, which included control and treatment groups – rhEPO and TDZD-8 groups (Figure 3.13).

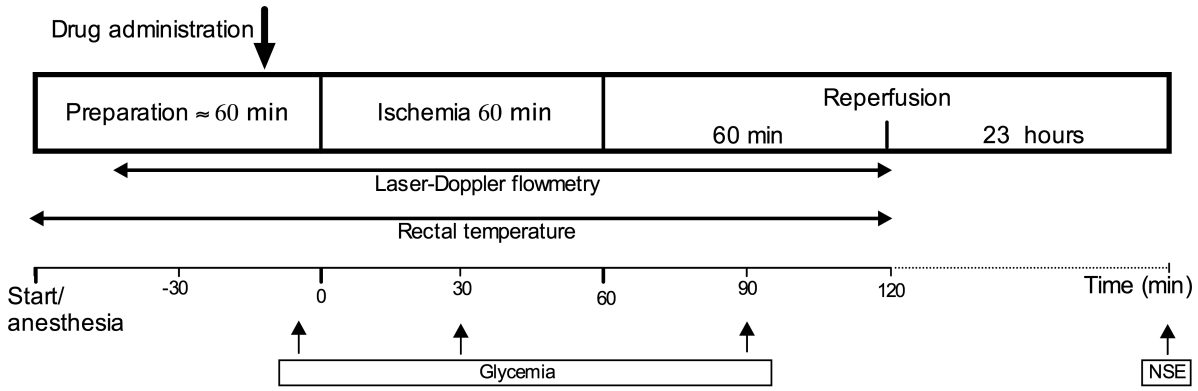


**Figure 3.13.** Study flow diagram of experiments depicting the course of experimental ischemia, timing of drug administration and monitoring. In all drug-treated groups a bolus of the selected drug was administered prior to ischemia. *NSE, neuron specific enolase.*

As shown, drug experiments were planned to comprise a 60-minute period ischemia rather than 90-minute ischemia, since I-R 60' group showed both lower mortality and an adequate amount of infarct volume/hemispheric edema to assess changes with drugs.

Due to timing, technical and financial constraints, some endpoints that were not evaluated during the setting up of the model could, however, be performed during the drug evaluation experiments phase. In accordance with STAIR preclinical recommendations[109,110], these additional endpoints included histological, biomarkers, immunohistochemical, and western blot procedures that will be detailed in corresponding sections.

# 4 NEUROPROTECTIVE EFFECTS OF ERYTHROPOIETIN

## 4.1 Background

Erythropoietin (EPO) is a natural hormone most notably recognized for its central role in erythropoiesis and successfully used for anemia treatment in the last two decades. Fetal liver, and postpartum kidney are the two major sites of synthesis. The finding that EPO and its receptor (EPOR) are expressed throughout the brain in glial cells, neurons, and endothelial cells, suggested that this glycoprotein could have hematopoiesis-independent effects on the nervous system[135,136]. Endogenously produced EPO and/or expression of the EPOR gives rise to autocrine and paracrine signaling in different organs particularly during hypoxia, toxicity and injury conditions. EPO mRNA levels have been shown to remain elevated in the brain for more than 24 hours during the duration of the hypoxic stimuli[137] and following ischemic/hypoxic injury, dramatic changes have been reported in the expression of EPO and its receptor within and around infarcts in human brain regions[138].

EPO is one of the gene products of HIF-1 and an increase in HIF in brain tissue after hypoxia has been demonstrated in several rodent models[84]. EPO binds the EPOR to initiate an auto-phosphorylation of the receptor-associated Janus kinase-2 that leads to phosphorylation/activation of several downstream signal cascades critical to regulate a variety of cell functions such as ionic balance, neurotransmitter synthesis and cell survival[139-141] (Figure 4.1).

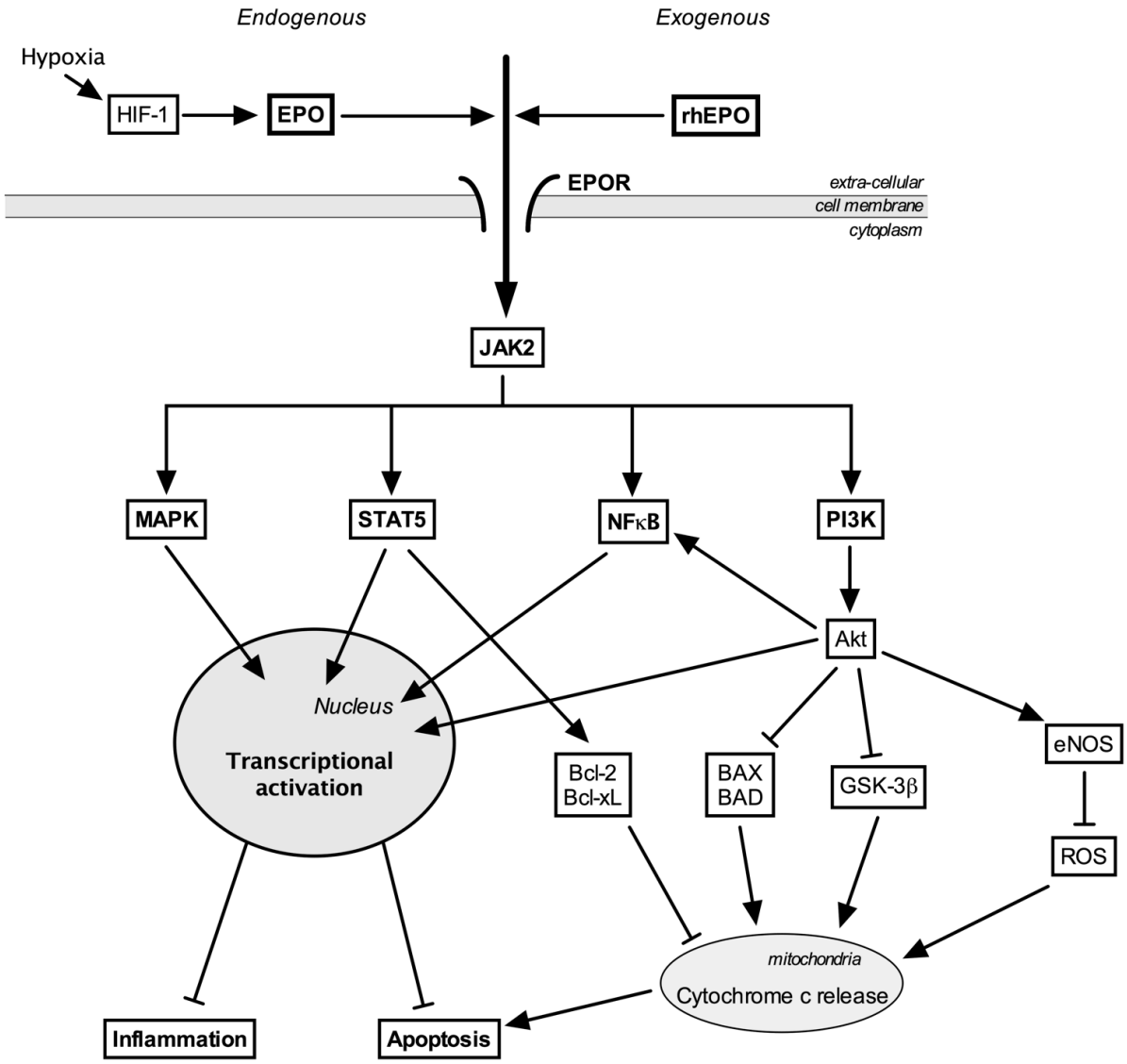


**Figure 4.1.** Neuroprotective signaling pathways employed by EPO. During hypoxia, HIF-1 is activated which induces the transcription of endogenous EPO. Endogenous and exogenous EPO binds the extra-cellular EPOR and JAK2 is phosphorylated leading to several downstream signaling pathways including MAPK, STAT5, NF-κB and the PI3K. Activated MAPK and NF-κB translocate into the nucleus and initiate transcription of genes encoding for proteins involved in the response to stress, including several molecules that regulate apoptosis and inflammation. STAT5 also translocates into the nucleus and triggers transcriptional activation of several genes encoding for anti-apoptotic molecules, such as Bcl-2 and Bcl-xL. Several apoptotic stimuli may trigger cytochrome c release from mitochondria to the cytosol to activate caspase cascade, which commits the cell to the death process. PI3K activation leads to Akt phosphorylation which inhibits GSK-3β and subsequent mitochondrial apoptotic initiator caspase-9 expression. Furthermore, phosphorylated-Akt also translocates into nucleus and induces cell survival genes transcription, activates

NF-κB and inhibits pro-apoptotic molecules such as BAX and BAD. Binding of EPO to its receptor on the endothelial cells leads to activation of PI3K/Akt pathway, causing activation of eNOS, which decreases ROS and an increase in NO production resulting in cerebral vasodilatation. Lines with arrows indicate activation and lines with flattened ends represent inhibitory effects. *Akt*, protein kinase B; *BAD*, Bcl-2-associated death promoter; *BAX*, Bcl-2-associated X protein; *Bcl-2*, B-cell lymphoma 2; eNOS, endothelial nitric oxide synthase; *EPO*, Erythropoietin; *EPOR*, erythropoietin receptor; *GSK-3β*, glycogen synthase kinase-3β; *HIF-1*, Hypoxia-inducible factor-1; *JAK2*, Janus-tyrosine kinase 2; *MAPK*, mitogen-activated protein kinase; *NF-κB*, nuclear factor-κB; *PI3K*, phosphoinositide 3-kinase; *rhEPO*, recombinant human erythropoietin; *ROS*, reactive oxygen species; *STAT5*, signal transducer and activator of transcription.

Several preclinical studies have shown protective and reparative effects of EPO for neurovascular unit following an I-R injury and that this hormone may work for the response in different timepoints and through indirect effects (Figure 4.2). Moreover, under ischemic conditions, *in vitro* and *in vivo* research has implicated EPO in neurogenesis regulating the production of neuronal progenitors by mammalian forebrain neural stem cells[142].

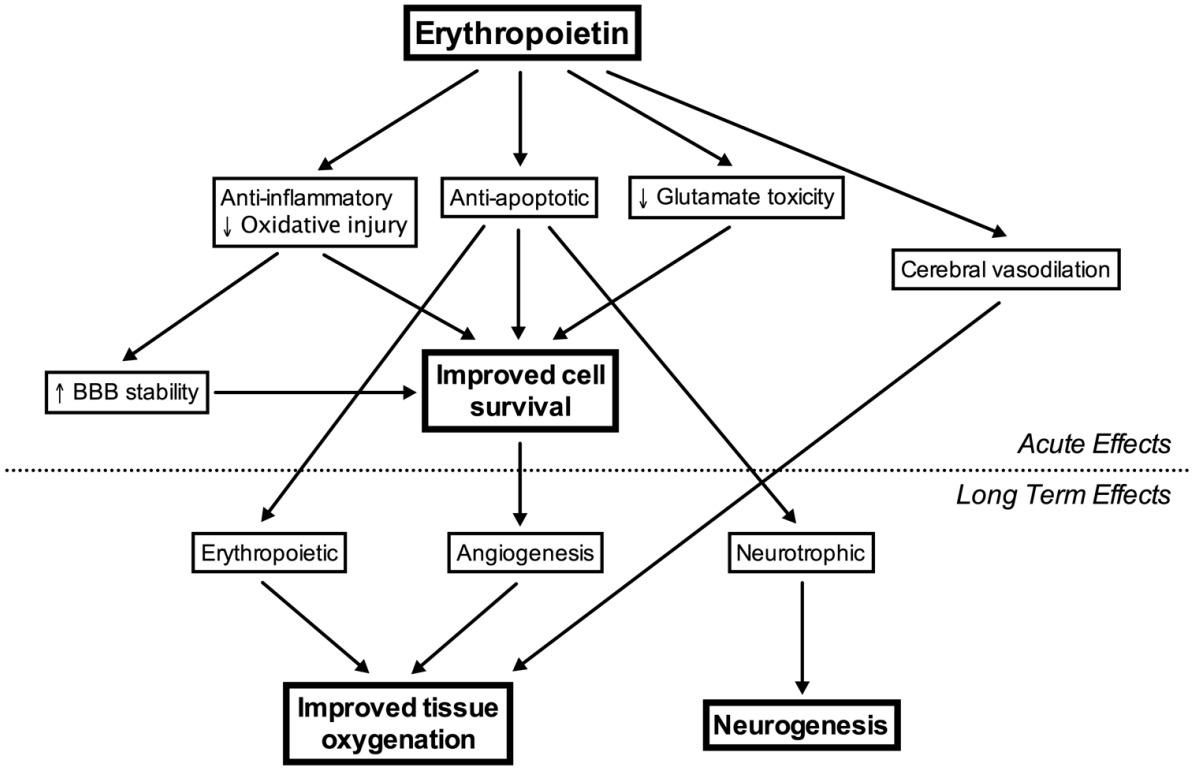


**Figure 4.2.** Schematic representation of possible EPO neuroprotection acute and long term effects. *BBB*, blood-brain barrier.

Preclinical research has also shown that a high-dose of systemically administered rhEPO crosses the BBB, leading to neuroprotective and neurotrophic effects[143-145]. As a result, several trials are currently ongoing to identify possible benefits in the usage of rhEPO for specific clinical situations requiring neuroprotection[146-148]. To our knowledge, we present the first animal study based on a MCA I-R model aiming to investigate the potential benefits of a single dose of 1.000 IU/kg intravenous rhEPO as a possible pretreatment against neuronal damage in neurovascular procedures that require transient cerebral artery occlusion. Research on translational pharmacokinetics showed that rhEPO 1.000 IU/kg per dose IV for neonatal encephalopathy[149] and for extremely low birth weight infants[150] reach drug exposure levels that afford optimal neuroprotection in animal models, and concluded this moderate dose is likely to minimize risks associated with a higher dose. Furthermore, selected dose and route has been used in several clinical trials with no additional safety concerns reported and thus, could be safely translated to the clinical setting[151-153].

## 4.2 Materials and Methods

A total of 28 adult male Wistar rats (240-340 g) housed under diurnal light conditions with unlimited access to food and water were used ($n$=14 per group).

### *4.2.1 Intervention*

Treatment group had rhEPO (epoietin β, F.Hoffmann-La Roche, Basel, Switzerland) administered at a dose of 1000 IU/kg IV in the tail vein, 10 minutes prior to the ischemia onset. Control group had the same volume of saline administered similarly. Allocation concealment was attained by having drug or saline individually prepared and labeled for each animal according to randomization by an independent investigator. The principal investigator, blinded to treatment, carried out all surgical procedures.

### *4.2.2 Middle Cerebral Artery Ischemia-Reperfusion*

Rats were food deprived 12 hours prior to surgery. Anesthesia was induced by IP administration of ketamine (80 mg/kg) and xylazine (8 mg/kg) mixture, supplemented as needed. Anesthetized rats were placed onto a thermostatically controlled heating pad, a rectal probe was inserted, and body temperature was monitored and maintained between 36.5°C and 37.5°C. Cerebral blood flow was monitored by LDF in the supply territory of the right MCA as previously detailed. Transient focal cerebral ischemia was induced by 60-minute right MCA occlusion followed by 24-hour reperfusion, as previously described (Figure 3.2). Briefly, the right CCA, ICA and ECA were exposed under the operating microscope and isolated from branches through a midline neck incision. The ECA was tied and cut at approximately 5 mm from the bifurcation and a loose 6-0 silk knot was placed around the ECA origin. After, microvascular clips were placed on the CCA and ICA, an ECA stump arteriotomy distal to the loose knot was performed and a 4-0 nylon silicone rubber-coated tip monofilament was inserted. The suture around the ECA stump and the intraluminal nylon filament was tightened to prevent bleeding and the clips were removed. The filament was gently introduced (19-21 mm) into the ICA to the level where the MCA branches out, until LDF signal decreased to less than 30% of baseline, occluding the right MCA at its origin at the circle of Willis. After a 60-minute period of ischemia, the thread was cautiously removed reestablishing the blood flow in the MCA. The ECA was permanently ligated at the level of bifurcation. Animals were allowed to recover.

Rats with CBF patterns suggesting subarachnoid hemorrhage, incomplete ischemia (CBF does not decrease to a maximum of 30% of baseline) or incomplete reperfusion (CBF does not recover to over 80% of baseline within 30 minutes of filament withdrawal) were excluded and replaced.

### *4.2.3 Neurological Examination*

At 24-hour into reperfusion, the previously described nine-point neurological scale (0=normal to 9=highest handicap (Table 3.1) was performed in the rats by the principal investigator, who was blinded to the treatment groups. Animals were then euthanized with anesthetic overdose.

### *4.2.4 Infarct Volume and Brain Edema Assessment*

To calculate the minimum sample size for infarct volume continuous variable, the formula $n=1+2C(s/d)^2$ was used[154], where '*s'* is the estimate of the population standard deviation of the variable, '*d*' corresponds to the effect size and 'C' is dependent on values for significance level (α) and power (1-β). Using a conservative approach, with a significance of $p=0.01$, a power of 90% (C=14.88), a SD for the infarct volume estimated from the pilot study of 9% (8.7%; for details, see Table 3.5) and a magnitude of the effect size to detect of 20%, a minimum of 8 rats per group ($n=7.03$) would be needed before the final infarct volume assessment.

As detailed in a previous chapter, brains were removed, placed in a brain matrix and sliced in 2-mm thick coronal sections, resulting in 6 slices per animal ($n=8$ per group). The sections were stained in 2% 2,3,5-TTC saline solution for 10 minutes at 37°C in the dark and fixed in 4% paraformaldehyde at 4°C overnight. Sections were scanned and analyzed using ImageJ software version 1.45. Brain infarction was visualized as areas of unstained (white) tissue, which contrasted from brick red stained areas of viable tissue. Summing the infarct area of each coronal slice and multiplying that number by the thickness of the sections allowed the calculation of the total infarct volume. Right and left hemispheric volumes were calculated similarly. The amount of infarction was expressed in absolute terms in cubic millimeters and as a percentage of contralateral hemisphere adjusted for brain edema[124]. An index of brain edema was assessed by calculating the percent increase of size of the ipsilateral (injured) hemisphere compared with the contralateral (uninjured) hemisphere. The described analysis was performed blindly to individual treatment by the principal investigator.

### *4.2.5 Determination of Neuron-Specific Enolase (NSE) Plasma Levels*

Blood samples were taken by puncture of the left cardiac ventricle prior to sacrifice. Blood was centrifuged at 10.000 rpm for 10 minutes and the isolated serum was frozen and stored until time of assay. Plasma NSE measurements were performed with an electrochemiluminescence immunoassay, using a sandwich technique with double monoclonal antibodies directed against NSE (Roche Diagnostics, Mannheim, Germany) and an Elecsys 2010 analyzer (Roche Diagnostics, Mannheim, Germany). Data were normalized to nanograms per mililiter of plasma.

### *4.2.6 Histology and Immunohistochemistry Procedures*

Rat brains were removed, fixed in 4% paraformaldehyde in phosphate buffered saline (PBS) for 72 hours at room temperature, dehydrated through a graded ethanol series and embedded in paraffin (*n*=3 per group). H&E staining was performed as previously described[155] and images were acquired using a brigthfield Axioscop microscope (Zeiss, Göttingen, Germany).

For Fluoro-Jade staining, 6 μm thick coronal sections were deparaffinized and rehydrated. Slides were first immersed in 100% alcohol for 3 minutes followed by 1 minute in 70% alcohol and 1 minute in distilled water. The slides were then transferred to a solution of 0.06% potassium permanganate for 15 minutes on a shaker table and protected from light. After, the slides were rinsed in distilled water for 1 minute and immersed in Fluoro-Jade B (Chemicon, CA, USA) staining solution 0.001% for 30 minutes with moderate agitation. Slides were rinsed for one minute in each of three distilled water washes and dried at room temperature. The dry slides were cleared by immersion in xylene for at least a minute before coverslipping with DPX (Fluka, WI, USA, or Sigma-Aldrich, MO, USA). The tissue was then examined using an epifluorescent AxioScope microscope (Zeiss, Göttingen, Germany) with blue (450-490 nm) excitation light. The number of positive Fluoro-Jade B neurons were counted in 4 sections of 0.16 $\mu m^2$ (*n*=3 per group) within the region of interest using ImageJ software version 1.45 and expressed as positive cells/section. A single blinded observer performed the analysis described.

For immunostaining, 6 μm thick coronal sections were submitted to antigen retrieval in 20 mM citrate buffer with 1.5% $H_2O_2$ for 15 minutes at room temperature in the dark, incubated for 10 minutes in Tris/EDTA buffer at 84°C and blocked for 1 hour at room temperature in 1% bovine serum albumin (BSA) in PBS. Primary antibody, rabbit anti-p-Akt (1:100, CellSignaling Technology, MA, USA) was used in 0.5% BSA in PBS overnight at 4°C. After washing in PBS, sections were incubated for 1 hour at room temperature with antibodies anti-rabbit coupled to AlexaFluor 568 (#A11077, 1:1000, Invitrogen, CA, USA) in 0.5% BSA in PBS, incubated for 20 minutes in 4,6-diamidino-2-phenylindole (DAPI) and mounted with Shandon Immu-Mount™ Aqueous Non-fluorescing Mounting Medium (Thermo Scientific, IL, USA). Tissue sections were visualized with an epifluorescent AxioScope microscope (Zeiss, Göttingen, Germany) and the number of total nuclei (DAPI staining) and the ones positive for p-Akt were counted to present the results as percentage of p-Akt-positive nuclei

(2 sections within the region of interest, *n*=3 per group). A single blinded observer performed the analysis described.

### *4.2.7 Western Blot Analysis*

For western blot analysis (N=3 per group), frozen tissue samples cells were lysed in a radioimmunoprecipitation assay (RIPA) buffer containing Tris 50 mM (pH 8.0), 5 mM EDTA (pH 8.0), 150 mM NaCl, 1% NP-40, 10% glycerol and 0.1% sodium dodecyl sulfate, and sonicated for 20 seconds. The lysate was centrifuged at 14.000 g for 10 minutes at 4ºC and the supernatants were collected and stored at -80ºC. Protein concentrations were determined using Nanodrop ND-1000. Cell extracts containing equal amounts of protein (100-150 µg) were separated on sodium dodecyl sulphate-polyacrylamide gel electrophoresis and transferred to a nitrocellulose membrane. The membranes were blocked with 5% non-fat milk, incubated with the primary antibody overnight at 4ºC (anti-rabbit p-Akt [1:1000, #12178, Cell Signaling, MA, USA] and anti-rabbit Akt [1:1000, #4691, Cell Signaling, MA, USA]), and then with a horseradish peroxidase-labeled secondary antibody for 1 hour at room temperature. After extensive washes, immunoreactive bands were detected by LumiGLO® (Cell Signaling, MA, USA) and visualized by autoradiography with Hyperfilm ECL. Phosphorylation levels of Akt were analyzed by the ratio of p-Akt to total Akt levels and expressed as fold change compared to contralateral MCAO hemisphere.

### *4.2.8 Statistical Analysis*

Statistical analysis was performed using GraphPad Prism software version 6.0. Parametric data were analyzed using Student's *t*-test for single comparisons between groups and non-parametric data (neurologic scores) were subjected to the two-tailed Mann-Whitney test. Data are presented as mean±SEM for *n* observations, where *n* represents the number of animals studied. For histological scoring and western blot analysis, each data point represents analyses of brain sections taken from 3 individual rats. A *p* value of less than or equal to 0.05 was the threshold considered for a statistically significant difference or association.

## 4.3 Results

All animals lost between 10 to 18% of body weight during the 24-hour recovery period with no significant differences between groups. Normothermia was maintained in all animals. There were no significant differences between groups with respect to CBF pattern and glycemia values during the procedure.

Results showed no difference between groups in the infarct volume. The total brain infarct volume was 265,46±13,88 $mm^3$ for the control group and 223,33±12,97 $mm^3$ for the treatment group. Expressed as a percentage[124], infarct volume was 28,02±1,73% in the control group and 25,71±1,41% in the rhEPO group (Figure 4.3).

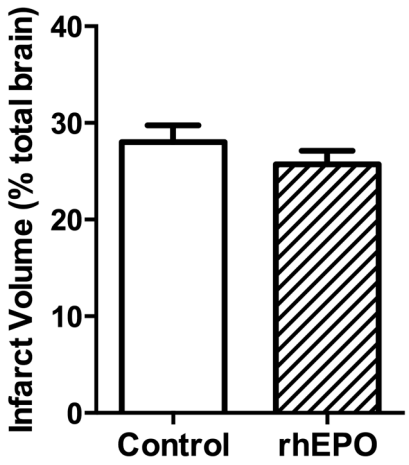


**Figure 4.3.** Bar graph comparing total infarct volume between control and rhEPO-treated groups. Infarct volumes are presented as percentages of the contralateral hemisphere. Data represent the mean±SEM (*n*=8 per group). Differences between groups were not significant (*p*=0,32).

Also, the number of positive Fluoro-Jade degenerating neurons in the interest area was similar between groups (Figure 4.4).

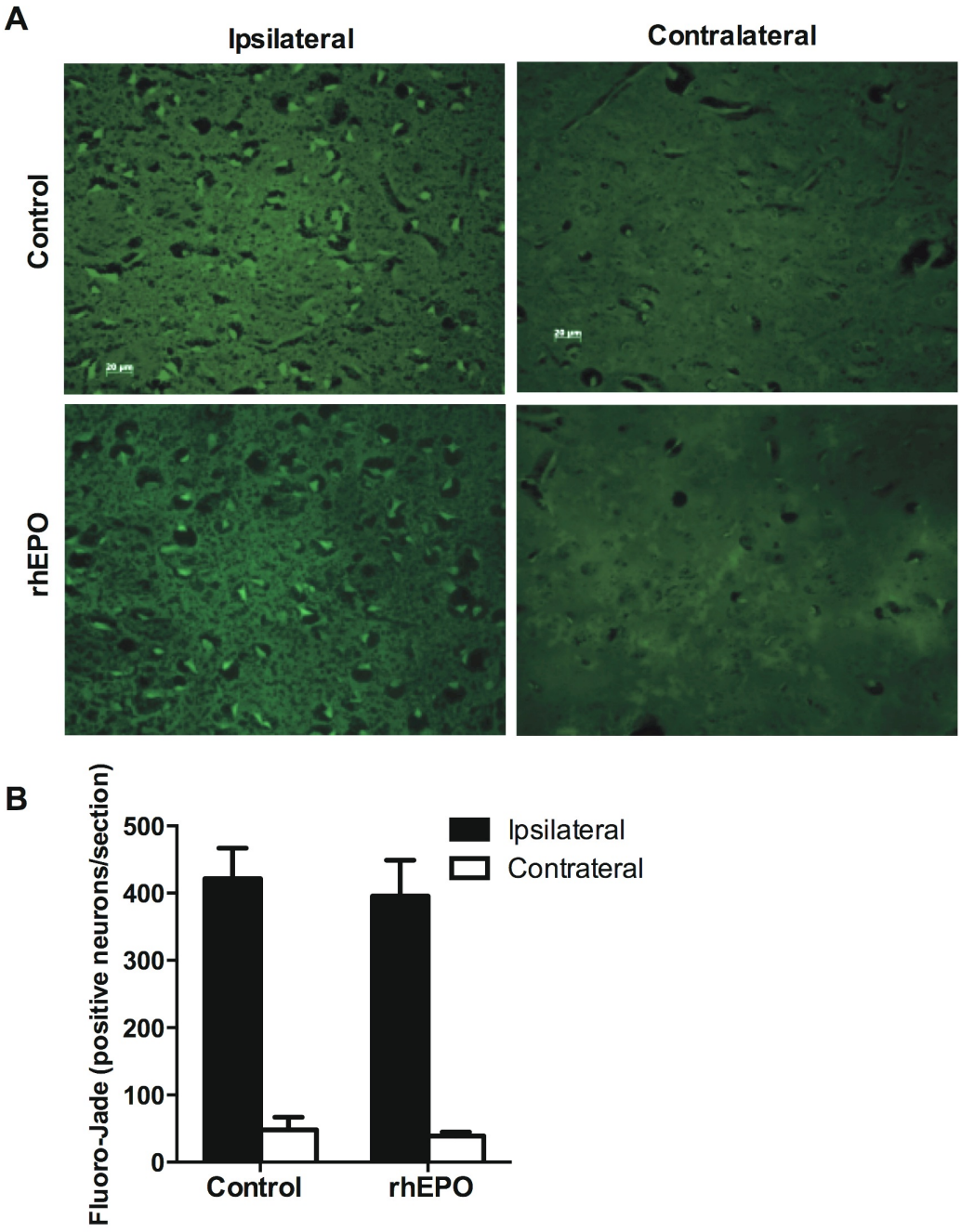


**Figure 4.4.** Comparison of degenerating neurons in both control and rhEPO-treated groups. *A*, Representative images of brain section stained for degenerating neurons using Fluoro-Jade, including both injured and contralateral hemispheres. Scale bar equals 20 μm. *B*, Bar graph comparing the number of positive Fluoro-Jade staining neurons per 0.16 $\mu m^2$ in 4 sections for each rat of the interest area. Data represents the mean±SEM (4 sections for each individual, *n*=3 per group). Values were non-significant.

Brain swelling index was significantly decreased in treatment group when compared to control group (2,11±0,46% and 9,74±1,39%, respectively, $p<0.001$) (Figure 4.5).

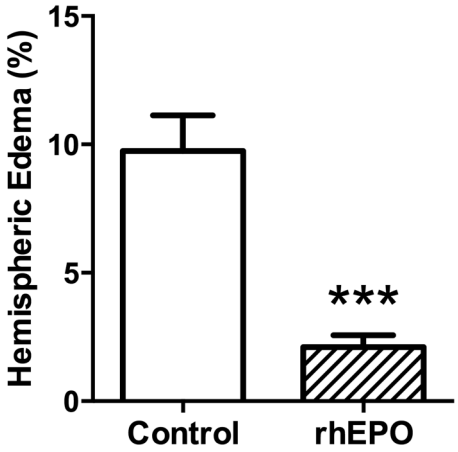


**Figure 4.5.** Bar graph depicting the percentage of hemispheric edema in both control and rhEPO-treated groups. Data represent the mean±SEM ($n$=8 per group). Values were significant, representing a 78% reduction of ipsilateral hemispheric edema in treatment group compared with control group. ***$p<0.001$.

Accordingly, H&E histological analysis of the brain parenchyma revealed neuropil spongiosis and perivascular edema, which was less marked in rhEPO-treated group (Figure 4.6).

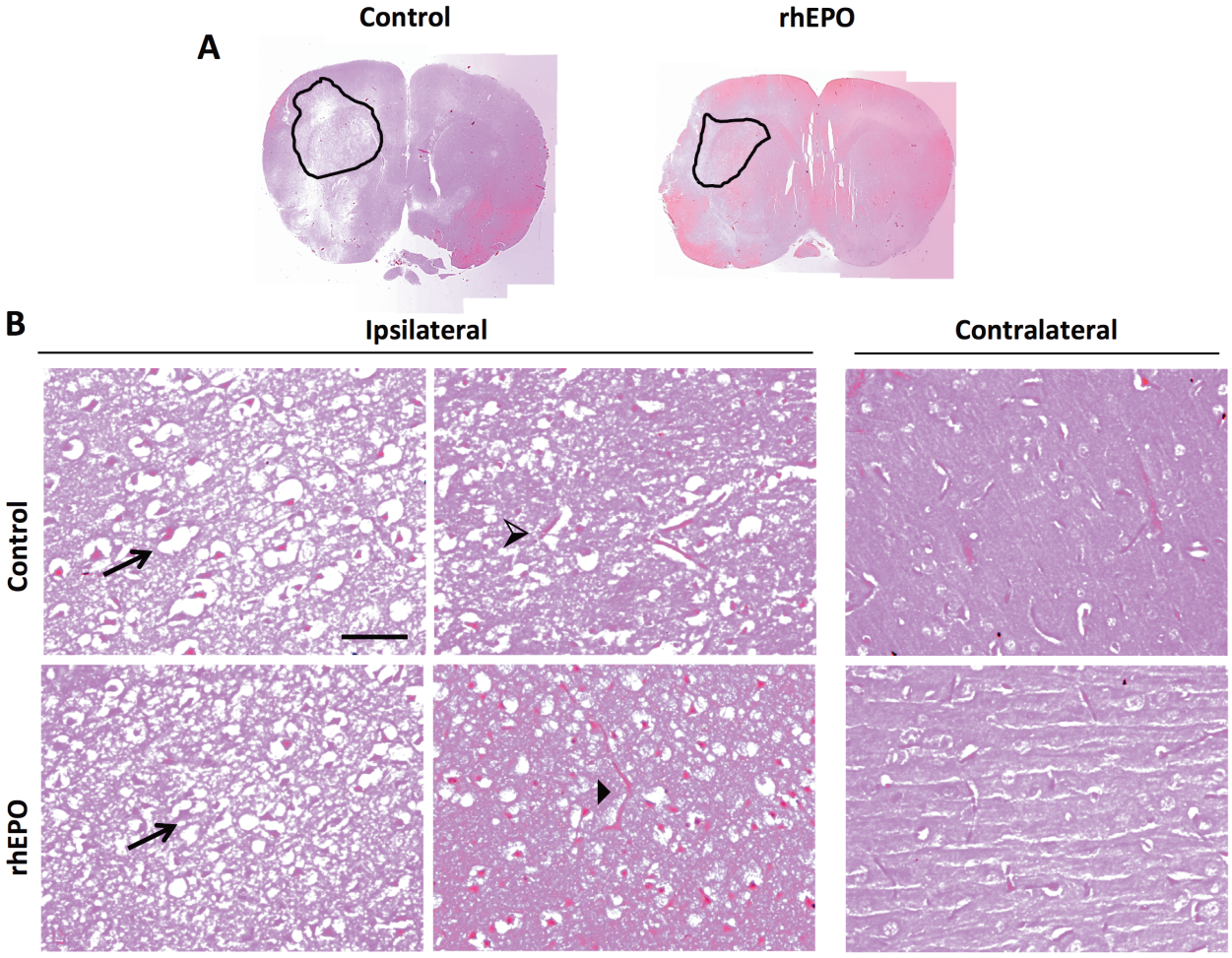


**Figure 4.6.** Representative photomicrographs H&E brain sections of control and rhEPO-treated rats. *A*, Whole brain section images with delineated infarct area. *B*, Cerebrovascular changes in the infarct area: neuropil spongiosis (arrows) and perivascular edema (➢) in control animals or its absence in rhEPO-treated ones (▸). Contralateral hemispheres had no relevant changes. Scale bar equals 200 μm.

Treatment group had significantly lower NSE plasma levels compared with control group (1,17±0,07 ng/ml compared to 1,88±0,07 ng/ml respectively, $p<0.001$) (Figure 4.7), a relevant parameter for assessing the prognosis of cerebral hypoxia-ischemia, and presented significantly less neurological deficits (median value of 7,5 point in the neurological score compared to 5 point respectively, $p<0.001$) (Figure 4.8).

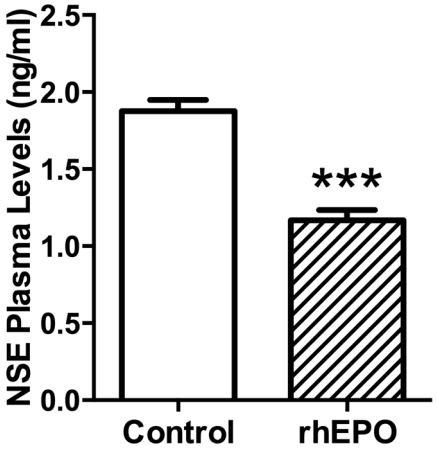


**Figure 4.7.** Bar graph showing a 38% reduction of NSE plasma levels at 24 hours of reperfusion in the rhEPO-treated group. Data represent the mean±SEM (*n*=8 for control and *n*=13 for treatment group). ****p*<0.001.

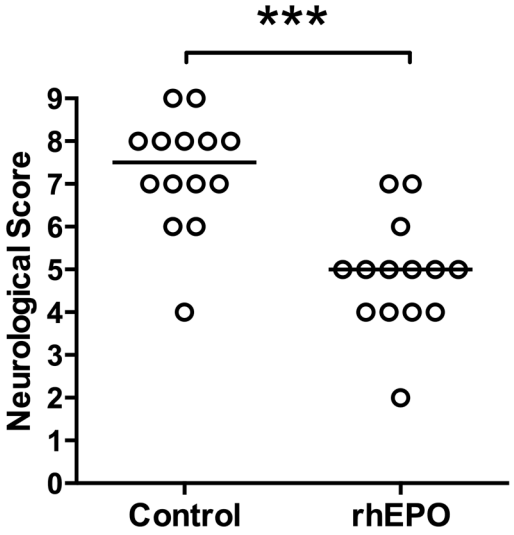


**Figure 4.8.** Scatter plot showing the effects of rhEPO at 24 hours on a 9-point neurologic score (*n*=14 per group). *Open circles* indicate values for individual animals. *Horizontal bars* indicate group median values. RhEPO significantly reduced neurologic deficits. ****p*<0.001, Mann-Whitney test.

Although it is believed that EPO activate/phosphorylate Akt, no differences between groups for p-Akt/Akt ratio in western blot and for percentage of p-Akt-positive nuclei in immunohistochemistry were found (Figs. 4.9 and 4.10).

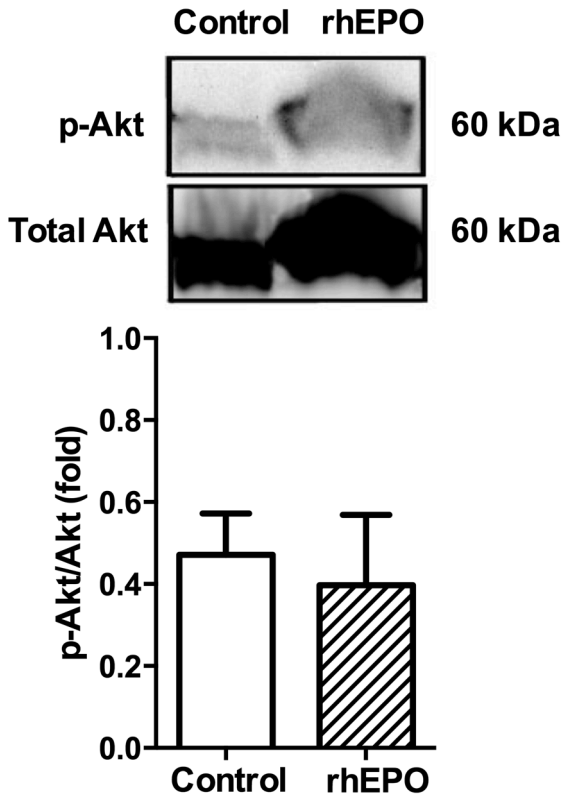


**Figure 4.9.** Western Blot showing expression of p-Akt and total Akt with a bar graph displaying the densitometric analysis of the relative intensity of p-Akt, normalized against total Akt. Data represent the mean±SEM (*n*=3 per group). Results did not show differences between groups.

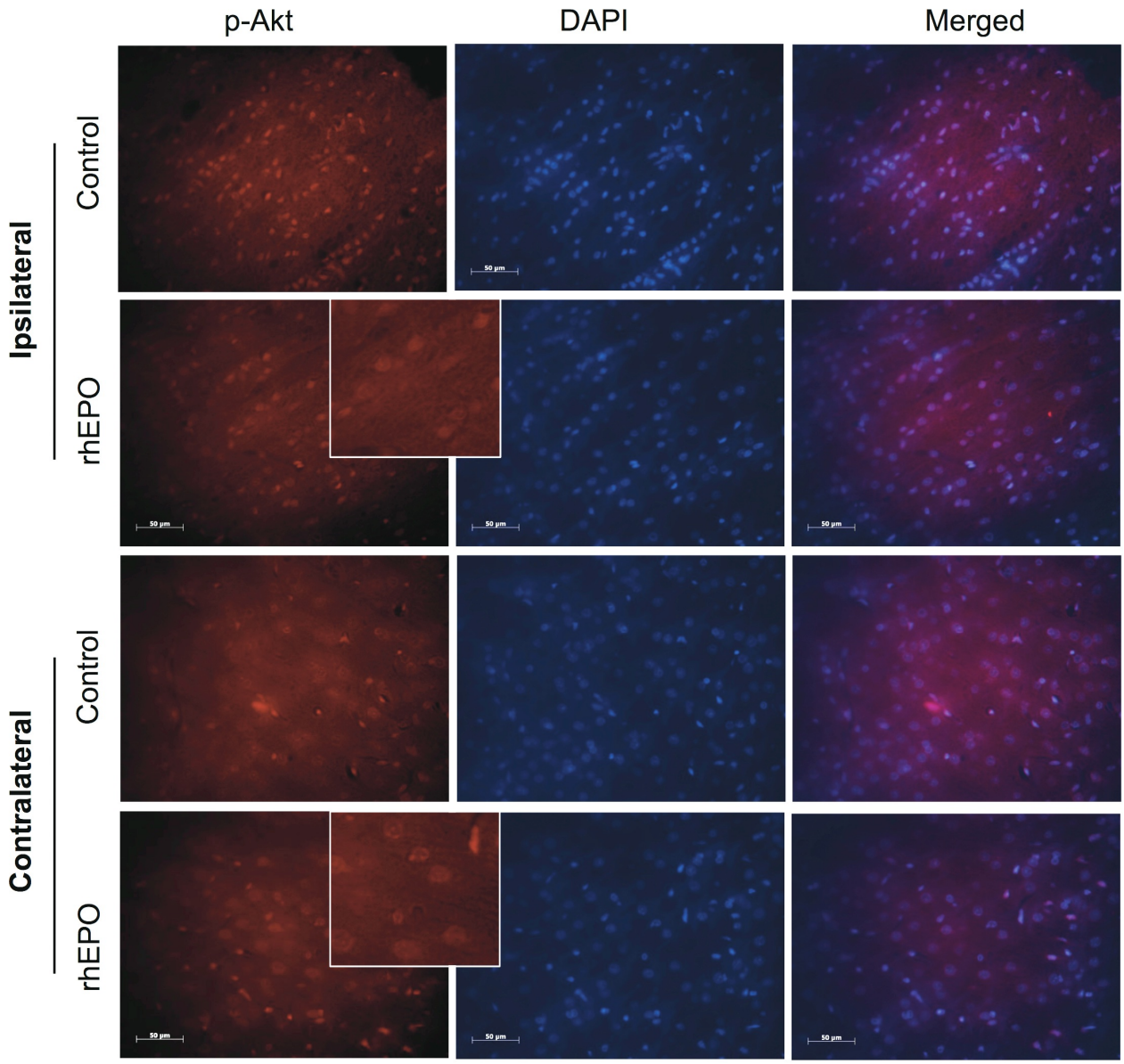


**Figure 4.10.** Akt phosphorylation in control and rhEPO-treated groups. Representative images of the infarct area of the I-R injured and contralateral hemispheres after double staining for p-Akt and nuclear DAPI. Insert shows p-Akt zoom-in images. Merged images are also presented. Scale bar equals 50 μm.

## 4.4 Discussion and Conclusions

Our study reveals that rhEPO exerts protective effects in focal cerebral I-R. This is in line with rhEPO tissue protective effects described in several I-R injury animal models, as demonstrated by our research group[156,157]. RhEPO has been consistently tested at high doses (>5.000 IU/kg) in permanent cerebral artery occlusion rodent models and shown to be more effective when administered within 6 hours after stroke onset[158]. We investigated the effects of a single moderate dose of rhEPO as a pretreatment (1.000 IU/kg) in an I-R rodent model. This dose has been safely tested in humans[151-153]. Our results suggest that a single 1.000 IU/kg rhEPO IV administration just prior to a transitory occlusion of a cerebral artery may decrease secondary brain insult, resulting in a better neurological outcome.

Regarding infarct volume outcome, we found no differences between groups at 24-hour reperfusion, although the improved neurological status and significantly lower NSE plasma levels observed at that point could indicate that this outcome may change in time between groups. NSE is an enzyme rapidly released by injured neurons. Lower NSE plasma levels in the treatment group may suggest a smaller penumbra area and a better clinical outcome. Plasma levels reach their maximum at 24 hours, and the best correlation between infarct size and plasma levels occurs at Day 3[159]. Plasma levels of this kinase have been found to be increased even before the onset of clinical symptoms and are strongly correlated with the clinical score and histological damage when clinical symptoms are present[159]. NSE plasma levels probably reflect neuronal cell death, suggesting that NSE is a reliable marker to follow neuronal damage[160].

Since its first description, Akt kinase has been gaining recognition as a key contributor to the cellular survival after neuronal injury[161,162]. There is evidence that EPO treatment activates this anti-apoptotic molecule[163,164]. Upon phosphorylation, the serine-threonine kinase Akt promotes cell survival by inactivating several targets, including GSK-3β, Bcl-2-associated death promoter (BAD) protein, Bcl-2-associated X protein (BAX) protein and caspase 9, or activates prosurvival molecules, suggesting that phosphoinositide 3-kinase (PI3K)/Akt/GSK-3β pathway is involved in the neuroprotective effect of rhEPO[163]. Akt phosphorylation is coupled to its nuclear translocation where it phosphorylates nuclear targets, suppressing the

transcription of death genes[165]. Unexpectedly, our results did not show an increase in the expression of p-Akt/Akt (western blot) or a p-Akt nuclear translocation (immunohistochemistry). The lack of PI3K/Akt/GSK-3β pathway activation could be explained by the use of lower rhEPO doses in our study when compared to previous ones. In fact, only up to 1% of systemically administered rhEPO crosses the BBB in primates[145] and small penetration into the BBB is expected even when administering up to 10.000 IU/kg IV at single doses[166]. This poor crossing ratio suggests that high doses of systemically administered rhEPO are needed for direct neuron protective purposes. On the other hand, it has been demonstrated that EPO significantly provides neuroprotection following traumatic brain injury in EPOR-null mice, that is, even in the absence of erythropoietin receptor in the neural cells, probably mediated through vascular protection[167]. We postulate that the benefits observed in prophylactic rhEPO administration were not due to a direct neuronal action in the infarct area but the result of an indirect effect in brain swelling as a consequence of diminished BBB disruption. This is also in line with the histological findings and lack of difference between treatment and control groups on the number of positive Fluoro-Jade cells that labels degenerating neurons.

Cerebral edema is a well-recognized factor for high morbidity and mortality in large territory ischemic strokes[168]. Brain edema following MCAO has been shown to gradually increase over the first 48 hours before peaking[169]. The reduction in brain edema from the early phase may reduce space-occupying effect and improve regional CBF in the penumbra phase of stroke. Here we suggest that rhEPO pretreatment is associated with reduced perivascular edema and a protection of the BBB from increased permeability. These effects are probably due to the activation of an EPOR-dependent intracellular pathway of the microvascular endothelium, which may inhibit transcription factor NF-κB, upregulate expression of tight junction proteins and improve abnormalities in the free radical system[170,171]. Reperfusion phase leads to generation of reactive oxygen radicals and lipid peroxidation that are highly noxious to brain capillary endothelial cells and its complex tight junctions, which are mostly responsible for the integrity of BBB[172]. EPO has been shown to increase NO synthesis in endothelial cells and, under oxidative stress conditions, NO may scavenge ROS[173,174]. This detoxification also prevents membrane lipid peroxidation and consequential additional disruption of BBB in I-R[170]. NF-κB transcriptional activation pathway has been considered a central regulator of

inflammatory response, critical to the regulation of apoptosis, and related to cell adhesion molecule expression in endothelial cells[175]. Liu[170] suggested the relation between the downregulation of NF-κB with the reversed expression of the tight junction associated proteins to be involved in the mechanism of protection of the BBB in I-R rats. We recognize some limitations on our study. We speculate rhEPO promotes BBB integrity but we did not show direct evidence or quantify BBB permeability changes. Also, it would be interesting to perform time course experiments, in particular because long-term effects were not evaluated. These dynamics would be of both experimental and clinical relevance.

EPO has been extensively studied in experimental cerebral ischemia, in which population target were mainly patients who have suffered from stroke[176]. Accordingly, the majority of work performed focuses on the potential effects of rhEPO after the induction of ischemia and/or used permanent cerebral artery occlusion models. Surprisingly, when reviewing the literature, only one unpublished study, presented as a poster, evaluated the use of EPO administered before induction of transient focal cerebral ischemia[177]. Data available from this trial is very scarce. In here, EPO was administered at a 5.000 IU/Kg dose 2 hours before transient MCAO. The results were compared to a saline administered group and authors concluded that although EPO did not reduce infarct size at 48 hours, it did improve infarct volume 7 days following reperfusion onset, suggesting a neurorestorative action of EPO. The technique performed for MCAO and timing of drug administration was not provided. Furthermore, the majority of studies usually administer extremely high doses of EPO, over 5.000 IU/kg, which limits its clinical importance.

Non-erythropoietic tissue-protective EPO variants have been developed, most notably asialo-EPO (AEPO), nasal formulations of low-sialic acid EPO (NeuroEPO), and carbamylated EPO (CEPO) in order to dissociate the erythropoietic effect from the tissue protective effect, and thus lessen side effects[178]. However, rhEPO possesses not only neuron antiapoptotic properties but also reduces BBB leakage, enhances blood flow, and promotes angiogenesis after brain injury. It is likely that these non-neuronal effects are not shared by EPO derivatives as part of EPO's rescue effects after systemic intravenous delivery in patients. Moreover, the clinical safety profile is still under investigation in clinical trials and further research is needed before EPO's variants could be used in patients[140].

We present first evidence that rhEPO pretreatment at a dose of 1.000 IU/Kg, which has a well-described safety profile in humans, reduces brain edema and preserves the penumbra functional neuronal pool following *in vivo* I-R-injury. Considering that a substantial proportion of the ischemic lesion could be attributed to mechanical compression induced by brain swelling, the development of effective drugs in attenuating the formation and progression of brain edema is crucial. Since rhEPO has a higher innate capacity to cross the BBB in humans than in rodents[179] and given the cerebroprotective effects observed in the present study, we believe that clinically available rhEPO could be a potential therapy to prevent neuronal injury induced by transient ischemia during neurovascular procedures. Further preclinical research is needed to completely understand the underlying mechanisms of rhEPO and BBB interactions. However, given the number of animal studies already done on cerebral ischemia where rhEPO works well, our investigation may provide supporting evidence for a translational clinical trial evaluating single bolus pretreatment of 1.000 IU/kg rhEPO in patients undergoing elective transient cerebral artery occlusion during cerebrovascular procedures.

# 5 NEUROPROTECTIVE EFFECTS OF TDZD-8

## 5.1 Background

Glycogen synthase kinase-3, a cytoplasmic serine/threonine protein kinase, was originally described as a component of the metabolic pathway of glycogen metabolism and has been involved in a wide range of cellular functions, including glucose metabolism, cytoskeletal integrity, gene expression, cell division, and apoptosis[180,181]. Several studies have implicated GSK-3 signaling transduction pathway in multiple central nervous system diseases, particularly stroke, traumatic brain injury and neurodegenerative conditions such as Alzheimer's disease, Parkinson's disease and amyotrophic lateral sclerosis[182,183].

GSK-3β, one of the two isoforms of GSK-3, is widespread both in developing and adult mammalian nervous system and its overexpression induces intrinsic apoptotic signaling pathway in neuronal cells following hypoxia/ischemia stimulus[184,185]. GSK-3β is constitutively active in cells, and a wide range of stimuli, including insulin, exerts some of its effects by deactivating it. Therefore, GSK-3β is primarily regulated by inhibition by numerous kinases, such as Akt, through phosphorylation at Ser9. GSK-3β may be, however, regulated by an activation pathway by phosphorylation at Tyr216 as a consequence of a proapoptotic stimulus, such as calcium overload. GSK-3β promotes apoptosis by inhibiting prosurvival transcription factors, such as CREB and heat shock factor-1, and facilitating proapoptotic transcription factors such as p53[186]. Moreover, GSK-3β has been shown to regulate neuroinflammation by modulating several pro-inflammatory mediators and cell autophagy after ischemic brain injury[187-189]. Additionally, there is growing evidence that GSK-3β is implicated in neurodegeneration, in particular in plaque formation and neurofibrillary tangle accumulation in Alzheimer disease[190].

Lithium is the classical example of a nonspecific GSK-3β inhibitor, which is known to inhibit the enzyme in a competitive manner by binding to its magnesium-binding sites, and demonstrated to be protective against several neurological insults, including cerebral ischemia, suggesting that reduction in activity of GSK-3β improves brain cell survival[183]. Furthermore, topical application of insulin-like growth factor-I (IGF-1), also a non-specific

GSK-3β inhibitor, significantly reduced infarct size after cerebral focal I-R in a rat model[191]. As non-selective inhibitors tend to also inhibit other kinases and may prove to be harmful, the acknowledgement of relation between GSK-3β and neuronal apoptosis lead to the development of specific antagonists. Martinez described small heterocyclic thiadiazolidinones (TDZDs) and their structure-activity relationships as the first non-ATP-competitive selective GSK-3β inhibitors[192]. TDZDs are small molecules with favorable absorption, distribution, metabolism, excretion and toxicity properties[193]. TDZD-8 is a BBB permeable compound[193,194] and appears to be one the most effective anti-inflammatory and tissue-protective thiadiazolidinone[190] in conditions such as stroke, spinal cord trauma, kidney injury, arthritis, or colitis[195-199] (Figure 5.1).

Furthermore, phase 2 and phase 3 clinical trials suggest that TDZDs have a favorable safety profile and may become clinically available for the treatment of diabetes or some neurological diseases in the near future[190,200,201].

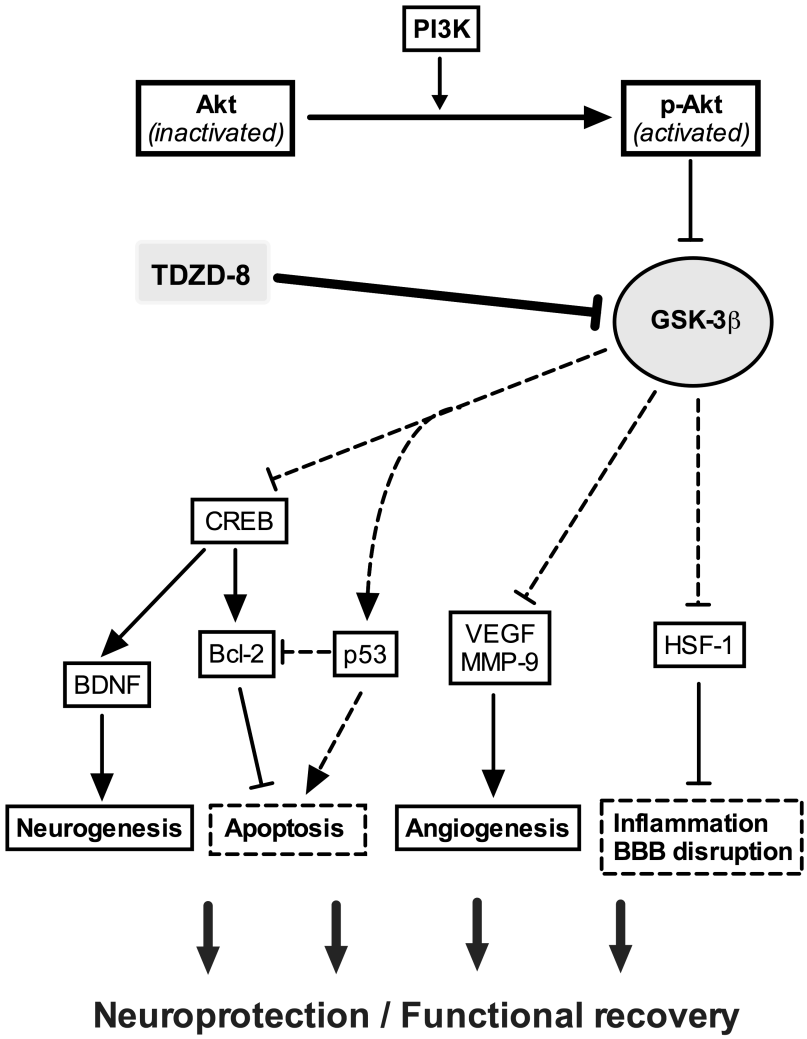


**Figure 5.1.** Proposed TDZD-8's neuroprotective effects against cerebral I-R. The inhibition of GSK-3β leads to disinhibition of several transcription factors such as CREB and HSF-1, and results in induction of major cytoprotective proteins such as BDNF, and the well-known antiapoptotic resident of the mitochondrial outer membrane Bcl-2. A decrease in GSK-3β activity further reduces the activity of pro-apoptotic protein p53 and its downregulating effect on Bcl-2. Counteraction of GSK-3 inhibition of VEGF and MMP-9 may enhance angiogenesis and neurovascular remodeling as medium/long-term effects. Taken together, these effects in reducing apoptosis, decreasing neuroinflammation, maintaining BBB integrity, and promoting both neurogenesis and angiogenesis may contribute to neuroprotection and functional recovery for an I-R insult. Lines with arrows indicate activation and lines with flattened ends represent inhibitory effects. Dashed lines represent pathways with possible reduced activity as a result of TDZD-8 treatment. *BBB*, blood-brain barrier; Bcl-*2*, B-cell lymphoma 2; *BDNF*, brain-derived neurotrophic factor; *CREB*, cAMP response element-binding protein; *GSK-3β*, glycogen synthase kinase-3β; *HSF-1*, heat shock factor-1; *MMP-9*, matrix metallopeptidase 9; *PI3K*, phosphoinositide 3-kinase; *VEGF*, vascular endothelial growth factor.

The aim of this experiment was to investigate the effects of a single dose of TDZD-8 (5 mg/Kg) as a possible pretreatment against neuronal damage in surgical transient cerebral artery occlusion during aneurysmal clipping. TDZD-8 doses were determined in accordance with effective previous studies of the central nervous system[196,202] and with the established therapeutic time window in the clinical setting.

## 5.2 Materials and Methods

A total of 28 adult male Wistar rats (240-340 g) housed under diurnal light conditions with unlimited access to food and water were used (*n*=14 per group).

### *5.2.1 Intervention*

Animals were randomly assigned to two different groups: TDZD-8 (4-benzyl-2-methyl-1,2,4-thiadiazolidine-3,5-dione, Sigma-Aldrich, St. Louis, MO, USA) treatment group in which a dose of 5 mg/kg 10 minutes previous to ischemia onset was administered in the tail vein IV or control group, in which animals administered saline IV. Allocation concealment was attained by having drug or saline individually prepared and labeled for each animal according to randomization by an independent investigator. The principal investigator, blinded to treatment, carried out all surgical procedures.

### *5.2.2 Surgical Procedure and Outcomes Assessment*

The surgical MCA I-R technique and outcomes assessment methodology at 24-hour (neurological examination, quantification of infarct volume and brain edema, determination of NSE plasma levels, evaluation of brain tissue by histology, immunohistochemistry and western blot techniques) were performed as detailed in the previous chapter (for details, see Chapter 4 Section 2).

## 5.3 Results

All animals lost between 10 to 18% of body weight during the 24-hour recovery period with no significant differences between groups. Normothermia was maintained in all animals. There were no significant differences between groups with respect to CBF pattern and glycemia values during the procedure.

Prophylactic administration of TDZD-8 resulted in significant differences between groups for most outcomes and endpoints evaluated. Infarct volume had a 48% reduction in treatment group when compared with control group (from 28,02±1,73% to 14,70±1,12%) (Figure 5.2).

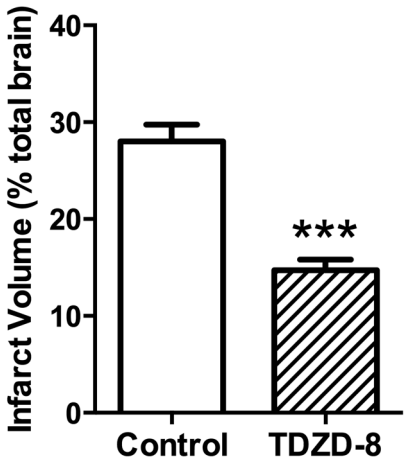


**Figure 5.2.** Bar graph comparing total infarct volume between groups. The whole brain infarct volume was 265,46±13,88 $mm^3$ for control group and 125,99±11,26 $mm^3$ for treatment group. Infarct volumes are presented as percentages of the total contralateral hemisphere. Data represent the mean±SEM (*n*=8 for each group). ****p*<0.001.

Treatment group had a 59% decrease in the ipsilateral hemispheric edema (9,74±1,39% compared to 3,99±0,56%) (Figure 5.3).

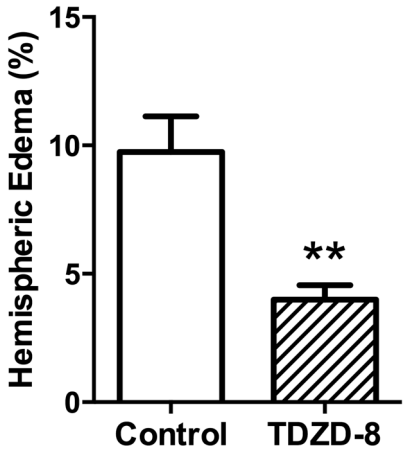


**Figure 5.3.** Bar graph comparing percentage of hemispheric edema between groups. Data represent the mean±SEM (*n*=8 per group). ***p*<0.001.

TDZD-8 administration prevented the rise of NSE plasma levels (0,20±0,06 ng/ml in treatment group compared to 1,88±0,07 ng/ml in control group) (Figure 5.4).

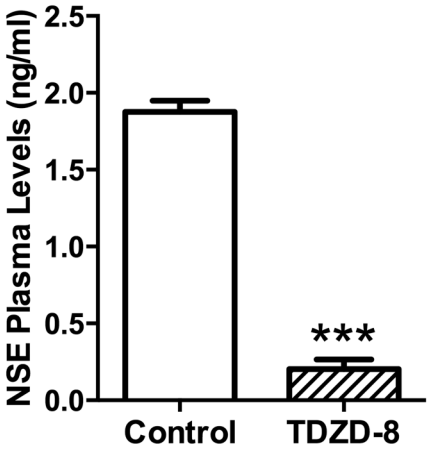


**Figure 5.4.** Bar graph showing NSE plasma levels at 24 hours of reperfusion in both control and treatment groups. Data represent the mean±SEM (*n*=8 for control group and *n*=13 for treatment group). ****p*<0.001.

Rats treated with TDZD-8 presented significantly less neurological deficits compared to the control group (Figure 5.5).

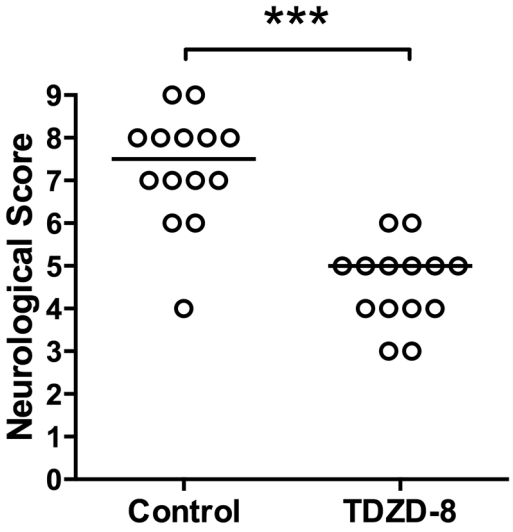


**Figure 5.5.** Scatter plot showing the effects of TDZD-8 at 24 hours on a 9-point neurologic score (*n*=14 per group). Open circles indicate values for individual animals. Horizontal bars indicate group median values. TDZD-8 significantly reduced neurologic deficits. ***$p<0.001$, Mann-Whitney test.

H&E staining neuropathological examination performed in the ischemic area showed less neuropil spongiosis and no perivascular edema on TDZD-8-treated group (Figure 5.6).

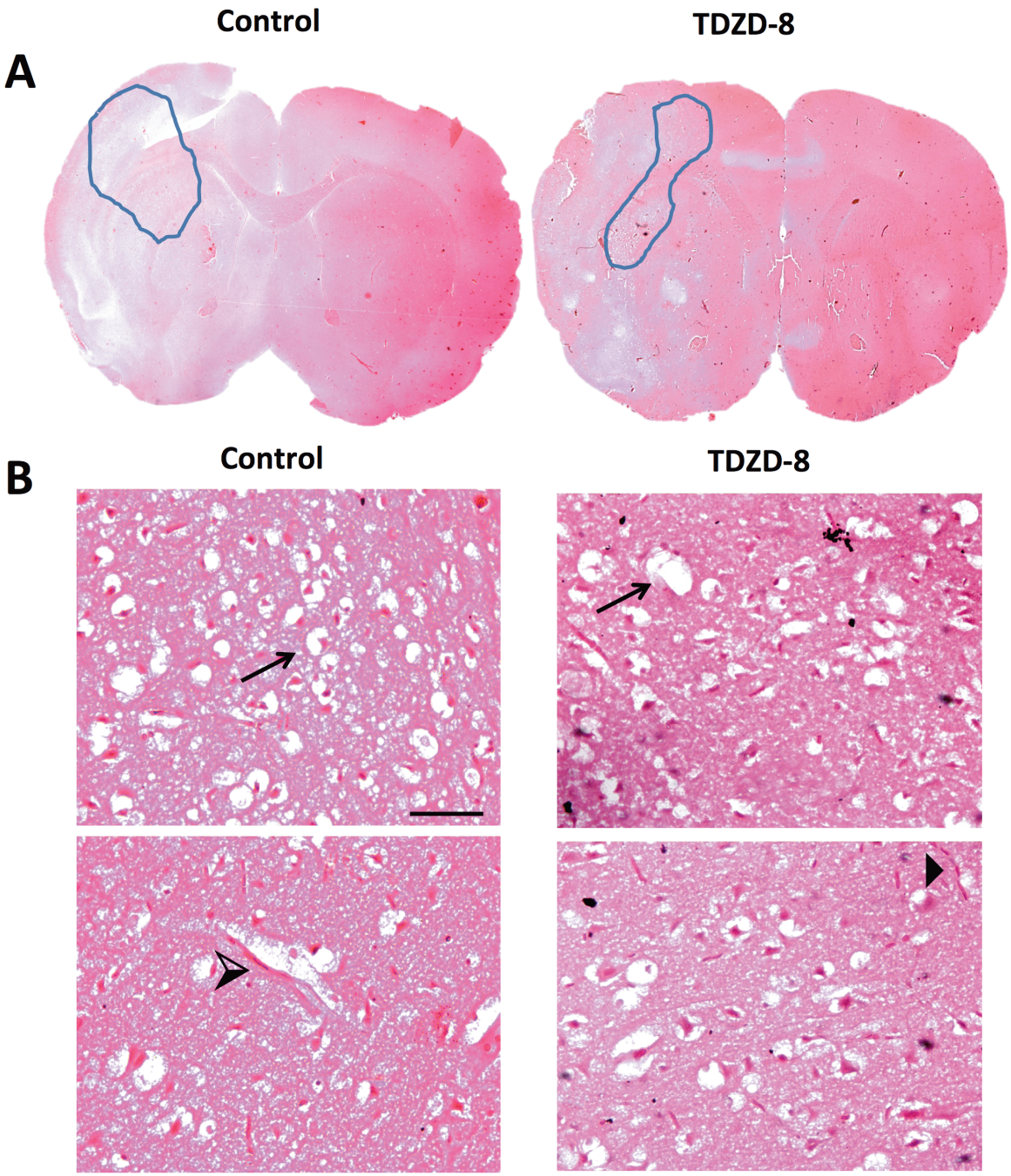


**Figure 5.6.** Representative photomicrographs H&E brain sections of control and TDZD-8-treated rats *A*, Whole brain section H&E images with delineated infarct area of control and TDZD-8-treated rats. *B*, Representative photomicrographs of cerebrovascular changes: neuropil spongiosis (arrows) and perivascular edema (➢) in control animals or its absence in TDZD-8-treated ones ( ▸ ). Scale bar equals 200 μm.

There was a 50% reduction in the number of degenerating Fluoro-Jade positive neurons in TDZD-8 treatment group (421,3±45,61 compared to 210,8±16,14 positive cells per section) (Figure 5.7).

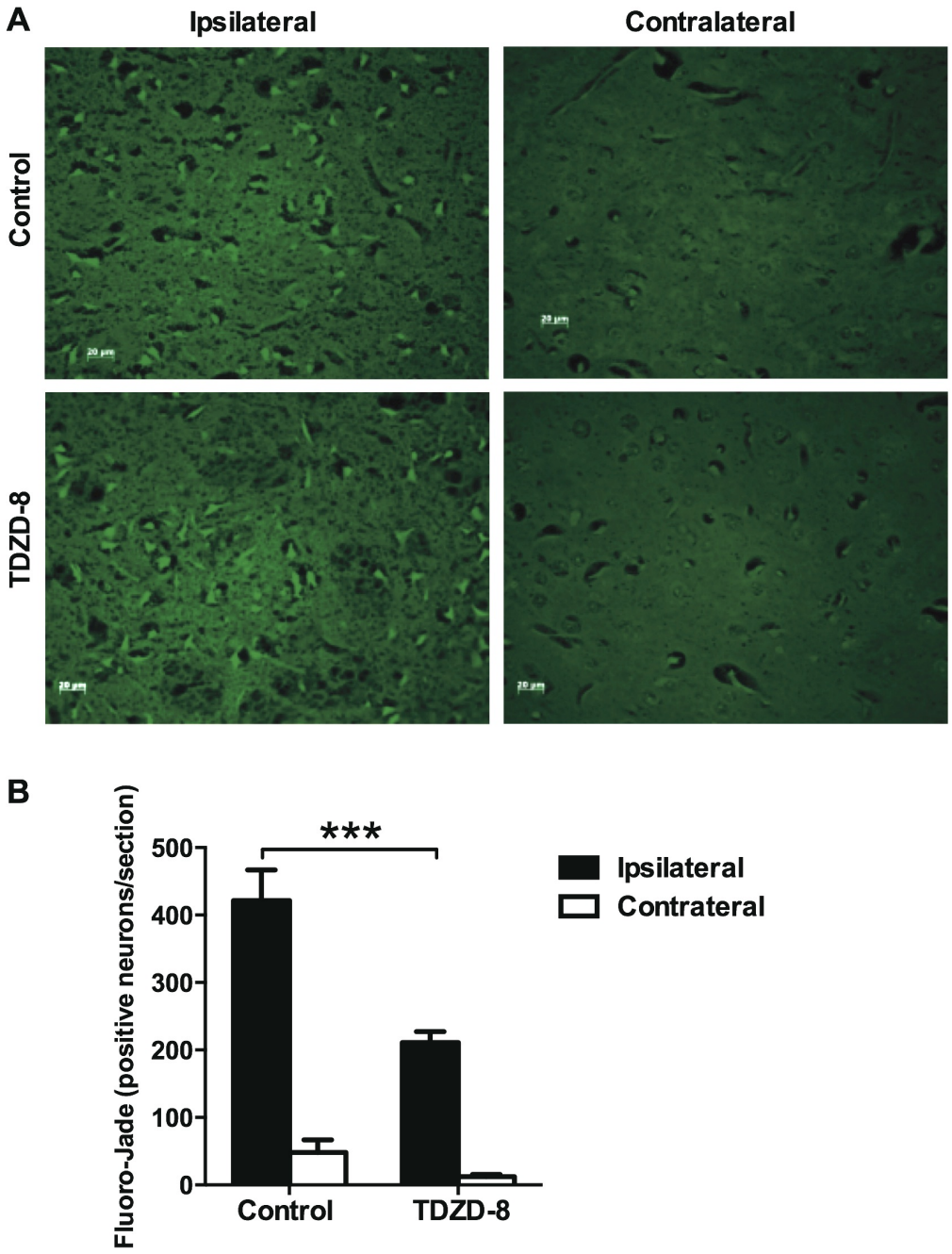


**Figure 5.7.** Comparison of degenerating neurons for the two hemispheres in both control and TDZD-8-treated groups. *A*, Representative images of brain section stained for degenerating neurons using Fluoro-Jade. Scale bar equals 20 μm. *B,* Bar graph comparing the number of positive Fluoro-Jade staining neurons per 0.16 $\mu m^2$ in 4 sections for each rat of the interest area (*n*=3). Data represent the mean±SEM (4 sections from *n*=3 per group). ****p*<0.001.

Western blot analysis of p-Akt and total Akt expression was non-significant between groups (Figure 5.8) but immunostaining techniques revealed that TDZD-8 significantly increases p-Akt nucleus translocation (22,7±3,44% of positive p-Akt nuclei in control group compared to 34,3±3,61% in treatment group) (Figs. 5.9 and 5.10).

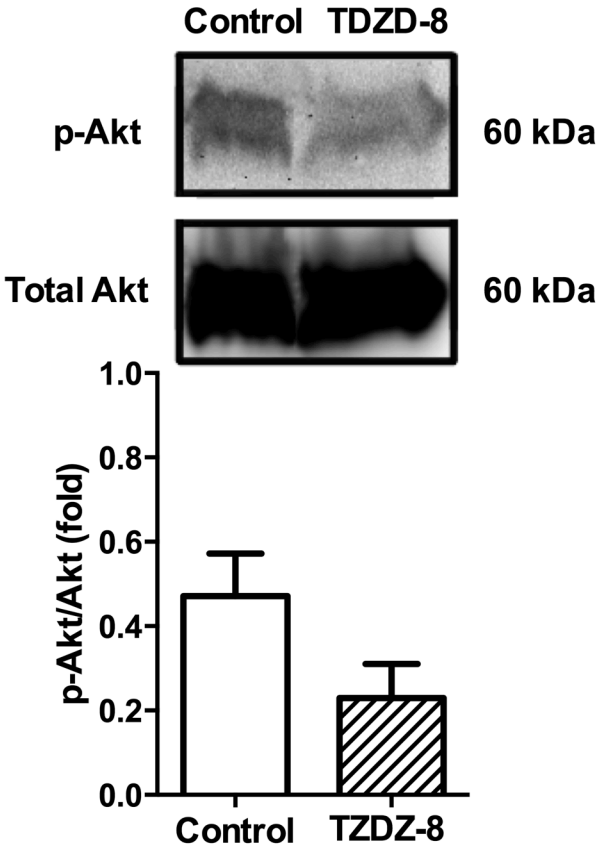


**Figure 5.8.** Western Blot showing expression of p-Akt and total Akt with a bar graph displaying the densitometric analysis for comparisons of p-Akt/Akt. Data represent the mean±SEM (*n*=3 per group). Results did not show differences between groups (*p*=0.14).

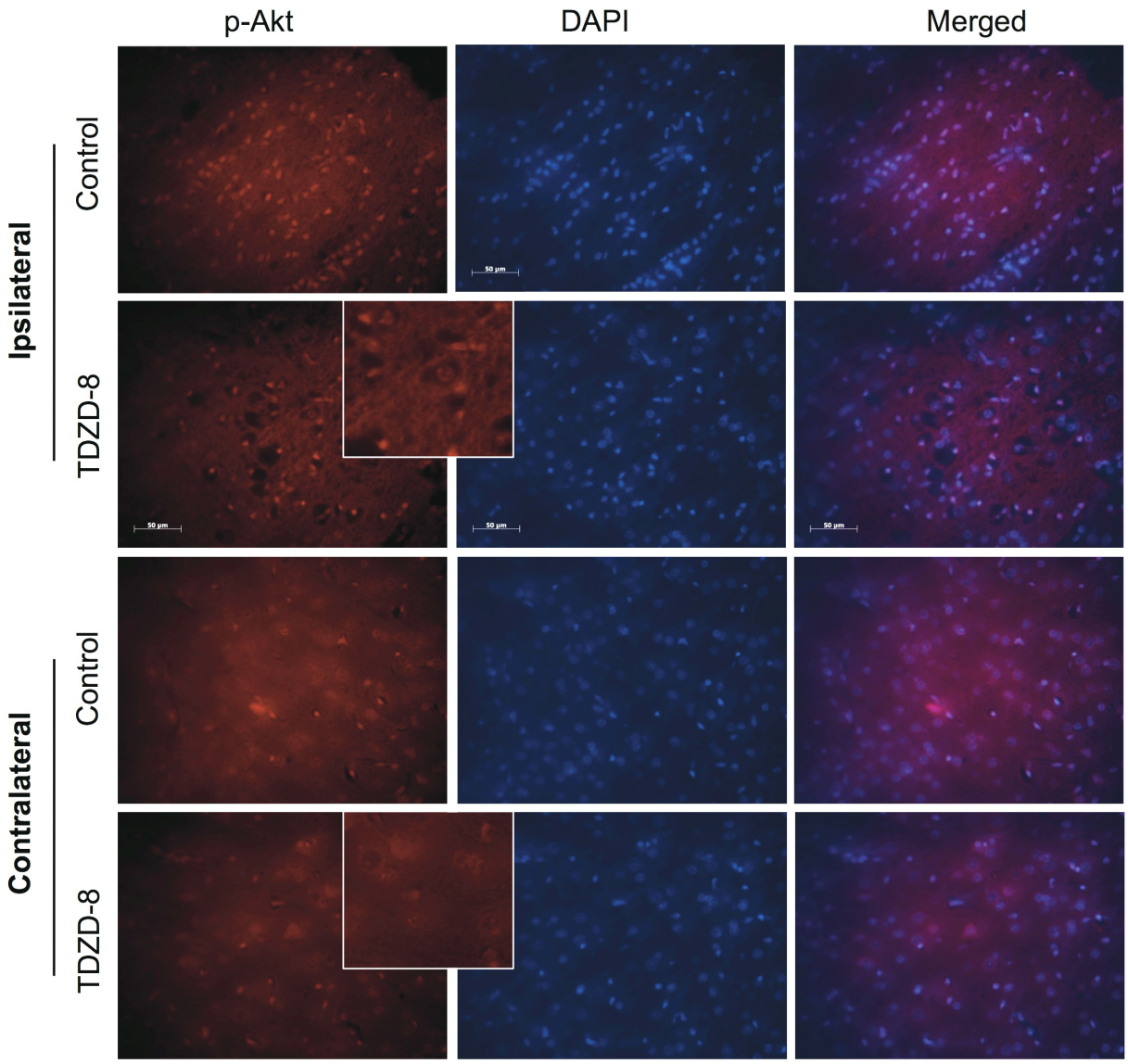


**Figure 5.9.** Akt phosphorylation in control and TDZD-8-treated groups. Representative images of the interest area of the I-R injured and contralateral hemispheres after double staining for p-Akt and nuclear DAPI. Merged images are also presented. Scale bar equals 50 μm.

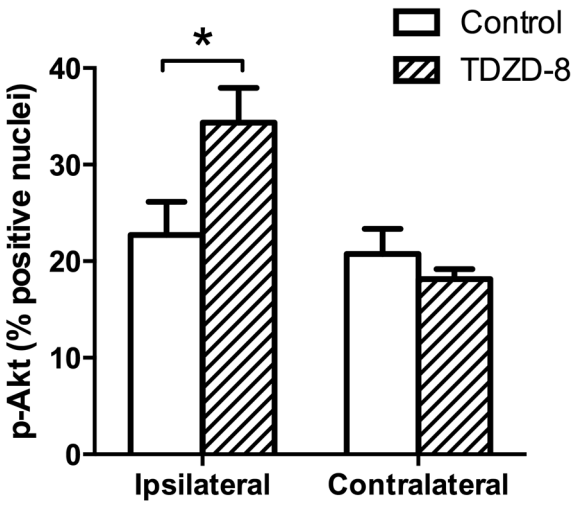


**Figure 5.10.** Bar graph representing the percentage of positive p-Akt nuclei in the interest area for both treatment and control groups, including comparisons to contralateral hemispheres. Data represent the mean±SEM (4 sections for each *n*=3 of each group). *$p$<0.005.

## 5.4 Discussion and Conclusions

To our knowledge, this study provides first evidence that a single TDZD-8 pretreatment dose protects rat brain against injury following 60-minute transient MCA ischemia. Our data demonstrates that for cerebral I-R injury, TDZD-8: (i) reduced brain damage extent, that is 48% reduction on the infarct volume and 59% reduction of the hemispheric edema; (ii) diminished the number of apoptotic/degenerating neurons; (iii) improved neurological performance at 24 hours and (iv) prevented plasma rise of NSE. NSE is assumed to be a reliable marker to follow-up neuronal damage since the plasma levels of NSE correlate with the extent of cerebral infarction[159,160]. Blood glucose levels during ischemia or reperfusion were not different between groups, indicating that the effects induced by TDZD-8 are independent from this variable.

GSK-3β inhibition has been shown to induce neuroprotective effects in cerebral ischemia by suppressing neuronal apoptosis and protecting against the loss of barrier integrity due to a decrease in the generation of several pro-inflammatory mediators and preventing leukocyte adhesion and migration into the brain[187,188,195]. Furthermore, GSK-3β inhibition is thought to promote autophagy activation in ischemic injury, an intracellular catabolic process by which

cells remove their damaged organelles for the maintenance of cellular homeostasis, and to induce astrocyte sensitization and tolerance to inflammatory molecules[189,203]. These prosurvival effects for the neurovascular unit are consistent with the histological findings, fewer positive degenerating/necrotic neurons stained with Fluro-Jade and lower NSE plasma levels seen in the treatment group. GSK-3β inhibition has been proposed to be a potent and effective therapeutic approach to attenuating inflammatory response associated with brain microvascular endothelial cells dysfunction, which includes preservation of BBB tightness by promoting tight junction protein stability[188,204]. Also, it is possible that TDZD-8 attenuates BBB disruption and consequential secondary brain injury.

The PI3K/Akt/GSK-3β pathway is a central mediator in signal transduction pathways that help to regulate cell growth, metabolism, inflammation and cell survival[162]. Akt's role in cell survival was first elucidated by Dudek, who demonstrated that IGF-1 promoted the survival of cerebellar cells and that this was mediated by Akt[161]. Following cerebral ischemia, p-Akt levels transiently increase in neurons, and this elevation is believed to be a neuroprotective response[162,205]. Activated protein kinase p-Akt phosphorylates a number of downstream cytosolic and nuclear proteins that regulate mitochondrial activity, cell growth, and cell survival. The cytosolic modulation include the inhibition of pro-apoptotic molecules such as BAD protein, BAX protein, caspases and GSK-3β itself[162,194,205]. Phosphorylated-Akt has been shown to translocate to the nucleus where it phosphorylates several other targets, such as p53 tumor suppressor and Forkhead box (FOX) transcription factors, inhibiting their activity and ability to induce the expression of death genes[206,207]. In conclusion, p-Akt is important to I-R because its actions may allow cells to escape apoptosis and retain their function.

We found that TDZD-8 did not affect total p-Akt expression in our I-R experiment, which may be explained by the fact that GSK-3β inhibition occurs downstream to the phosphorylation site of Akt and its potential targets (Figs. 4.1 and 5.1). Interestingly, an increased translocation of p-Akt into the nucleus was observed following TDZD-8 treatment, suggesting Akt signaling pathway activation. Accordingly, phosphorylation of Akt appears to be essential for its intranuclear permanence[206] and recent evidence indicates that Akt plays its roles by regulating its phosphorylation state, rather than its protein expression[208,209]. We recognize complete mechanism of action by which TDZD-8 acts in focal cerebral I-R is

lacking and requires further investigation.

The efficacy of intraoperative drugs most commonly used during aneurismal clipping surgery offer limited neuroprotection. It has been recently described that thiadiazolidinones compounds have potent anti-inflammatory and tissue-protective effects. Our study suggests that neuroprotective effects induced by TDZD-8 are likely due to a complex and mixed synergic interaction between GSK-3β inhibition and Akt modulation, which acts in the neurovascular unit. In conclusion, TDZD-8 is neuroprotective *in vivo* and may have a role in the clinical setting as a pretreatment against neuronal damage induced by transient cerebral artery occlusion during cerebrovascular procedures.

# 6 SUMMARY PROTOCOL FOR CLINICAL TRIAL

Our research supports a translational clinical trial to evaluate use of a single pretreatment dose of rhEPO (1.000 IU/kg) in patients undergoing transient cerebral artery occlusion during surgical clipping of IA, aiming to evaluate morbidity, volume of brain infarct, extent of brain edema, overall survival, quality of life, incidence of vasospasm, and incidence of adverse treatment events. Even though higher doses of EPO were shown to promote neuroprotection by protecting penumbral cells against apoptosis, we have demonstrated that intravenous rhEPO pretreatment at a 1.000 IU/kg dose reduces brain edema and preserves the penumbra functional neuronal pool following rodent I-R injury. Moreover, research on translational pharmacokinetics showed that rhEPO 1.000 IU/kg per dose IV for neonatal encephalopathy[149] and for extremely low birth weight infants[150] reach drug exposure levels that afford optimal neuroprotection in animal models, and concluded this moderate dose is likely to minimize risks associated with a higher dose. Also, this dose and route of rhEPO has been used in other several clinical trials with no identified additional safety concerns[151-153] Overall, EPO complies the important general clinical rules of a neuroprotective drug: it should be safe, readily available, relatively inexpensive, require no special equipment, and target mechanisms of injury to improve outcome. EPO is widely available, affordable and has proven safe in over two decades of clinical use for erythropoiesis.

A putative clinical trial would be carried out in conformation with the spirit and the letter of the Declaration of Helsinki, in accordance with the International Conference on Harmonisation (ICH) Good Clinical Practice Guidelines and would require both approvals of the National Competent Authority and the author's institutional Review Board. Its registration in www.clinicaltrials.gov would be filled thereafter.

A summary protocol is proposed below:

**Title**

Eritropoietin as pretreatment for transient cerebral ischemia during aneurysmal surgery: multicentre randomized clinical trial of efficacy and safety

**Objective and purpose**

To establish the effectiveness and safety of the use of a single pretreatment dose of rhEPO (1.000 IU/kg) in patients undergoing surgical clipping of IA that require at least a period of transient cerebral artery occlusion. The decision to use temporary clipping would be at the discretion of the neurosurgeon. The number of temporary clips applied would be counted and the maximal and total time of temporary occlusion recorded.

The following tested hypotheses would be that administration of single pretreatment dose of rhEPO (1.000 IU/kg) in patients undergoing transient cerebral artery occlusion during surgical clipping of IA would: 1. improve short and long-term clinical course; 2. reduce the rate of brain infarct; 3. reduce the rate of brain swelling.

**Study Type**

Phase 3 interventional trial

**Allocation**

Randomized (web-based electronic platform); 1:1 randomization

**Design**

Endpoint Classification: Efficacy/Safety Study
Intervention Model: Parallel Assignment
Masking: Double blind (subject, outcomes assessor)
Primary Purpose: Treatment
Participating Centres: Multicentre

**Arms**

**Active Arm:** Intraoperative intravenous single bolus of 1.000 IU/kg rhEPO administration over 30 minutes, at the beginning of surgery and at least 10 minutes before the transient occlusion of a cerebral artery during an aneurysmal surgery

**Control Arm:** No intervention

**Primary outcome**

1. National Institutes of Health Stroke Score (NIHSS) (Time Frame: baseline, discharge date/Day 7, Day 30, Day 90)

**Key secondary outcome**

1. Acute stroke – presence and lesion volume measured by magnetic resonance imaging (MRI)[210,211] (within 12 to 72 hours post-operative)

**Other secondary outcomes**

1. Cerebral edema – presence and lesion volume measured by MRI (within 12 to 72 hours post-operative)
2. Modified Ranking Scale (mRS) (time frame: baseline, discharge date/Day 7, Day 30, Day 90)
3. Vasospasm – transcranial Doppler (TCD) according Lindegaard ratio (graded as normal, mild and severe; time frame: regularly until postoperative Day 21)
4. Adverse events related to rhEPO – including deep vein thrombosis, pulmonary embolism, seizures, arterial thrombosis such as myocardial infarct/ischemia, hypersensitivity reactions, hypertensive crisis.
5. All-cause mortality (time frame: post-operative day 28)

**Types of participants**

Eligibility: >18 years and <70 years

Gender: Both

**Inclusion criteria**

- Age 18-70 years
- Proposed surgical clipping of a diagnosed IA (regardless rupture, number, location or type of aneurysm)
- Signed informed consent by patient or proxy

**Exclusion criteria**

- Hunt and Hess grade 4 or 5 at admission
- Uncorrected coagulopathy
- Previous stroke, dementia, severe Parkinson's disease, mental disorders, limb dysfunction caused by any diseases or other conditions that may affect therapeutic efficacy or functional assessment.
- Pregnancy
- Transient cerebral artery occlusion during the surgical procedure was not required
- Unable to undergo MRI
- Hemoglobin>15 g/dl before surgery
- Uncontrolled hypertension
- Severe coronary, peripheral artery or carotid disease, including recent myocardial infarction
- Chronic renal failure
- Suspected or known additional disease process that threatens life expectancy (e.g. malignancy)
- Any other condition that in the opinion of the investigator should preclude study participation

If sufficient information would be available, the following **subgroup analyses** could be performed:

1. to determine differences between treatment groups in patients with SAH, i.e. ruptured aneurysm
2. to determine differences between treatment groups in patients with different aneurysm locations

**Duration of follow-up**

90 days

**Estimated enrollment**

Sample size calculations were performed for both primary and key secondary outcomes.

**Primary outcome:** 2144 patients

Using a significance of p=0.05 and a power of 80% (ability to detect a difference between groups), assuming an overall rate of symptomatic stroke due to transient clipping of 17%[30,31] and an effect size of 25%, that is, assuming that rhEPO therapeutic effect decreases this outcome to 13%, a minimum of 1072 patients per group will be needed before the final analysis.

**Key secondary outcome**: 702 patients

Using a significance of p=0.05 and a power of 80%, assuming an overall rate of the primary outcome 'stroke' of 40%[30,31,33,34], and an effect size of 25%, that is, assuming that rhEPO therapeutic effect decreases this outcome to 30%, a minimum of 702 patients will be needed before the final analysis.

Planned interim analyses with sample size re-assessments will be performed every 70 patients. For instance, if treatment had an effect size of 50%, that is, rhEPO therapeutic effect decreases rate of primary outcome from 17% to 8.5%, a total of 476 patients would be enough to demonstrate treatment effect.

**Timeline**

5 years

# 7 FINAL COMMENTS

Surgical or endovascular interventions are the options for treatment of IAs. As endovascular techniques gain popularity, the aneurysms that are being sent for clipping are fewer and more complex. Therefore, surgical aneurysms are increasingly challenging for microvascular neurosurgeons. Temporary clip applications will remain essential.

Any strategy to reduce intraoperative risks to minimum is critical, which may include intraoperative physiological monitoring, vascular clips design or cerebroprotective drugs. Research is still looking for an effective neuroprotective drug that may be used in daily practice. The translational disappointments have created a great deal of pessimism regarding the future of neuroprotection trials in humans. However, the smaller number of neurosurgical patients requiring temporary clipping are being disregarded by the large number of patients with spontaneous stroke. Neurosurgical patients could benefit from best timing/route for drug administration and from strict physiological variables control, raising chances of clinical success. The concerns on differences between animal and human studies may explain why most preclinical trials evaluating neuroprotective agents have been using either permanent cerebral ischemia models or treatment drug administration after the onset of ischemia, as the clinical world would require in patients with ongoing stroke. This research was designed for the assessment of drugs that could be used against cerebral injury due to intraoperative transient ischemia. Experimental planning, animal model and drug selection, as well as effective dose selection, considering dose-limiting toxicity in humans, route of administration, and time-window to treatment were major concerns to approach the clinical problem.

There is a multiplicity of mechanisms causing brain injury following cerebral I-R. In this study, we evaluated neuroprotective compounds with a possible multimodal mode of action. This concept considers the use of agents with potential recovery-enhancing properties besides its possible neuroprotective effects. We have studied a promising drug with well-known anti-inflammatory actions, TDZD-8, on a MCA I-R rodent model, with very encouraging results. Phase 3 clinical trials for marketing approval of this molecule are still ongoing, which limits its clinical use. Furthermore, we present the first study based on the same animal model to evaluate potential benefits of a single moderate dose of intravenous rhEPO, suitable for

translation to humans, administered prior the ischemia onset. Even though higher doses of EPO were shown to promote neuroprotection by protecting penumbral cells against apoptosis, our results demonstrate that 1.000 IU/kg rhEPO pretreatment dose may also attenuate cerebral I-R injury. Contrary to what one would expect, results suggest that protective outcome of rhEPO is more a result of an indirect effect in brain edema due to BBB preservation rather than direct neuronal antiapoptotic actions. These effects are in line with the emerging concept of neurovascular unit protection, which emphasizes that all cell types in the brain, including neurons, glial and vascular elements, must be considered for rescue and preservation. Since rhEPO is widely available, affordable, and with a well-known safety profile in humans, a translational clinical trial evaluating single bolus pretreatment dose of 1.000 UI/kg in patients undergoing elective transient cerebral artery occlusion during aneurysm surgery was planned.

The writing of this thesis allowed my introduction into animal research. It was interesting to realize that, as with real life surgery, small pitfalls can lead to unpleasant events. The most difficult step in accomplishing this work was, by far, setting up and establishing the animal model. Therefore, this work was not meant to end here. It is reassuring that methodology is being further improved and other experiments are being planned.

Nevertheless, it will be very gratifying once this thesis results in a clinical trial in a nearby future.

# 8 BIBLIOGRAPHIC REFERENCES


1. Penn DL, Komotar RJ, Sander Connolly E. Hemodynamic mechanisms underlying cerebral aneurysm pathogenesis. J Clin Neurosci 2011;18:1435-1438.
2. Vlak MH, Algra A, Brandenburg R, Rinkel GJ. Prevalence of unruptured intracranial aneurysms, with emphasis on sex, age, comorbidity, country, and time period: a systematic review and meta-analysis. Lancet Neurol. 2011;10:626-636.
3. Linn FH, Rinkel GJ, Algra A, van Gijn J. Incidence of subarachnoid hemorrhage: role of region, year, and rate of computed tomography: a meta-analysis. Stroke 1996;27:625-629.
4. Ohkuma H, Fujita S, Suzuki S. Incidence of aneurysmal subarachnoid hemorrhage in Shimokita, Japan, from 1989 to 1998. Stroke 2002;33:195-199.
5. The ACROSS Group. Epidemiology of Aneurysmal Subarachnoid Hemorrhage in Australia and New Zealand: Incidence and Case Fatality From the Australasian Cooperative Research on Subarachnoid Hemorrhage Study (ACROSS). Stroke 2000;31:1843-1850.
6. Hop JW, Rinkel GJ, Algra A, van Gijn J. Case-fatality rates and functional outcome after subarachnoid hemorrhage: a systematic review. Stroke 1997;28:660-664.
7. Hackett ML, Anderson CS. Health outcomes 1 year after subarachnoid hemorrhage: An international population-based study. The Australian Cooperative Research on Subarachnoid Hemorrhage Study Group. Neurology 2000;55:658-662.
8. Morgagni GB. De sedibus et causis morborum per anatomen indagatis libri quinque. Venetiis: ex Thypographia Remondiniana; 1761.
9. Quinke HU. Lumbalpunction. Berl Klin Wochenschr 1895;32:889-891.
10. Moniz E. L'encephalographie arterielle, son importance dans la localization des temeurs cerebrales. Rev Neurol 1927;2:72-90.
11. Dott NW. Intracranial aneurysms: cerebral arterio-radiography: surgical treatment. Edinburgh Med J 1933;40:219-234.
12. Dandy WE. Intracranial aneurysm of the internal carotid artery: cured by operation. Ann Surg 1938;107:654-659.
13. Pool JL, Colton RP. The dissecting microscope for intracranial vascular surgery. J Neurosurg 1966;25:315-318.

14. Yasargil MG, Fox JL. The microsurgical approach to intracranial aneurysms. Surg Neurol 1975;3:7-14.
15. Luessenhop AJ, Velasquez AC. Observation on the tolerance of the intracranial arteries to catheterization. J Neurosurg 1964;21:85-91.
16. Serbinenko FA. Balloon catheterization and occlusion of major cerebral vessels. J Neurosurg 1974;41:125-145.
17. Guglielmi G, Viñuela F, Dion J, Duckwiler G. Electrothrombosis of saccular aneurysms via endovascular approach. Part 2: Preliminary clinical experience. J Neurosurg 1991;75:8-14.
18. Guglielmi G, Viñuela F, Sepetka I, Macellari V. Electrothrombosis of saccular aneurysms via endovascular approach. Part 1: Electrochemical basis, technique, and experimental results. J Neurosurg 1991;75:1-7.
19. Pool JL. Aneurysms of the anterior communicating (ACC) artery - indications for surgery. Trans Am Neurol Assoc 1961;86:232-233.
20. Batjer HH, Frankfurt AI, Purdy PD, Smith SS, Samson DS. Use of etomidate, temporary arterial occlusion, and intraoperative angiography in surgical treatment of large and giant cerebral aneurysms. J Neurosurg 1988;68:234-240.
21. Buchthal A, Belopavlovic M, Mooij JJ. Evoked potential monitoring and temporary clipping in cerebral aneurysm surgery. Acta Neurochir (Wien) 1988;93:28-36.
22. Fortuny LA, Adams CB, Briggs M. Surgical mortality in an aneurysm population: effects of age, blood pressure and preoperative neurological state. J Neurol Neurosurg Psychiatry 1980;43:879-882.
23. Lanzino G, Kassell NF, Germanson TP, Kongable GL, Truskowski LL, Torner JC, Jane JA. Age and outcome after aneurysmal subarachnoid hemorrhage: why do older patients fare worse? J Neurosurg 1996;85:410-418.
24. Ogilvy CS, Carter BS, Kaplan S, Rich C, Crowell RM. Temporary vessel occlusion for aneurysm surgery: risk factors for stroke in patients protected by induced hypothermia and hypertension and intravenous mannitol administration. J Neurosurg 1996;84:785-791.
25. Schramm J, Koht A, Schmidt G, Pechstein U, Taniguchi M, Fahlbusch R. Surgical and electrophysiological observations during clipping of 134 aneurysms with evoked potential monitoring. Neurosurgery 1990;26:61-70.

26. Kühnel TS, Müller GH. Experimental animal studies of clip-induced microvascular trauma. Microsurgery 2004;24:241-247.
27. Woertgen C, Rothoerl RD, Albert R, Schebesch KM, Ullrich OW. Effects of temporary clipping during aneurysm surgery. Neurol Res 2008;30:542-546.
28. Dujovny M, Kossovsky N, Munoz G, Langhi R, Nelson D, Fein JM. Reduced vascular trauma after temporary occlusion with modified Biemer and Yasargil clips. J Microsurg 1981;2:195-201.
29. Samson D, Batjer HH, Bowman G, Mootz L, Krippner WJ Jr, Meyer YJ, Allen BC. A clinical study of the parameters and effects of temporary arterial occlusion in the management of intracranial aneurysms. Neurosurgery 1994;34:22-28.
30. Ferch R, Pasqualin A, Pinna G, Chioffi F, Bricolo A. Temporary arterial occlusion in the repair of ruptured intracranial aneurysms: an analysis of risk factors for stroke. J Neurosurg 2002;97:836-842.
31. Ha SK, Lim DJ, Seok BG, Kim SH, Park JY, Chung YG. Risk of stroke with temporary arterial occlusion in patients undergoing craniotomy for cerebral aneurysm. J Korean Neurosurg Soc 2009;46:31-37.
32. Jabre A, Symon L. Temporary vascular occlusion during aneurysm surgery. Surg Neurol 1987;27:47-63.
33. Lavine SD, Masri LS, Levy ML, Giannotta SL. Temporary occlusion of the middle cerebral artery in intracranial aneurysm surgery: time limitation and advantage of brain protection. J Neurosurg 1997;87:817-824.
34. Umredkar A, Gupta SK, Khandelwal N, Chhabra R, Mathuriya SN, Pathak A, Tiwari MK, Mukherjee KK, Mohindra S, Singla N, Salunke P. Intracerebral infarcts following clipping of intracranial aneurysms: incidence, clinical correlation and outcome. Br J Neurosurg 2010;24:156-162.
35. David CA, Prado R, Dietrich WD. Cerebral protection by intermittent reperfusion during temporary focal ischemia in the rat. J Neurosurg 1996;85:923-928.
36. Goldman MS, Anderson RE, Meyer FB. Effects of intermittent reperfusion during temporal focal ischemia. J Neurosurg 1992;77:911-916.
37. Steinberg GK, Panahian N, Sun GH, Maier CM, Kunis D. Cerebral damage caused by interrupted, repeated arterial occlusion versus uninterrupted occlusion in a focal ischemic model. J Neurosurg 1994;81:554-559.

38. Astrup J, Siesjö BK, Symon L. Thresholds in cerebral ischemia - the ischemic penumbra. Stroke 1981;12:723-725.
39. Lo EH. A new penumbra: transitioning from injury into repair after stroke. Nat Med 2008;14:497-500.
40. Karaszewski B, Wardlaw JM, Marshall I, Cvoro V, Wartolowska K, Haga K, Armitage PA, Bastin ME, Dennis MS. Early brain temperature elevation and anaerobic metabolism in human acute ischaemic stroke. Brain 2009;132:955-964.
41. Li J, Yu W, Li XT, Qi SH, Li B. The effects of propofol on mitochondrial dysfunction following focal cerebral ischemia-reperfusion in rats. Neuropharmacology 2014;77:358-368.
42. Pundik S, Xu K, Sundararajan S. Reperfusion brain injury: focus on cellular bioenergetics. Neurology 2012;79(13S1):S44-S51.
43. Starkov AA, Chinopoulos C, Fiskum G. Mitochondrial calcium and oxidative stress as mediators of ischemic brain injury. Cell Calcium 2004;36:257–264.
44. Khatri R, McKinney AM, Swenson B, Janardhan V. Blood-brain barrier, reperfusion injury, and hemorrhagic transformation in acute ischemic stroke. Neurology 2012;79:S52-57.
45. Bodalia A, Li H, Jackson MF. Loss of endoplasmic reticulum Ca2+ homeostasis: contribution to neuronal cell death during cerebral ischemia. Acta Pharmacol Sin 2013;34:49-59.
46. Bano D, Munarriz E, Chen HL, Ziviani E, Lippi G, Young KW, Nicotera P. The plasma membrane Na+/Ca2+ exchanger is cleaved by distinct protease families in neuronal cell death. Ann N Y Acad Sci 2007;1099:451-455.
47. Kristián T, Siesjö BK. Calcium in ischemic cell death. Stroke 1998;29:705–718.
48. Chen J, Nagayama T, Jin K, Stetler RA, Zhu RL, Graham SH, Simon RP. Induction of caspase-3-like protease may mediate delayed neuronal death in the hippocampus after transient cerebral ischemia. J Neurosci 1998;18:4914-4928.
49. Sun GY, Shelat PB, Jensen MB, He Y, Sun AY, Simonyi A. Phospholipases A2 and inflammatory responses in the central nervous system. Neuromolecular Med 2010;12:133-148.

50. Han Q, Liu S, Li Z, Hu F, Zhang Q, Zhou M, Chen J, Lei T, Zhang H. DCPIB, a potent volume-regulated anion channel antagonist, Attenuates microglia-mediated inflammatory response and neuronal injury following focal cerebral ischemia. Brain Res 2014;1542:176-185.
51. Kweon HJ, Suh BC. Acid-sensing ion channels (ASICs): therapeutic targets for neurological diseases and their regulation. BMB Rep 2013;46:295-304.
52. Weilinger NL, Maslieieva V, Bialecki J, Sridharan SS, Tang PL, Thompson RJ. Ionotropic receptors and ion channels in ischemic neuronal death and dysfunction. Acta Pharmacol Sin 2013;34:39-48.
53. Zhang H, Cao HJ, Kimelberg HK, Zhou M. Volume regulated anion channel currents of rat hippocampal neurons and their contribution to oxygen-and-glucose deprivation induced neuronal death. PLoS One. 2011;6:e16803.
54. Szatkowski M, Barbour B, Attwell D. Non-vesicular release of glutamate from glial cells by reversed electrogenic glutamate uptake. Nature 1990;348:443–446.
55. Coulter DA, Eid T. Astrocytic Regulation of Glutamate Homeostasis in Epilepsy. Glia 2012;60:1215–1226.
56. Peng PL, Zhong X, Tu W, Soundarapandian MM, Molner P, Zhu D, Lau L, Liu S, Liu F, Lu Y. ADAR2-dependent RNA editing of AMPA receptor subunit GluR2 determines vulnerability of neurons in forebrain ischemia. Neuron 2006;49:719-733.
57. Fabricius M, Fuhr S, Bhatia R, Boutelle M, Hashemi P, Strong AJ, Lauritzen M. Cortical spreading depression and peri-infarct depolarization in acutely injured human cerebral cortex. Brain 2006;129:778-790.
58. Dreier JP, Major S, Manning A, Woitzik J, Drenckhahn C, Steinbrink J, Tolias C, Oliveira-Ferreira AI, Fabricius M, Hartings JA, Vajkoczy P, Lauritzen M, Dirnagl U, Bohner G, Strong AJ; COSBID study group. Cortical spreading ischaemia is a novel process involved in ischaemic damage in patients with aneurysmal subarachnoid haemorrhage. Brain. 2009;132:1866-1881.
59. Gill R, Andiné P, Hillered L, Persson L, Hagberg H. The effect of MK-801 on cortical spreading depression in the penumbral zone following focal ischaemia in the rat. J Cereb Blood Flow Metab 1992;12:371-379.
60. Adibhatla RM, Hatcher JF. Altered lipid metabolism in brain injury and disorders. Subcell Biochem 2008;49:241-268.

61. Chen H, Yoshioka H, Kim GS, Jung JE, Okami N, Sakata H, Maier CM, Narasimhan P, Goeders CE, Chan PH. Oxidative stress in ischemic brain damage: mechanisms of cell death and potential molecular targets for neuroprotection. Antioxid Redox Signal. 2011;14:1505-1517.
62. Murakami K, Kondo T, Kawase M, Li Y, Sato S, Chen SF, Chan PH. Mitochondrial susceptibility to oxidative stress exacerbates cerebral infarction that follows permanent focal cerebral ischemia in mutant mice with manganese superoxide dismutase deficiency. J Neurosci 1998;18:205–213.
63. Liu L, Zhang R, Liu K, Zhou H, Yang X, Liu X, Tang M, Su J, Dong Q. Tissue kallikrein protects cortical neurons against in vitro ischemia-acidosis/reperfusion-induced injury through the ERK1/2 pathway. Exp Neurol 2009;219:453-465.
64. Yang Y, Ke-Zhou L, Ning GM, Wang ML, Zheng XX. Dynamics of nitric oxide and peroxynitrite during global brain ischemia/reperfusion in rat hippocampus: NO-sensor measurement and modeling study. Neurochem Res 2008;33:73-80.
65. Warner DS, Sheng H, Batinic-Haberle I. Oxidants, antioxidants and the ischemic brain. J Exp Biol 2004;207:3221–3231.
66. Liu Y, Wang D, Wang H, Qu Y, Xiao X, Zhu Y. The protective effect of HET0016 on brain edema and blood-brain barrier dysfunction after cerebral ischemia/reperfusion. Brain Res 2014;1544:45-53.
67. Wang X, Jiang CM, Wan HY, Wu JL, Quan WQ, Wu KY, Li D. Neuroprotection against permanent focal cerebral ischemia by ginkgolides A and B is associated with obstruction of the mitochondrial apoptotic pathway via inhibition of c-Jun N-terminal kinase in rats. J Neurosci Res. 2014;92:232-242
68. Crack PJ, Taylor JM. Reactive oxygen species and the modulation of stroke. Free Radic Biol Med 2005;38:1433–1444.
69. Doyle KP, Simon RP, Stenzel-Poore MP. Mechanisms of ischemic brain damage. Neuropharmacology 2008;55:310-318.
70. Ekshyyan O, Aw TY. Apoptosis: a key in neurodegenerative disorders. Curr Neurovasc Res 2004;1:355-371.
71. Eldadah BA, Faden AI. Caspase pathways, neuronal apoptosis, and CNS injury. J Neurotrauma 2000;17:811-829.

72. Terai K, Matsuo A, McGeer EG, McGeer PL. Enhancement of immunoreactivity for NF-kappa B in human cerebral infarctions. Brain Res 1996;739:343-349.
73. Kim GW, Kondo T, Noshita N, Chan PH. Manganese superoxide dismutase deficiency exacerbates cerebral infarction after focal cerebral ischemia/reperfusion in mice: implications for the production and role of superoxide radicals. Stroke 2002;33:809–815.
74. Gerriets T, Walberer M, Ritschel N, Tschernatsch M, Mueller C, Bachmann G, Schoenburg M, Kaps M, Nedelmann M. Edema formation in the hyperacute phase of ischemic stroke. Laboratory investigation. J Neurosurg 2009;111:1036-1042.
75. Spatz M. Past and recent BBB studies with particular emphasis on changes in ischemic brain edema. Acta Neurochir Suppl 2010;106:21-27.
76. Giffard RG, Yenari MA. Many mechanisms for hsp70 protection from cerebral ischemia. J Neurosurg Anesthesiol 2004;16:53-61.
77. Pérez-de Puig I, Miró F, Salas-Perdomo A, Bonfill-Teixidor E, Ferrer-Ferrer M, Márquez-Kisinousky L, Planas AM. IL-10 deficiency exacerbates the brain inflammatory response to permanent ischemia without preventing resolution of the lesion. J Cereb Blood Flow Metab 2013;33:1955-1966.
78. Schneider A, Krüger C, Steigleder T, Weber D, Pitzer C, Laage R, Aronowski J, Maurer MH, Gassler N, Mier W, Hasselblatt M, Kollmar R, Schwab S, Sommer C, Bach A, Kuhn HG, Schäbitz WR. The hematopoietic factor G-CSF is a neuronal ligand that counteracts programmed cell death and drives neurogenesis. J Clin Invest 2005;115:2083-2098.
79. Zhang J, Shi Q, Yang P, Xu X, Chen X, Qi C, Zhang J, Lu H, Zhao B, Zheng P, Zhang P, Liu Y. Neuroprotection of neurotrophin-3 against focal cerebral ischemia/reperfusion injury is regulated by hypoxia-responsive element in rats. Neuroscience 2012;222:1-9.
80. Zhang L, Zhao H, Zhang X, Chen L, Zhao X, Bai X, Zhang J. Nobiletin protects against cerebral ischemia via activating the p-Akt, p-CREB, BDNF and Bcl-2 pathway and ameliorating BBB permeability in rat. Brain Res Bull 2013;96:45-53.
81. Puyal J, Vaslin A, Mottier V, Clarke PG. Postischemic treatment of neonatal cerebral ischemia should target autophagy. Ann Neurol 2009;66:378-389.
82. Levine B, Kroemer G. Autophagy in aging, disease and death: the true identity of a cell death impostor. Cell Death Differ 2009;16:1-2.

83. Helton R1, Cui J, Scheel JR, Ellison JA, Ames C, Gibson C, Blouw B, Ouyang L, Dragatsis I, Zeitlin S, Johnson RS, Lipton SA, Barlow C. Brain-specific knock-out of hypoxia-inducible factor-1alpha reduces rather than increases hypoxic-ischemic damage. J Neurosci 2005;25:4099-4107.
84. Fan X, Heijnen CJ, van der Kooij MA, Groenendaal F, van Bel F. The role and regulation of hypoxia-inducible factor-1alpha expression in brain development and neonatal hypoxic-ischemic brain injury. Brain Res Rev. 2009;62:99-108.
85. Ginsberg MD. Neuroprotection for ischemic stroke: past, present and future. Neuropharmacology 2008;55:363-389.
86. Del Zoppo GJ. The neurovascular unit in the setting of stroke. J Intern Med 2010;267:156–171.
87. Maki T, Hayakawa K, Pham LD, Xing C, Lo EH, Arai K. Biphasic mechanisms of neurovascular unit injury and protection in CNS diseases. CNS Neurol Disord Drug Targets 2013;12:302-215.
88. Bulusu S, Kassam AB, Houlden DA, Alkherayf F. Intraoperative neurophysiological monitoring during circulatory arrest using deep hypothermia: A case report during brain aneurysm clipping. Neurodiagn J 2013;53:121-141.
89. Chen L, Lang L, Zhou L, Song D, Mao Y. Bypass or not? Adjustment of surgical strategies according to motor evoked potential changes in large middle cerebral artery aneurysm surgery. World Neurosurg 2012;77:398.
90. Klein KU, Stadie A, Fukui K, Schramm P, Werner C, Oertel J, Engelhard K, Fischer G. Measurement of cortical microcirculation during intracranial aneurysm surgery by combined laser-Doppler flowmetry and photospectrometry. Neurosurgery 2011;69:391-398.
91. Wicks RT, Pradilla G, Raza SM, Hadelsberg U, Coon AL, Huang J, Tamargo RJ. Impact of changes in intraoperative somatosensory evoked potentials on stroke rates after clipping of intracranial aneurysms. Neurosurgery 2012;70:1114-1124.
92. Cerejo A, Silva PA, Dias C, Vaz R. Monitoring of brain oxygenation in surgery of ruptured middle cerebral artery aneurysms. Surg Neurol Int 2011;2:70.
93. Cerejo A, Silva PA, Dias C, Vaz R. Monitoring of brain tissue oxygenation in surgery of middle cerebral artery incidental aneurysms. Surg Neurol Int 2011;2:37.

94. El Beheiry H. Protecting the brain during neurosurgical procedures: strategies that can work. Curr Opin Anaesthesiol 2012;25:548-555.
95. Van der Worp HB, Sena ES, Donnan GA, Howells DW, Macleod MR. Hypothermia in animal models of acute ischaemic stroke: a systematic review and meta-analysis. Brain 2007;130:3063-3074.
96. De Georgia MA, Krieger DW, Abou-Chebl A, Devlin TG, Jauss M, Davis SM, Koroshetz WJ, Rordorf G, Warach S. Cooling for Acute Ischemic Brain Damage (COOL AID): a feasibility trial of endovascular cooling. Neurology. 2004;63:312-317.
97. Hemmen TM, Raman R, Guluma KZ, Meyer BC, Gomes JA, Cruz-Flores S, Wijman CA, Rapp KS, Grotta JC, Lyden PD; ICTuS-L Investigators. Intravenous thrombolysis plus hypothermia for acute treatment of ischemic stroke (ICTuS-L): final results. Stroke 2010;41:2265-2270.
98. Kimme P, Fridrikssen S, Engdahl O, Hillman J, Vegfors M, Sjöberg F. Moderate hypothermia for 359 operations to clip cerebral aneurysms. Br J Anaesth 2004;93:343-347.
99. Tang XN, Yenari MA. Hypothermia as a cytoprotective strategy in ischemic tissue injury. Ageing Res Rev 2010;9:61-68.
100. Todd MM, Hindman BJ, Clarke WR, Torner JC; Intraoperative Hypothermia for Aneurysm Surgery Trial (IHAST) Investigators. Mild intraoperative hypothermia during surgery for intracranial aneurysm. N Engl J Med 2005;352:135-45.
101. Krieger DW, De Georgia MA, Abou-Chebl A, Andrefsky JC, Sila CA, Katzan IL, Mayberg MR, Furlan AJ. Cooling for acute ischemic brain damage (COOL AID): an open pilot study of induced hypothermia in acute ischemic stroke. Stroke 2001;32:1847-1854.
102. Hindman BJ, Bayman EO, Pfisterer WK, Torner JC, Todd MM; IHAST Investigators. No association between intraoperative hypothermia or supplemental protective drug and neurologic outcomes in patients undergoing temporary clipping during cerebral aneurysm surgery: findings from the Intraoperative Hypothermia for Aneurysm Surgery Trial. Anesthesiology 2010;112:86-101.
103. Li LR, You C, Chaudhary B. Intraoperative mild hypothermia for postoperative neurological deficits in intracranial aneurysm patients. Cochrane Database Syst Rev 2012 DOI: 10.1002/14651858.CD008445.pub2

104. Zhao ZX, Wu C, He M. A systematic review of clinical outcomes, perioperative data and selective adverse events related to mild hypothermia in intracranial aneurysm surgery. Clin Neurol Neurosurg 2012;114:827-832.
105. Lyden PD, Hemmen TM, Grotta J, Rapp K, Raman R. Endovascular therapeutic hypothermia for acute ischemic stroke: ICTuS 2/3 protocol. Int J Stroke 2014;9:117-125.
106. Michenfelder JD. The interdependency of cerebral function and metabolic effects following massive doses of thiopental in the dog. Anesthesiology 1974;41:231-236.
107. Nussmeier NA, Arlund C, Slogoff S. Neuropsychiatric complications after cardiopulmonary bypass: cerebral protection by a barbiturate. Anesthesiology 1986;64:165-170.
108. O'Collins VE, Macleod MR, Donnan GA, Horky LL, van der Worp BH, Howells DW. 1,026 experimental treatments in acute stroke. Ann Neurol 2006;59:467–77.
109. Fisher M, Feuerstein G, Howells DW, Hurn PD, Kent TA, Savitz SI, Lo EH; STAIR Group. Update of the stroke therapy academic industry roundtable preclinical recommendations. Stroke 2009;40:2244-2250.
110. Stroke Therapy Academic Industry Roundtable (STAIR). Recommendations for standards regarding preclinical neuroprotective and restorative drug development. Stroke 1999;30:2752-2758.
111. Sutherland BA, Minnerup J, Balami JS, Arba F, Buchan AM, Kleinschnitz C. Neuroprotection for ischaemic stroke: translation from the bench to the bedside. Int J Stroke 2012;7:407-418.
112. Coyle P. Arterial patterns of the rat rhinencephalon and related structures. Exp Neurol 1975;49:671-690.
113. Alexis NE, Back T, Zhao W, Dietrich WD, Watson BD, Ginsberg MD. Neurobehavioral consequences of induced spreading depression following photothrombotic middle cerebral artery occlusion. Brain Res 1996;706:273-282.
114. Jones BJ, Roberts DJ. The quantiative measurement of motor incoordination in naive mice using an acelerating rotarod. J Pharm Pharmacol 1968;20:302-304.
115. Justicia C, Martín A, Rojas S, Gironella M, Cervera A, Panés J, Chamorro A, Planas AM. Anti-VCAM-1 antibodies did not protect against ischemic damage either in rats or in mice. J Cereb Blood Flow Metab 2006;26:421-432.

116. Stroemer RP, Kent TA, Hulsebosch CE. Enhanced neocortical neural sprouting, synaptogenesis, and behavioral recovery with D-amphetamine therapy after neocortical infarction in rats. Stroke 1998;29:2381-2393.
117. Sughrue ME, Mocco J, Komotar RJ, Mehra A, D'Ambrosio AL, Grobelny BT, Penn DL, Connolly ES Jr. An improved test of neurological dysfunction following transient focal cerebral ischemia in rats. J Neurosci Methods 2006;151:83-89.
118. Alexis NE, Dietrich WD, Green EJ, Prado R, Watson BD. Nonocclusive common carotid artery thrombosis in the rat results in reversible sensorimotor and cognitive behavioral deficits. Stroke 1995;26:2338-2346.
119. Horie N, Maag AL, Hamilton SA, Shichinohe H, Bliss TM, Steinberg GK. Mouse model of focal cerebral ischemia using endothelin-1. J Neurosci Methods 2008;173:286-290.
120. Koizumi J, Yoshida Y, Nakazawa T, Ooneda G. Experimental studies of ischemic brain edema, I: a new experimental model of cerebral embolism in rats in which recirculation can be introduced in the ischemic area. Jpn J Stroke 1986;8:1-8.
121. Wang Y, Chang CF, Morales M, Chiang YH, Harvey BK, Su TP, Tsao LI, Chen S, Thiemermann C. Diadenosine tetraphosphate protects against injuries induced by ischemia and 6-hydroxydopamine in rat brain. J Neurosci 2003;23:7958-7965.
122. Zhang RL, Chopp M, Zhang ZG, Jiang Q, Ewing JR. A rat model of focal embolic cerebral ischemia. Brain Res 1997;766:83-92.
123. Bederson JB, Pitts LH, Germano SM, Nishimura MC, Davis RL, Bartkowski HM. Evaluation of 2,3,5-triphenyltetrazolium chloride as a stain for detection and quantification of experimental cerebral infarction in rats. Stroke 1986;17(6):1304-1308.
124. Swanson RA, Morton MT, Tsao-Wu G, Savalos RA, Davidson C, Sharp FR. A semiautomated method for measuring brain infarct volume. J Cereb Blood Flow Metab 1990;10:290-293.
125. Walberer M, Stolz E, Müller C, Friedrich C, Rottger C, Blaes F, Kaps M, Fisher M, Bachmann G, Gerriets T. Experimental stroke: ischaemic lesion volume and oedema formation differ among rat strains (a comparison between Wistar and Sprague-Dawley rats using MRI). Lab Anim 2006;40:1-8.

126. Peeling J, Corbett D, Del Bigio MR, Hudzik TJ, Campbell M, Palmer GC. Rat middle cerebral artery occlusion correlations between histopathology, T2-weighted magnetic resonance imaging, and behavioral indices. J Stroke Cerebrovasc Dis 2001;10:166-77.
127. Reglodi D, Somogyvari-Vigh A, Vigh S, Kozicz T, Arimura A. Delayed systemic administration of PACAP38 is neuroprotective in transient middle cerebral artery occlusion in the rat. Stroke 2000;31:1411-1417.
128. Warner DS, Takaoka S, Wu B, Ludwig PS, Pearlstein RD, Brinkhous AD, Dexter F. Electroencephalographic burst suppression is not required to elicit maximal neuroprotection from pentobarbital in a rat model of focal cerebral ischemia. Anesthesiology 1996;84:1475-1484.
129. Sakai H, Sheng H, Yates RB, Ishida K, Pearlstein RD, Warner DS. Isoflurane provides long-term protection against focal cerebral ischemia in the rat. Anesthesiology 2007;106:92-99.
130. Calloni RL, Winkler BC, Ricci G, Poletto MG, Homero WM, Serafini EP, Corleta OC. Transient middle cerebral artery occlusion in rats as an experimental model of brain ischemia. Acta Cir Bras 2010;25:428-433.
131. Mouw G, Zechel JL, Zhou Y, Lust WD, Selman WR, Ratcheson RA. Caspase-9 inhibition after focal cerebral ischemia improves outcome following reversible focal ischemia. Metab Brain Dis 2002;17:143-151.
132. Alkayed NJ, Harukuni I, Kimes AS, London ED, Traystman RJ, Hurn PD. Gender-linked brain injury in experimental stroke. Stroke 1998;29:159-165.
133. Johnson MP, McCarty DR, Chmielewski PA. Temporal dependent neuroprotection with propentofylline (HWA 285) in a temporary focal ischemia model. Eur J Pharmacol 1998;346:151-157.
134. Hayashi T, Abe K, Itoyama Y. Reduction of ischemic damage by application of vascular endothelial growth factor in rat brain after transient ischemia. J Cereb Blood Flow Metab. 1998;18:887-895.
135. Hasselblatt M, Ehrenreich H, Siren AL. The brain erythropoietin system and its potential for therapeutic exploitation in brain disease. J Neurosurg Anesthesiol 2006;18:132–138.

136. Masuda S, Okano M, Yamagishi K, Nagao M, Ueda M, Sasaki R. A novel site of erythropoietin production. Oxygen-dependent production in cultured rat astrocytes. J Biol Chem 1994;269:19488-19493.
137. Chikuma M, Masuda S, Kobayashi T, Nagao M, Sasaki R. Tissue-specific regulation of erythropoietin production in the murine kidney, brain, and uterus. Am J Physiol Endocrinol Metab 2000;279:1242–1248.
138. Sirén AL, Knerlich F, Poser W, Gleiter CH, Bruck W, Ehrenreich H. Erythropoietin and erythropoietin receptor in human ischemic/hypoxic brain. Acta Neuropathol (Berl) 2001;101:271–276.
139. Ponce LL, Navarro JC, Ahmed O, Robertson CS. Erythropoietin neuroprotection with traumatic brain injury. Pathophysiology 2013;20:31-38.
140. Velly L, Pellegrini L, Guillet B, Bruder N, Pisano P. Erythropoietin 2nd cerebral protection after acute injuries: a double-edged sword? Pharmacol Ther 2010;128:445-459.
141. Vogel J, Gassmann M. Erythropoietic and non-erythropoietic functions of erythropoietin in mouse models. J Physiol 2011;15:1259-1264.
142. Shingo T, Sorokan ST, Shimazaki T, Weiss S. Erythropoietin regulates the in vitro and in vivo production of neuronal progenitors by mammalian forebrain neural stem cells. J Neurosci 2001;21:9733-9743.
143. Brines ML, Ghezzi P, Keenan S, Agnello D, de Lanerolle NC, Cerami C, Itri LM, Cerami A. Erythropoietin crosses the blood-brain barrier to protect against experimental brain injury. Proc Natl Acad Sci U S A 2000;97:10526-10531.
144. Celik M, Gökmen N, Erbayraktar S, Akhisaroglu M, Konakc S, Ulukus C, Genc S, Genc K, Sagiroglu E, Cerami A, Brines M. Erythropoietin prevents motor neuron apoptosis and neurologic disability in experimental spinal cord ischemic injury. Proc Natl Acad Sci U S A 2002;99:2258-2263.
145. Juul SE, McPherson RJ, Farrell FX, Jolliffe L, Ness DJ, Gleason CA. Erytropoietin concentrations in cerebrospinal fluid of nonhuman primates and fetal sheep following high-dose recombinant erythropoietin. Biol Neonate 2004;85:138-144.

146. National Library of Medicine (US). Efficacy of Erythropoietin to Improve Survival and Neurological Outcome in Hypoxic Ischemic Encephalopathy (Neurepo). Bethesda (MD): National Library of Medicine, 2000 (http://clinicaltrials.gov/show/NCT01732146) [Accessed March 18, 2014]
147. National Library of Medicine (US). Erythropoetin Neuroprotection for Neonatal Cardiac Surgery. Bethesda (MD): National Library of Medicine, 2000 (http://clinicaltrials.gov/show/NCT00513240) [Accessed March 18, 2014]
148. National Library of Medicine (US). Trial of Erythropoietin Neuroprotection in Extremely Preterm Infants (PENUT). Bethesda (MD): National Library of Medicine, 2000 (http://clinicaltrials.gov/show/NCT01378273) [Accessed March 18, 2014]
149. Wu YW, Bauer LA, Ballard RA, Ferriero DM, Glidden DV, Mayock DE, Chang T, Durand DJ, Song D, Bonifacio SL, Gonzalez FF, Glass HC, Juul SE. Erythropoietin for neuroprotection in neonatal encephalopathy: safety and pharmacokinetics. Pediatrics 2012;130:683-691.
150. Juul SE, McPherson RJ, Bauer LA, Ledbetter KJ, Gleason CA, Mayock DE. A phase I/II trial of high-dose erythropoietin in extremely low birth weight infants: pharmacokinetics and safety. Pediatrics 2008;122:383-391.
151. Dame C, Langer J, Koller BM, Fauchère JC, Bucher HU. Urinary erythropoietin concentrations after early short-term infusion of high-dose recombinant epo for neuroprotection in preterm neonates. Neonatology 2012;102:172-177.
152. Gao D, Ning N, Niu X, Dang Y, Dong X, Wei J, Zhu C. Erythropoietin treatment in patients with acute myocardial infarction: a meta-analysis of randomized controlled trials. Am Heart J 2012;164:715-727.
153. Prunier F, Bière L, Gilard M, Boschat J, Mouquet F, Bauchart JJ, Charbonnier B, Genée O, Guérin P, Warin-Fresse K, Durand E, Lafont A, Christiaens L, Abi-Khalil W, Delépine S, Benard T, Furber A. Single high-dose erythropoietin administration immediately after reperfusion in patients with ST-segment elevation myocardial infarction: results of the erythropoietin in myocardial infarction trial. Am Heart J 2012;163:200-207.
154. Dell RB, Holleran S, Ramakrishnan R. Sample size determination. ILAR J. 2002;43:207-213.

155. Fischer AH, Jacobson KA, Rose J, Zeller R. Hematoxylin and eosin staining of tissue and cell sections. CSH Protoc 2008 [DOI:10.1101/pdb.prot4986].
156. Maio R, Sepodes B, Patel NS, Thiemermann C, Mota-Filipe H, Costa P. Erythropoietin preserves the integrity and quality of organs for transplantation after cardiac death. Shock 2011;35:126-133.
157. Sepodes B, Maio R, Pinto R, Sharples E, Oliveira P, McDonald M, Yaqoob M, Thiemermann C, Mota-Filipe H. Recombinant human erythropoietin protects the liver from hepatic ischemia-reperfusion injury in the rat. Transpl Int 2006;19:919-926.
158. Minnerup J, Heidrich J, Rogalewski A, Schäbitz WR, Wellmann J. The efficacy of erythropoietin and its analogues in animal stroke models: a meta-analysis. Stroke 2009;40:3113-3120.
159. Gelderblom M, Daehn T, Schattling B, Ludewig P, Bernreuther C, Arunachalam P, Matschke J, Glatzel M, Gerloff C, Friese MA, Magnus T. Plasma levels of neuron specific enolase quantify the extent of neuronal injury in murine models of ischemic stroke and multiple sclerosis. Neurobiol Dis 2013;59:177-82.
160. Ahmad O, Wardlaw J, Whiteley WN. Correlation of levels of neuronal and glial markers with radiological measures of infarct volume in ischaemic stroke: a systematic review. Cerebrovasc Dis 2012;33:47-54.
161. Dudek H, Datta SR, Franke TF, Birnbaum MJ, Yao R, Cooper GM, Segal RA, Kaplan DR, Greenberg ME. Regulation of neuronal survival by the serine-threonine protein kinase Akt. Science 1997;275:661-665.
162. Zhao H, Sapolsky RM, Steinberg GK. Phosphoinositide-3-kinase/akt survival signal pathways are implicated in neuronal survival after stroke. Mol Neurobiol 2006;34:249–270.
163. Shang Y, Wu Y, Yao S, Wang X, Feng D, Yang W. Protective effect of erythropoietin against ketamine-induced apoptosis in cultured rat cortical neurons: involvement of PI3K/Akt and GSK-3 beta pathway. Apoptosis 2007;12:2187-2195.
164. Shen J, Wu Y, Xu JY, Zhang J, Sinclair SH, Yanoff M. ERK- and Akt-dependent neuroprotection by erythropoietin (EPO) against glyoxal-AGEs via modulation of Bcl-xL, Bax, and BAD. Invest Ophthalmol Vis Sci 2010;51:35-46.
165. Brunet A, Bonni A, Zigmond MJ, Lin MZ, Juo P, Hu LS. Akt promotes cell survival by phosphorylating and inhibiting a Forkhead transcription factor. Cell 1999;96:857-868.

166. Fu A, Hui EK, Lu JZ, Boado RJ, Pardridge WM. Neuroprotection in stroke in the mouse with intravenous erythropoietin-Trojan horse fusion protein. Brain Res 2011;19:203-207.
167. Xiong Y, Mahmood A, Qu C, Kazmi H, Zhang ZG, Noguchi CT, Schallert T, Chopp M. Erythropoietin improves histological and functional outcomes after traumatic brain injury in mice in the absence of the neural erythropoietin receptor. J Neurotrauma 2010;27:205-215.
168. Walberer M, Ritschel N, Nedelmann M, Volk K, Mueller C, Tschernatsch M, Stolz E, Blaes F, Bachmann G, Gerriets T. Aggravation of infarct formation by brain swelling in a large territorial stroke: a target for neuroprotection? J Neurosurg 2008;109:287-293.
169. Silasi G, MacLellan CL, Colbourne F. Use of telemetry blood pressure transmitters to measure intracranial pressure (ICP) in freely moving rats. Curr Neurovasc Res 2009;6:62-69.
170. Liu K, Sun T, Wang P, Liu YH, Zhang LW, Xue YX: Effects of erythropoietin on blood-brain barrier tight junctions in ischemia-reperfusion rats. J Mol Neurosci 2013;49:369-379.
171. Martínez-Estrada OM, Rodríguez-Millán E, González-De Vicente E, Reina M, Vilaró S, Fabre M. Erythropoietin protects the in vitro blood-brain barrier against VEGF-induced permeability. Eur J Neurosci 2003;18:2538-2544.
172. Bahcekapili N, Uzüm G, Gökkusu C, Kuru A, Ziylan YZ. The relationship between erythropoietin pretreatment with blood-brain barrier and lipid peroxidation after ischemia/reperfusion in rats. Life Sci 2007;80:1245-1251.
173. Banerjee D, Rodriguez M, Nag M, Adamson JW. Exposure of endothelial cells to recombinant human erythropoietin induces nitric oxide synthase activity. Kidney Int 2000;57:1895-1904.
174. Utepbergenov DI, Mertsch K, Sporbert A, Tenz K, Paul M, Haseloff RF, Blasig IE. Nitric oxide protects blood-brain barrier in vitro from hypoxia/reoxygenation-mediated injury. FEBS Lett 1998;424:197-201.
175. Harari OA, Liao JK: NF-κB and innate immunity in ischemic stroke. Ann N Y Acad Sci 2010;1207:32-40.

176. Jerndal M, Forsberg K, Sena ES, Macleod MR, O'Collins VE, Linden T, Nilsson M, Howells DW. A systematic review and meta-analysis of erythropoietin in experimental stroke. J Cereb Blood Flow Metab 2010;30:961-968.
177. Dahlberg SA, Xu L, Hess DC, Hohnadel E, Hill WD, Fagan SC: Erythropoietin and erythropoietin mimetic peptide in focal cerebral ischemia. Stroke 35:279, 2004 (poster presentation, abstract only).
178. Sirén AL, Fasshauer T, Bartels C, Ehrenreich H. Therapeutic potential of erythropoietin and its structural or functional variants in the nervous system. Neurotherapeutics 2009;6:108-127.
179. Ehrenreich H, Hasselblatt M, Dembowski C, Cepek L, Lewczuk P, Stiefel M, Rustenbeck HH, Breiter N, Jacob S, Knerlich F, Bohn M, Poser W, Rüther E, Kochen M, Gefeller O, Gleiter C, Wessel TC, De Ryck M, Itri L, Prange H, Cerami A, Brines M, Sirén AL. Erythropoietin therapy for acute stroke is both safe and beneficial. Mol Med 2002;8:495-505.
180. Dugo L, Collin M, Thiemermann C. Glycogen synthase kinase 3beta as a target for the therapy of shock and inflammation. Shock 2007;27:113-123.
181. Embi N, Rylatt DB, Cohen P. Glycogen synthase kinase-3 from rabbit skeletal muscle: separation from cyclic-AMP-dependent protein kinase and phosphorylase kinase. Eur J Biochem 1980;107:519-27.
182. Lei P, Ayton S, Bush AI, Adlard PA. GSK-3 in Neurodegenerative Diseases. Int J Alzheimers Dis 2011:189246.
183. Xu J, Culman J, Blume A, Brecht S, Gohlke P. Chronic treatment with a low dose of lithium protects the brain against ischemic injury by reducing apoptotic death. Stroke. 2003;34:1287-1292.
184. Sasaki C, Hayashi T, Zhang WR, Warita H, Manabe Y, Sakai K, Abe K. Different expression of glycogen synthase kinase-3beta between young and old rat brains after transient middle cerebral artery occlusion. Neurol Res 2001;23:588-592.
185. Wood-Kaczmar A, Kraus M, Ishiguro K, Philpott KL, Gordon-Weeks PR. An alternatively spliced form of glycogen synthase kinase-3beta is targeted to growing neurites and growth cones. Mol Cell Neurosci 2009;42:184-194.
186. Jacobs KM, Bhave SR, Ferraro DJ, Jaboin JJ, Hallahan DE, Thotala D. GSK-3β: A Bifunctional Role in Cell Death Pathways. Int J Cell Biol 2012;2012:930710.

187. Green HF, Nolan YM. GSK-3 mediates the release of IL-1β, TNF-α and IL-10 from cortical glia. Neurochem Int 2012;61:666-671.
188. Ramirez SH, Fan S, Zhang M, Papugani A, Reichenbach N, Dykstra H, Mercer AJ, Tuma RF, Persidsky Y. Inhibition of glycogen synthase kinase 3beta (GSK3beta) decreases inflammatory responses in brain endothelial cells. Am J Pathol 2010;176:881-892.
189. Zhou X, Zhou J, Li X, Guo C, Fang T, Chen Z. GSK-3β inhibitors suppressed neuroinflammation in rat cortex by activating autophagy in ischemic brain injury. Biochem Biophys Res Commun 2011;411:271-275.
190. Martinez A, Castro A, Dorronsoro I, Alonso M. Glycogen synthase kinase 3 (GSK-3) inhibitors as new promising drugs for diabetes, neurodegeneration, cancer, and inflammation. Med Res Rev 2002;22:373-384.
191. Wang JM, Hayashi T, Zhang WR, Sakai K, Shiro Y, Abe K. Reduction of ischemic brain injury by topical application of insulin-like growth factor-I after transient middle cerebral artery occlusion in rats. Brain Res 2000;859:381-385.
192. Martinez A, Alonso M, Castro A, Pérez C, Moreno FJ. First non-ATP competitive glycogen synthase kinase 3 beta (GSK-3beta) inhibitors: thiadiazolidinones (TDZD) as potential drugs for the treatment of Alzheimer's disease. J Med Chem 2002;45:1292-1299.
193. Saitoh M, Kunitomo J, Kimura E, Iwashita H, Uno Y, Onishi T, Uchiyama N, Kawamoto T, Tanaka T, Mol CD, Dougan DR, Textor GP, Snell GP, Takizawa M, Itoh F, Kori M. 2-{3-[4-(Alkylsulfinyl)phenyl]-1-benzofuran-5-yl}-5-methyl-1,3,4-oxadiazole derivatives as novel inhibitors of glycogen synthase kinase-3beta with good brain permeability. J Med Chem 2009;52:6270-6286.
194. Perez DI, Gil C, Martinez A: Beta-Amyloid, Tau Protein and Glucose Metabolism. In: Martinez A, ed. Emerging drugs and targets for Alzheimer’s Disease. Cambridge: Royal Society of Chemistry; 2010:173-193.
195. Collino M, Thiemermann C, Mastrocola R, Gallicchio M, Benetti E, Miglio G, Castiglia S, Danni O, Murch O, Dianzani C, Aragno M, Fantozzi R. Treatment with the glycogen synthase kinase-3beta inhibitor, TDZD-8, affects transient cerebral ischemia/reperfusion injury in the rat hippocampus. Shock 2008;30:299-307.

196. Cuzzocrea S, Genovese T, Mazzon E, Crisafulli C, Di Paola R, Muià C, Collin M, Esposito E, Bramanti P, Thiemermann C. Glycogen synthase kinase-3 beta inhibition reduces secondary damage in experimental spinal cord trauma. J Pharmacol Exp Ther 2006;318:79-89.
197. Cuzzocrea S, Mazzon E, Di Paola R, Muià C, Crisafulli C, Dugo L, Collin M, Britti D, Caputi AP, Thiemermann C. Glycogen synthase kinase-3beta inhibition attenuates the degree of arthritis caused by type II collagen in the mouse. Clin Immunol 2006;120:57-67.
198. Dugo L, Abdelrahman M, Murch O, Mazzon E, Cuzzocrea S, Thiemermann C. Glycogen synthase kinase-3beta inhibitors protect against the organ injury and dysfunction caused by hemorrhage and resuscitation. Shock 2006;25:485-491.
199. Whittle BJ, Varga C, Posa A, Molnar A, Collin M, Thiemermann C. Reduction of experimental colitis in the rat by inhibitors of glycogen synthase kinase-3beta. Br J Pharmacol 2006;147:575-582.
200. Clinical trials 2013. A Double-Blind, Placebo-Controlled, Randomized, Parallel-Group Study Evaluating the Safety, Tolerability, and Efficacy of Two Different Oral Doses of NP031112, a GSK-3 Inhibitor, Versus Placebo in the Treatment of Patients With Mild-to-Moderate Progressive Supranuclear Palsy. www.clinicaltrials.gov. http://www.clinicaltrials.gov/ct2/show/NCT01049399?term=NP031112&rank=1. Accessed 16-03-2014.
201. Del Ser T, Steinwachs KC, Gertz HJ, et al. Treatment of Alzheimer's disease with the GSK-3 inhibitor tideglusib: a pilot study. J Alzheimers Dis 2013;33:205-215.
202. Aguilar-Morante D, Morales-Garcia JA, Sanz-SanCristobal M, Garcia-Cabezas MA, Santos A, Perez-Castillo A. Inhibition of glioblastoma growth by the thiadiazolidinone compound TDZD-8. PLoS One 2010;5:e13879.
203. Beurel E, Jope RS. Glycogen synthase kinase-3 regulates inflammatory tolerance in astrocytes. Neuroscience 2010;169:1063-1070.
204. Ramirez SH, Fan S, Dykstra H, Rom S, Mercer A, Reichenbach NL, Gofman L, Persidsky Y. Inhibition of glycogen synthase kinase 3β promotes tight junction stability in brain endothelial cells by half-life extension of occludin and claudin-5. PLoS One. 2013;8:e55972.

205. Noshita N, Lewén A, Sugawara T, Chan PH. Evidence of phosphorylation of Akt and neuronal survival after transient focal cerebral ischemia in mice. J Cereb Blood Flow Metab 2001;21:1442-1450.
206. Xuan Nguyen TL, Choi JW, Lee SB, Ye K, Woo SD, Lee KH, Ahn JY. Akt phosphorylation is essential for nuclear translocation and retention in NGF-stimulated PC12 cells. Biochem Biophys Res Commun 2006;349:789-798.
207. Yamaguchi A, Tamatani M, Matsuzaki H, Namikawa K, Kiyama H, Vitek MP, Mitsuda N, Tohyama M. Akt activation protects hippocampal neurons from apoptosis by inhibiting transcriptional activity of p53. J Biol Chem 2001;276:5256-5264.
208. Lan R, Xiang J, Zhang Y, Wang GH, Bao J, Li WW, Zhang W, Xu LL, Cai DF. PI3K/Akt Pathway Contributes to Neurovascular Unit Protection of Xiao-Xu-Ming Decoction against Focal Cerebral Ischemia and Reperfusion Injury in Rats. Evid Based Complement Alternat Med. 2013:2013:459-467.
209. Xie R, Cheng M, Li M, Xiong X, Daadi M, Sapolsky RM, Zhao H. Akt isoforms differentially protect against stroke-induced neuronal injury by regulating mTOR activities. J Cereb Blood Flow Metab 2013;33:1875-1885.
210. Saunders DE, Clifton AG, Brown MM. Measurement of infarct size using MRI predicts prognosis in middle cerebral artery infarction. Stroke 1995;26:2272-2276.
211. Tourdias T, Renou P, Sibon I, Asselineau J, Bracoud L, Dumoulin M, Rouanet F, Orgogozo JM, Dousset V. Final cerebral infarct volume is predictable by MR imaging at 1 week. AJNR Am J Neuroradiol. 2011;32:352-358.

# 9 PUBLICATIONS

1. Ratilal BO, Arroja MM, Rocha JP, Fernandes AM, Barateiro AP, Brites DM, Pinto RM, Sepodes BM, Mota-Filipe HD. Neuroprotective effects of erythropoietin pretreatment in a rodent model of transient middle cerebral artery occlusion. **Journal of Neurosurgery** 2014 Jul;121(1):55-62.

2. Ratilal BO, Rocha JP, Fernandes AM, Arroja MM, Barateiro AP, Brites DM, Pinto RM, Sepodes BM, Mota-Filipe HD. TDZD-8 pre-treatment in transient middle cerebral artery occlusion. **Biomedicine & Aging Pathology** 2014 Oct;4(4):361-367.

**DOI:** 10.3171/2014.2.JNS132197


# Neuroprotective effects of erythropoietin pretreatment in a rodent model of transient middle cerebral artery occlusion

## Laboratory investigation

**Bernardo Oliveira Ratilal, M.Sc.,[1] Mariana Moreira Coutinho Arroja, B.Sc.,[2] Joao Pedro Fidalgo Rocha, Ph.D.,[2] Adelaide Maria Afonso Fernandes, Ph.D.,[3] Andreia Pereira Barateiro, Ph.D.,[3] Dora Maria Tuna Oliveira Brites, Ph.D.,[3] Rui Manuel Amaro Pinto, Ph.D.,[2] Bruno Miguel Nogueira Sepodes, Ph.D.,[2] and Helder Dias Mota-Filipe, Ph.D.[2]**

*[1]Department of Neurosurgery, Hospital de São José, Centro Hospitalar de Lisboa Central; [2]Pharmacology & Translational Research, Faculdade de Farmácia, Universidade de Lisboa; and [3]Department of Biochemistry and Human Biology, Faculdade de Farmácia, Universidade de Lisboa, Portugal*

*Object*. There is an unmet clinical need to develop neuroprotective agents for neurosurgical and endovascular procedures that require transient cerebral artery occlusion. The aim in this study was to explore the effects of a single dose of recombinant human erythropoietin (rhEPO) before middle cerebral artery (MCA) occlusion in a focal cerebral ischemia/reperfusion model.

*Methods*. Twenty-eight adult male Wistar rats were subjected to right MCA occlusion via the intraluminal thread technique for 60 minutes under continuous cortical perfusion monitoring by laser Doppler flowmetry. Rats were divided into 2 groups: control and treatment. In the treated group, rhEPO (1000 IU/kg intravenously) was administered 10 minutes before the onset of the MCA ischemia. At 24-hour reperfusion, animals were examined for neurological deficits, blood samples were collected, and animals were killed. The following parameters were evaluated: brain infarct volume, ipsilateral hemispheric edema, neuron-specific enolase plasma levels, parenchyma histological features (H & E staining), Fluoro-Jade–positive neurons, p-Akt and total Akt expression by Western blot analysis, and p-Akt–positive nuclei by immunohistochemical investigation.

*Results*. Infarct volume and Fluoro-Jade staining of degenerating neurons in the infarct area did not vary between groups. The severity of neurological deficit ($p < 0.001$), amount of brain edema (78% reduction in treatment group, $p < 0.001$), and neuron-specific enolase plasma levels ($p < 0.001$) were reduced in the treatment group. Perivascular edema was histologically less marked in the treatment group. No variations in the expression or localization of p-Akt were seen.

*Conclusions*. Administration of rhEPO before the onset of 60-minute transient MCA ischemia protected the brain from this insult. It is unlikely that rhEPO pretreatment leads to direct neuronal antiapoptotic effects, as supported by the lack of Akt activation, and its benefits are most probably related to an indirect effect on brain edema as a consequence of blood-brain barrier preservation. Although research on EPO derivatives is increasing, rhEPO acts through distinct neuroprotective pathways and its clinical safety profile is well known. Clinically available rhEPO is a potential therapy for prevention of neuronal injury induced by transitory artery occlusion during neurovascular procedures.
*(http://thejns.org/doi/abs/10.3171/2014.2.JNS132197*

**Key Words** • **neuroprotection** • **rat** • **recombinant human erythropoietin** • **transient focal cerebral ischemia** • **vascular disorders**

Transient vessel occlusion may be unavoidable during neurosurgical or endovascular procedures and might lead to brain damage. Unlike in stroke patients, to which most cerebral ischemia animal studies refer,[19,28] in patients undergoing neurovascular procedures the onset of temporary artery occlusion can be planned in advance, allowing the best timing for preventive maneuvers or neuroprotective drug administration to be performed, even before the onset of ischemia.

The risk of brain infarction with temporary artery occlusion in patients undergoing clip ligation for cerebral aneurysm has been reported to be as high as 45%.[16] Brain

*Abbreviations used in this paper:* BBB = blood-brain barrier; BSA = bovine serum albumin; CBF = cerebral blood flow; CCA = common carotid artery; ECA = external carotid artery; EPO, EPOR = erythropoietin, erythropoietin receptor; GSK-3β = glycogen synthase kinase–3β; ICA = internal carotid artery; I/R = ischemia/reperfusion; MCA = middle cerebral artery; NF-κB = nuclear factor–kappa B; NSE = neuron-specific enolase; PBS = phosphate-buffered saline; PI3K = phosphatidylinositol 3–kinase; rhEPO = recombinant human EPO.

This article contains some figures that are displayed in color online but in black-and-white in the print edition.

tolerance to reperfusion injury depends on several features, such as the degree, size, location, and duration of the ischemia; presence of subarachnoid blood; timing of surgery; patient's age; body temperature; genetic factors; and other comorbidities. Reperfusion injury is attributed to numerous events, including inflammatory response, oxidative stress, loss of blood-brain barrier (BBB) integrity, cerebral edema, and hemorrhagic transformation.[22] Particularly, focal ischemia followed by reperfusion leads to severe damage to the BBB integrity, allowing water and macromolecules to cross into brain tissue as early as 20–45 minutes following permanent middle cerebral artery (MCA) occlusion.[15] The detrimental edema further reduces focal blood flow, and induces cell necrosis and apoptosis.[37] Furthermore, widespread interactions among BBB disruption, edema formation, and lower blood flow become a vicious cycle, which accelerates brain damage.

Erythropoietin (EPO), a 30.4-kD glycoprotein, is a natural hormone originally identified for its role in erythropoiesis and successfully used for anemia treatment in the last 2 decades. The finding that EPO and its receptor (EPOR) are expressed throughout the brain in glial cells, neurons, and endothelial cells suggested that EPO could have hematopoiesis-independent effects on the nervous system.[18,27] Endogenously produced EPO and/or expression of EPOR gives rise to autocrine and paracrine signaling in different organs, particularly during hypoxia, toxicity, and injury conditions. In the brain, EPO mRNA levels have been shown to remain elevated for more than 24 hours during the duration of the hypoxic stimuli.[8] Accordingly, following ischemic/hypoxic injury, dramatic changes have been reported in the expression of EPO and EPOR within and around infarcts in human brain regions.[36] Erythropoietin has been shown to regulate a variety of cell functions such as ionic balance, neurotransmitter synthesis, and cell survival.[40,41] Research has also shown that a high dose of systemically administered recombinant human EPO (rhEPO) crosses the BBB, leading to neuroprotective and neurotrophic effects.[5,7] As a result, several trials are currently ongoing to identify possible benefits in the usage of rhEPO for specific clinical situations requiring neuroprotection (http://clinicaltrials.gov/show/NCT01732146; http://clinicaltrials.gov/show/NCT00513240; http://clinicaltrials.gov/show/NCT01378273).

To our knowledge, we present the first animal study based on an MCA ischemia/reperfusion (I/R) model aiming to investigate the potential benefits of a single dose of 1000 IU/kg intravenous rhEPO as a possible pretreatment against neuronal damage in neurovascular procedures that require transient cerebral artery occlusion. The selected dose and route has been used in several clinical trials with no identified additional safety concerns, and thus could be safely translated to the clinical setting.[9,13,29]

## Methods

A total of 28 adult male Wistar rats weighing between 240 and 340 g and housed under diurnal light conditions with unlimited access to food and water were used (14 per group). Animal care followed the recommendations of the European Convention for the Protection of Vertebrate Animals Used for Experimental and Other Scientific Purposes (Council Directive 86/609/EEC) and National Law 1005/92 (rules for protection of experimental animals). The Institutional Animal Care and Use Committee approved all animal procedures. All efforts were made to minimize animal suffering and to reduce the number of animals used.

### *Erythropoietin Administration*

A dose of 1000 IU/kg rhEPO (epoietin β, Hoffmann-La Roche) was administered intravenously in the tail vein 10 minutes before the onset of ischemia. The control group had the same volume of saline administered similarly.

### *Middle Cerebral Artery Ischemia-Reperfusion*

Food was withheld from rats 12 hours prior to surgery. Anesthesia was induced by intraperitoneal administration of a ketamine (80 mg/kg) and xylazine (8 mg/kg) mixture, supplemented as needed. Anesthetized rats were placed on a thermostatically controlled heating pad, a rectal probe was inserted, and body temperature was monitored and maintained between 36.5°C and 37.5°C. Transient focal cerebral ischemia was induced by 60-minute right MCA occlusion followed by 24-hour reperfusion, as reported.[24] Briefly, under the operating microscope, the right common carotid artery (CCA), internal carotid artery (ICA), and external carotid artery (ECA) were exposed and isolated from branches through a midline neck incision. The ECA was tied and cut at approximately 5 mm from the bifurcation and a loose 6-0 silk knot was placed around the ECA origin. Afterward, microvascular clips were placed on the CCA and ICA, an ECA stump arteriotomy distal to the loose knot was performed, and a 4-0 nylon silicone monofilament with a rubber-coated tip (Doccol Corp.) was inserted. The suture that had been placed around the ECA stump and intraluminal nylon filament was tightened to prevent bleeding and the clips were removed. The filament was then gently introduced (19–21 mm) into the ICA to the level where the MCA branches out, until the laser Doppler signal decreased to less than 30% of baseline, occluding the right MCA at its origin at the circle of Willis. After a 60-minute period of ischemia the thread was cautiously removed, reestablishing the blood flow in the MCA. The ECA was permanently ligated at the level of bifurcation. Animals were allowed to recover and then were killed with an anesthetic overdose at 24 hours into reperfusion.

### *Blood Flow Measurements*

Cortical cerebral blood flow (CBF) was monitored by laser Doppler flowmetry (PeriFlux 4000 System, Probe 407; Perimed Instruments) in the supply territory of the right MCA where transient ischemia was to be induced; CBF was measured before, during occlusion, and within 1 hour of reperfusion. A small bur hole was drilled 2 mm posterior to the bregma and 3.5 mm lateral to the midline, and the micro-Doppler probe was positioned above the dura mater in a holder glued to the bone. Steady-state baseline values were recorded before occlusion, and the

CBF measured during occlusion and reperfusion was expressed as a percentage of the baseline values. Rats with CBF patterns suggesting subarachnoid hemorrhage, incomplete ischemia (CBF did not decrease to a maximum of 30% of baseline), or incomplete reperfusion (CBF did not recover to more than 80% of baseline within 30 minutes of filament withdrawal) were excluded and replaced.

*Neurological Examination*

At 24 hours, a 9-point-scale neurological test (0 = normal to 9 = highest handicap) was performed in the rats, as previously described.[20] Four tests were performed by an observer who was blinded to the treatment groups to assess the following: 1) spontaneous activity (moving/exploring = 0, moving without exploration = 1, no displacement = 2); 2) laterality in movement (symmetrical = 0, left drifting when elevated by the tail = 1, spontaneous left drifting = 2, circling to the left without displacement or spinning = 3); 3) resistance to left forepaw stretching (no stretching allowed = 0, stretching allowed = 1, no resistance = 2); and 4) parachute reflex (symmetrical = 0, asymmetrical = 1, contralateral forelimb retracted = 2). Scores for each test were added to obtain the final neurological score.

*Infarct Volume and Brain Edema Assessment*

The brains were removed, placed in a brain matrix (World Precision Instrument), and sliced in 2-mm-thick coronal sections, beginning 2 mm from the frontal pole and ending rostral to the corticocerebellar junction, resulting in 6 slices per animal (8 rats per group). The sections were stained in 2% 2,3,5-triphenyltetrazolium chloride (Sigma-Aldrich) saline solution for 10 minutes at 37°C in the dark and fixed in 4% paraformaldehyde at 4°C overnight. Sections were scanned and analyzed using ImageJ software (version 1.45). Brain infarction was visualized as areas of unstained (white) tissue, which contrasted from brick-red–stained areas of viable tissue. Summing the infarct area of each coronal slice and multiplying that number by the thickness of the sections allowed the calculation of the total infarct volume. Right and left hemisphere volumes were calculated similarly. The amount of infarction was expressed in absolute terms in cubic millimeters and as a percentage of the infarct volume in the whole forebrain, adjusted for brain edema.[38] An index of brain edema was assessed by calculating the percent increase of size of the ipsilateral (injured) hemisphere compared with the contralateral (uninjured) hemisphere. A single observer blinded to the individual treatment performed the analysis described.

*Determination of Neuron-Specific Enolase Plasma Levels*

Blood samples were taken by puncture of the left cardiac ventricle prior to killing. Blood was centrifuged at 10,000 rpm for 10 minutes and the isolated serum was frozen and stored until time of assay. Serum neuron-specific enolase (NSE) measurements were performed with an electrochemiluminescence immunoassay by using a sandwich technique with double monoclonal antibodies directed against NSE and an Elecsys 2010 analyzer (antibodies and apparatus both from Roche Diagnostics). Data were normalized to nanograms per milliliter of plasma.

*Histological and Immunohistochemical Procedures*

Rat brains were removed, fixed in 4% paraformaldehyde in phosphate-buffered saline (PBS) for 72 hours at room temperature, dehydrated through a graded ethanol series, and embedded in paraffin (3 per group). Then, H & E staining was performed as previously described[11] and images were acquired using a bright-field microscope (Axioskop, Zeiss).

For Fluoro-Jade staining, 6-μm-thick coronal sections were deparaffinized and rehydrated. Slides were first immersed in 100% alcohol for 3 minutes, followed by 1 minute in 70% alcohol and 1 minute in distilled water. The slides were then transferred to a solution of 0.06% potassium permanganate for 15 minutes on a shaker table and protected from light. After that the slides were rinsed in distilled water for 1 minute and immersed in Fluoro-Jade B (Chemicon) staining solution 0.001% for 30 minutes with moderate agitation. Slides were rinsed for 1 minute in each of 3 distilled water washes and dried at room temperature. The dry slides were cleared by immersion in xylene for at least 1 minute before coverslipping with DPX (Fluka or Sigma-Aldrich. The tissue was then examined using an epifluorescent microscope (Axioskop, Zeiss) with blue (450–490 nm) excitation light. The number of positive Fluoro-Jade B–positive neurons was counted in 4 sections of 0.16 $\mu m^2$ (3 per group) within the region of interest by using ImageJ software version 1.45 and the total was expressed as positive cells/section.

For immunostaining, 6-μm-thick coronal sections were submitted to antigen retrieval in 20 mM citrate buffer with 1.5% $H_2O_2$ for 15 minutes at room temperature in the dark, incubated for 10 minutes in Tris/EDTA buffer at 84°C, and blocked for 1 hour at room temperature in 1% bovine serum albumin (BSA) in PBS. Primary antibody, rabbit anti–p-Akt (1:100, Cell Signaling Technology) was used in 0.5% BSA in PBS overnight at 4°C. After washing in PBS, sections were incubated for 1 hour at room temperature with anti–rabbit antibodies coupled to AlexaFluor 568 (#A11077, 1:1000; Invitrogen) in 0.5% BSA in PBS, incubated for 20 minutes in DAPI, and mounted with Shandon Immu-Mount Aqueous Nonfluorescing Mounting Medium (Thermo Scientific). Tissue sections were visualized with an epifluorescent microscope (Axioskop, Zeiss), and the total number of nuclei (those with DAPI staining) and those positive for p-Akt were counted to present the results as percentage of p-Akt–positive nuclei (2 sections within the region of interest; 3 per group).

*Western Blot Analysis*

For Western blot analysis (3 per group), cells from frozen tissue samples were lysed in RIPA (radioimmunoprecipitation assay) buffer containing Tris 50 mM (pH 8.0), 5 mM EDTA (pH 8.0), 150 mM NaCl, 1% NP-40, 10% glycerol, and 0.1% sodium dodecyl sulfate, and sonicated for 20 seconds. The lysate was centrifuged at 14,000 *g* for 10 minutes at 4°C and the supernatants were collected and stored at −80°C. Protein concentrations

were determined using Nanodrop ND-1000. Cell extracts containing equal amounts of protein (100–150 μg) were separated on sodium dodecyl sulfate-polyacrylamide gel electrophoresis and transferred to a nitrocellulose membrane. The membranes were blocked with 5% nonfat milk, incubated with the primary antibodies overnight at 4°C (anti–rabbit p-Akt [1:1000, #12178; Cell Signaling], and anti–rabbit Akt [1:1000, #4691; Cell Signaling]), and then with a horseradish peroxidase-labeled secondary antibody for 1 hour at room temperature. After extensive washes, immunoreactive bands were detected by LumiGLO (Cell Signaling) and visualized by autoradiography with Hyperfilm ECL. Phosphorylation levels of Akt were analyzed by the ratio of p-Akt to total Akt levels and expressed as "-fold" change.

*Statistical Analysis*

Statistical analysis was performed using GraphPad Prism software, version 6.0. Parametric data were analyzed using the Student t-test for single comparisons between groups, and nonparametric data (neurological scores) were subjected to the 2-tailed Mann-Whitney test. Data are presented as the mean ± SEM for "n" observations, where "n" represents the number of animals studied. For histological scoring and Western blot analysis, each data point represents analyses of brain sections obtained in 3 individual rats. A p value of ≤ 0.05 was the threshold for a statistically significant difference or association.

## Results

All animals lost between 10% and 18% of body weight during the 24-hour recovery period, with no significant differences between groups. Normothermia was maintained in all animals. There were no significant differences between groups with respect to CBF pattern and glycemia values during the procedure.

Results showed no difference between groups in the infarct volume. The total brain infarct volume was 265.46 ± 13.88 $mm^3$ for the control group and 223.33 ± 12.97 $mm^3$ for the treatment group. Expressed as a percentage,[38] infarct volume was 28.02% ± 1.73% in the control group and 25.71% ± 1.41% in the rhEPO group (Fig. 1). Also, the number of positive Fluoro-Jade degenerating neurons in the area of interest was similar between groups (Fig. 2). Brain swelling index was significantly decreased in the treatment group when compared with the control group (2.11% ± 0.46% and 9.74% ± 1.39%, respectively; $p < 0.001$) (Fig. 3). Accordingly, histological analysis of the brain parenchyma (with H & E staining) revealed neuropil spongiosis and perivascular edema, which was less marked in the rhEPO-treated group (Fig. 4). The treatment group had significantly lower NSE plasma levels compared with the control group (1.17 ± 0.07 ng/ml compared with 1.88 ± 0.07 ng/ml; $p < 0.001$) (Fig. 5). This was a relevant parameter for assessing the prognosis of cerebral hypoxia-ischemia, and presented significantly reduced neurological deficits ($p < 0.001$) (Fig. 6). Although it is believed that EPO activates Akt, no differences were found between groups for the p-Akt/Akt ratio in Western blot analysis (Fig. 7) and for percentage of p-Akt–positive nuclei in immunohistochemical studies (data not shown).

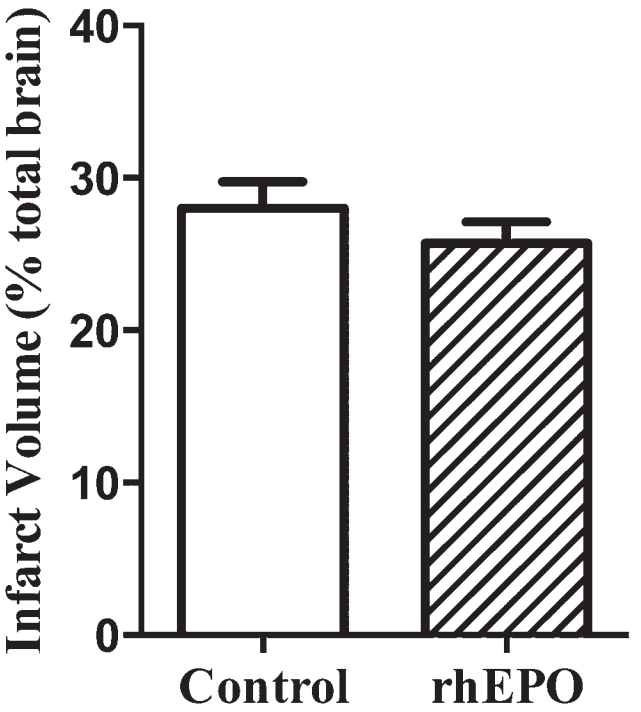


Fig. 1. Bar graph comparing total infarct volume between control and rhEPO-treated groups. Infarct volumes are presented as percentages of the total volume of forebrain. Data represent the mean ± SEM (8 per group). Differences between groups were not significant.

## Discussion

Our study reveals that rhEPO exerts protective effects in focal cerebral I/R. This is in line with the tissue-protective effects of rhEPO described in several animal models of I/R injury, as demonstrated by our research group.[25,30] Recombinant human EPO has been consistent-

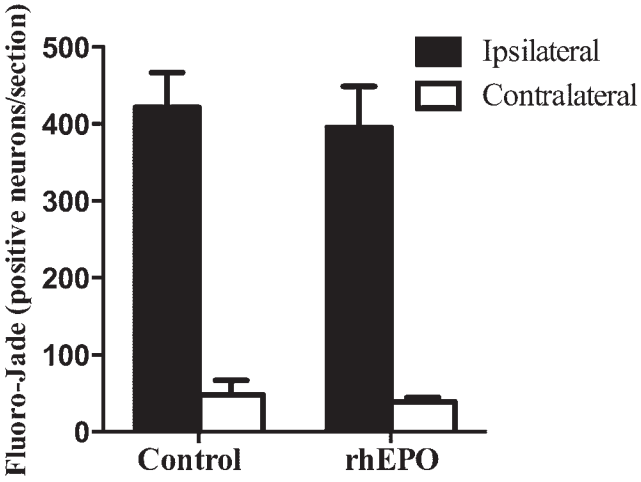


Fig. 2. Bar graph comparing the number of positive Fluoro-Jade neurons in the area of interest in the ipsilateral and contralateral hemispheres. Data represent the mean ± SEM (4 × 0.16–$\mu m^2$ sections for each specimen; 3 per group). Values were not significant.

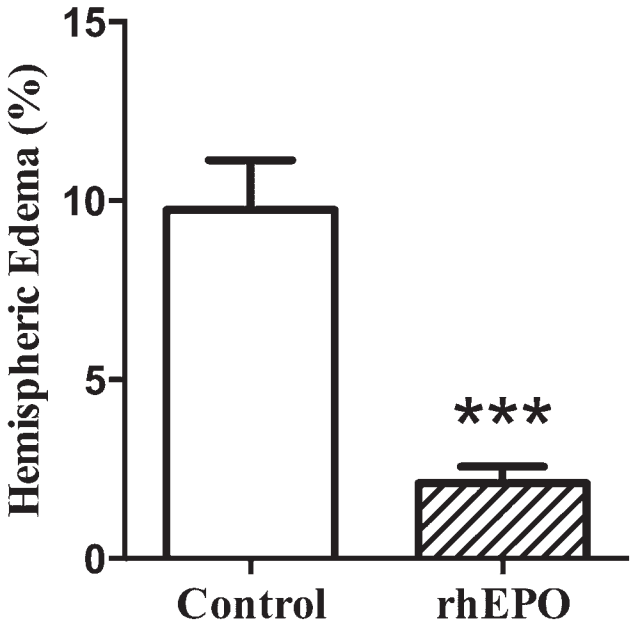


**Fig. 3.** Bar graph depicting the percentage of hemispheric edema in both control and rhEPO-treated groups. Data represent the mean ± SEM (8 per group). Values were significant, representing a 78% reduction of ipsilateral hemispheric edema in the treatment group compared with control group. ***p < 0.001.

ly tested at high doses (> 5000 IU/kg) in rodent models of permanent cerebral artery occlusion, and has been shown to be more effective when administered within 6 hours after stroke onset.[28] We investigated the effects of a single lower dose of rhEPO as a pretreatment (1000 IU/kg) in an I/R rodent model. The dose used has been safely tested in humans.[9,13,29] Our results suggest that intravenous administration of a single 1000-IU/kg dose of rhEPO just prior to a transitory occlusion of a cerebral artery may decrease secondary brain insult, resulting in a better neurological outcome.

Regarding infarct volume outcome, we found no differences between groups at 24-hour reperfusion, although the improved neurological status and significantly lower NSE plasma levels observed at that point could indicate that this outcome may change over time between groups. Because NSE is an enzyme that is rapidly released by injured neurons, lower NSE plasma levels in the treatment group may suggest a smaller penumbra area and a better clinical outcome. Plasma levels reach their maximum at 24 hours, and the best correlation between infarct size and plasma levels occurs at Day 3.[14] Plasma levels of this kinase have been found to be increased even before the onset of clinical symptoms, and are strongly correlated with the clinical score and histological damage when clinical symptoms are present.[14] The NSE plasma levels probably reflect neuronal cell death, suggesting that NSE is a reliable marker when used to follow neuronal damage.[1]

There is evidence that EPO treatment activates the antiapoptotic molecule Akt.[31,32] On phosphorylation, the serine-threonine kinase Akt promotes cell survival by inactivating several targets, including cell-death antagonist BCL-2, glycogen synthase kinase–3β (GSK-3β), and caspase-9, or else it activates prosurvival molecules,[33] suggesting that the phosphatidylinositol 3–kinase (PI3K)/

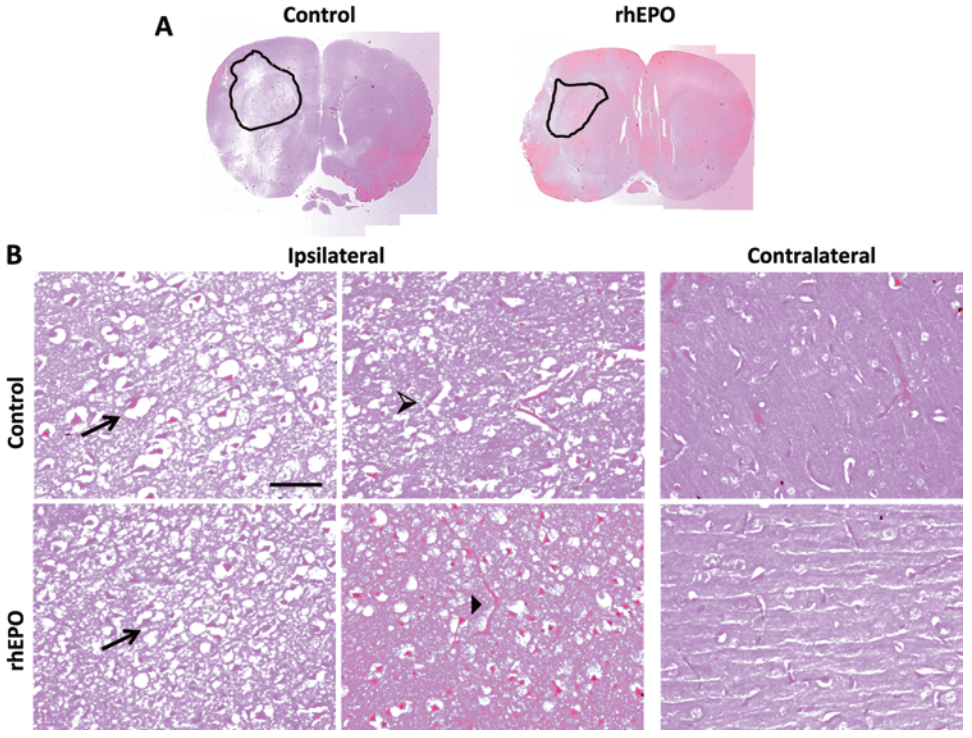


**Fig. 4.** Representative photomicrographs of brain sections obtained in control and rhEPO-treated rats. **A:** Whole-brain-section images with delineated infarct areas. **B:** Cerebrovascular changes in the infarct area: neuropil spongiosis *(arrows)* and perivascular edema *(black-and-white arrowhead)* in control animals or its absence *(black arrowhead)* in rhEPO-treated ones. Contralateral hemispheres had no relevant changes. H & E. Bar = 200 μm.

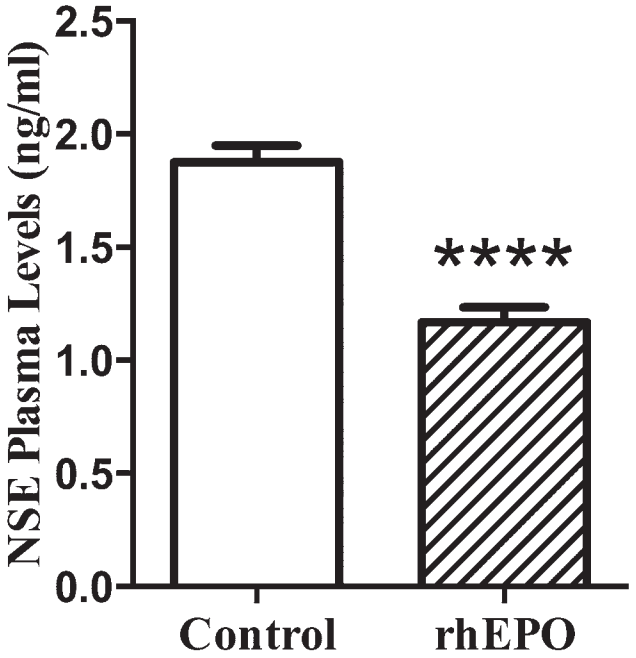


**Fig. 5.** Bar graph showing a 38% reduction of NSE plasma levels at 24 hours of reperfusion in the rhEPO-treated group. Data represent the mean ± SEM (n = 8 for control and 13 for treatment group). ****p < 0.001.

Akt/GSK-3β pathway is involved in the neuroprotective effect of rhEPO.[31] Phosphorylation of Akt is coupled to its nuclear translocation where it phosphorylates nuclear targets, suppressing the transcription of death genes.[6] Unexpectedly, our results did not show an increase in the

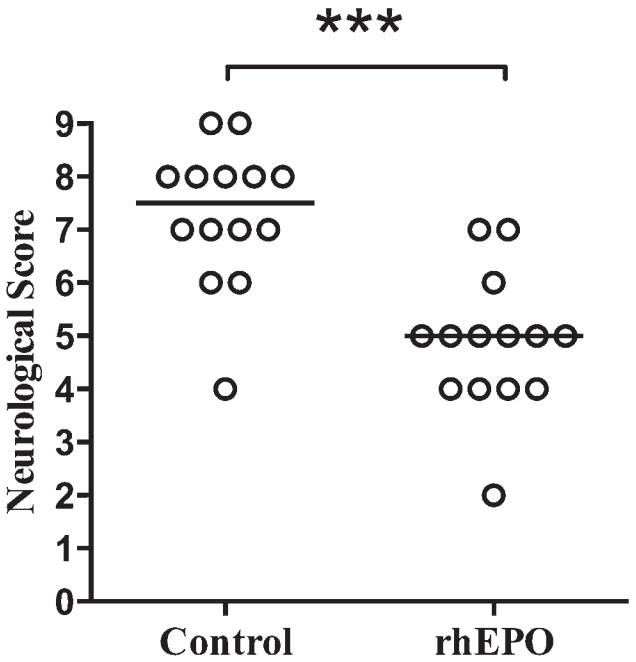


**Fig. 6.** Scatterplot showing the effects of rhEPO at 24 hours on a 9-point neurological scale (14 per group). *Open circles* indicate values for individual animals. *Horizontal bars* indicate group median values. The rhEPO significantly reduced neurological deficits. ***p < 0.001, Mann-Whitney test.

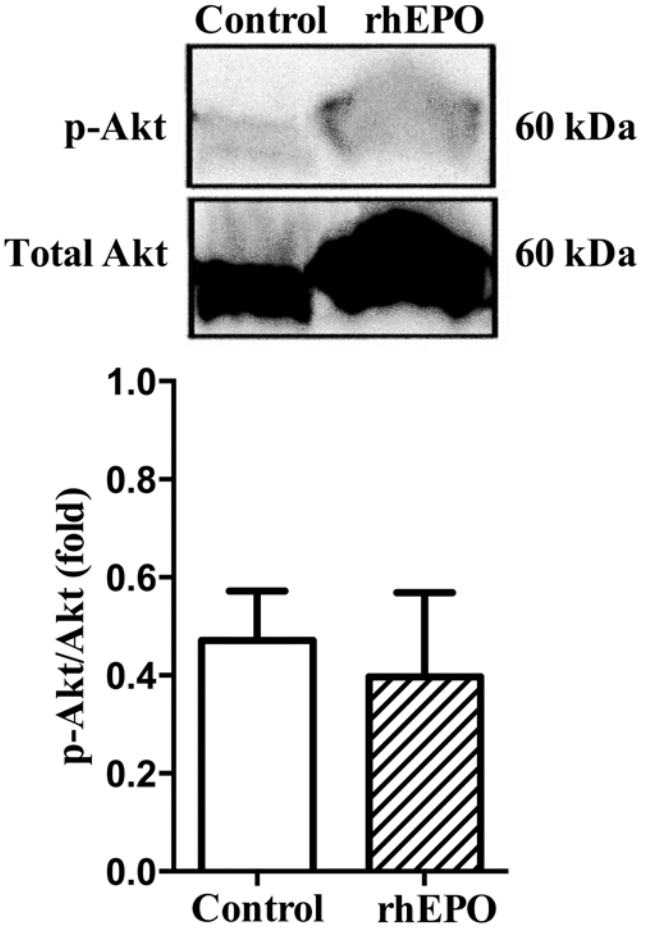


**Fig. 7.** Western blot showing expression of p-Akt and total Akt, with a bar graph showing the densitometric analysis of the relative intensity of p-Akt, normalized against total Akt. Data represent the mean ± SEM (3 per group). Results did not show differences between groups.

expression of p-Akt/Akt (Western blot) or a p-Akt nuclear translocation (immunohistochemistry). The lack of PI3K/Akt/GSK-3β pathway activation could be explained by the use of lower rhEPO doses in our study when compared with previous ones.[19,28] In fact, only up to 1% of systemically administered rhEPO crosses the BBB in primates,[21] and poor penetration into the BBB is expected even when administering up to 10,000 IU/kg intravenously as single doses.[12] This poor crossing ratio suggests that high doses of systemically administered rhEPO are needed for direct neuron-protective purposes.

On the other hand, Xiong et al.[43] have previously demonstrated that EPO significantly provides neuroprotection following traumatic brain injury in EPOR-null mice; that is, even in the absence of EPOR in the neural cells, probably mediated through vascular protection. We postulate that the benefits observed in prophylactic rhEPO administration were not due to a direct neuronal action in the infarct area but were the result of an indirect effect on brain swelling as a consequence of diminished BBB disruption. This is also in line with the histological findings and lack of difference between treatment and control groups in the number of positive Fluoro-Jade cells that label degenerating neurons.

Cerebral edema is a well-recognized factor for high morbidity and mortality in large-territory ischemic strokes.[42] Brain edema following MCA occlusion has been shown to increase gradually over the first 48 hours before peaking.[34] The reduction in brain edema from the early phase may reduce the space-occupying effect and improve regional CBF in the penumbra phase of stroke. Here we suggest that rhEPO pretreatment is associated with reduced perivascular edema and with protection of the BBB from increased permeability. These effects are probably due to activation of an EPOR-dependent intracellular pathway of the microvascular endothelium, which may inhibit the transcription factor nuclear factor–kappa B (NF-κB), upregulate expression of tight-junction proteins, and improve abnormalities in the free-radical system.[23,26]

The reperfusion phase leads to generation of reactive oxygen radicals and lipid peroxidation that are highly noxious to the brain's capillary endothelial cells and its complex tight junctions, which are mostly responsible for the integrity of the BBB.[2,4] Erythropoietin has been shown to increase nitric oxide synthesis in endothelial cells and, under oxidative stress conditions, nitric oxide may scavenge reactive oxygen species.[3,39] This detoxification also prevents membrane lipid peroxidation and consequential additional disruption of the BBB in I/R.[2] The NF-κB transcriptional activation pathway has been considered a central regulator of inflammatory response, critical to the regulation of apoptosis, and related to cell adhesion molecule expression in endothelial cells.[17] Liu et al.[23] suggested that the relation between the downregulation of NF-κB and the reversed expression of the tight junction–associated proteins is involved in the mechanism of protection of the BBB in rats with I/R injury.

We recognize some limitations on our study. We speculate that rhEPO promotes BBB integrity but we did not show direct evidence or quantify BBB permeability changes. Also, it would be interesting to perform time course experiments. These dynamics would be of both experimental and clinical relevance.

Nonerythropoietic tissue-protective EPO variants have been developed, most notably asialo-EPO (AEPO), intranasal formulations of low-sialic-acid EPO (Neuro-EPO), and carbamylated EPO (CEPO) to dissociate the erythropoietic effect from the tissue-protective effect, and thus lessen side effects.[36] However, rhEPO possesses not only neuron antiapoptotic properties but also reduces BBB leakage, enhances blood flow, and promotes angiogenesis after brain injury. It is likely that these nonneuronal effects are not shared by EPO derivatives as part of EPO's rescue effects after systemic intravenous delivery in patients. Moreover, the clinical safety profile is still under investigation in clinical trials and further research is needed before EPO variants could be used in patients.[40]

## Conclusions

We present the first evidence that rhEPO pretreatment at a dose of 1000 IU/kg, which has its safety profile in humans well described, reduces brain edema and preserves the penumbra functional neuronal pool following in vivo I/R injury. Considering that a substantial proportion of the ischemic lesion could be attributed to mechanical compression induced by brain swelling, the development of effective drugs to attenuate the formation and progression of brain edema is crucial. Because rhEPO has a higher innate capacity to cross the BBB in humans than in rodents,[10] and given the neuroprotective effects observed in the present study, we believe that clinically available rhEPO could be a potential therapy to prevent neuronal injury induced by transient ischemia during neurovascular procedures. Further research is needed to completely understand the underlying mechanisms of rhEPO and BBB interactions. A translational clinical trial could be supported.

### Acknowledgments

We acknowledge Prof. Anna Planas and her group for their help and advice on setting up this animal model. We thank Prof. João Lobo Antunes for his valuable comments in preparing this manuscript.

### Disclosure

The authors report no conflict of interest concerning the materials or methods used in this study or the findings specified in this paper.

Author contributions to the study and manuscript preparation include the following. Conception and design: Ratilal, Rocha, Fernandes, Sepodes, Mota-Filipe. Acquisition of data: Ratilal, Arroja, Rocha, Fernandes, Barateiro, Pinto. Analysis and interpretation of data: Ratilal, Arroja, Rocha, Sepodes. Drafting the article: Ratilal, Arroja, Rocha, Sepodes. Critically revising the article: all authors. Reviewed submitted version of manuscript: all authors. Approved the final version of the manuscript on behalf of all authors: Ratilal. Statistical analysis: Ratilal, Rocha. Study supervision: Brites, Mota-Filipe.

### References

1. Ahmad O, Wardlaw J, Whiteley WN: Correlation of levels of neuronal and glial markers with radiological measures of infarct volume in ischaemic stroke: a systematic review. **Cerebrovasc Dis 33:**47–54, 2012
2. Bahcekapili N, Uzüm G, Gökkusu C, Kuru A, Ziylan YZ: The relationship between erythropoietin pretreatment with blood-brain barrier and lipid peroxidation after ischemia/reperfusion in rats. **Life Sci 80:**1245–1251, 2007
3. Banerjee D, Rodriguez M, Nag M, Adamson JW: Exposure of endothelial cells to recombinant human erythropoietin induces nitric oxide synthase activity. **Kidney Int 57:**1895–1904, 2000
4. Blasig IE, Mertsch K, Haseloff RF: Nitronyl nitroxides, a novel group of protective agents against oxidative stress in endothelial cells forming the blood-brain barrier. **Neuropharmacology 43:**1006–1014, 2002
5. Brines ML, Ghezzi P, Keenan S, Agnello D, de Lanerolle NC, Cerami C, et al: Erythropoietin crosses the blood-brain barrier to protect against experimental brain injury. **Proc Natl Acad Sci U S A 97:**10526–10531, 2000
6. Brunet A, Bonni A, Zigmond MJ, Lin MZ, Juo P, Hu LS, et al: Akt promotes cell survival by phosphorylating and inhibiting a Forkhead transcription factor. **Cell 96:**857–868, 1999
7. Celik M, Gökmen N, Erbayraktar S, Akhisaroglu M, Konakc S, Ulukus C, et al: Erythropoietin prevents motor neuron apoptosis and neurologic disability in experimental spinal cord ischemic injury. **Proc Natl Acad Sci U S A 99:**2258–2263, 2002
8. Chikuma M, Masuda S, Kobayashi T, Nagao M, Sasaki R: Tissue-specific regulation of erythropoietin production in the murine kidney, brain, and uterus. **Am J Physiol Endocrinol Metab 279:**E1242–E1248, 2000

9. Dame C, Langer J, Koller BM, Fauchère JC, Bucher HU: Urinary erythropoietin concentrations after early short-term infusion of high-dose recombinant Epo for neuroprotection in preterm neonates. **Neonatology 102:**172–177, 2012
10. Ehrenreich H, Hasselblatt M, Dembowski C, Cepek L, Lewczuk P, Stiefel M, et al: Erythropoietin therapy for acute stroke is both safe and beneficial. **Mol Med 8:**495–505, 2002
11. Fischer AH, Jacobson KA, Rose J, Zeller R: Hematoxylin and eosin staining of tissue and cell sections. **Cold Spring Harbor Protoc 5:**1–2, 2008
12. Fu A, Hui EK, Lu JZ, Boado RJ, Pardridge WM: Neuroprotection in stroke in the mouse with intravenous erythropoietin-Trojan horse fusion protein. **Brain Res 1369:**203–207, 2011
13. Gao D, Ning N, Niu X, Dang Y, Dong X, Wei J, et al: Erythropoietin treatment in patients with acute myocardial infarction: a meta-analysis of randomized controlled trials. **Am Heart J 164:**715–727.e1, 2012
14. Gelderblom M, Daehn T, Schattling B, Ludewig P, Bernreuther C, Arunachalam P, et al: Plasma levels of neuron specific enolase quantify the extent of neuronal injury in murine models of ischemic stroke and multiple sclerosis. **Neurobiol Dis 59:**177–182, 2013
15. Gerriets T, Walberer M, Ritschel N, Tschernatsch M, Mueller C, Bachmann G, et al: Edema formation in the hyperacute phase of ischemic stroke. Laboratory investigation. **J Neurosurg 111:**1036–1042, 2009
16. Ha SK, Lim DJ, Seok BG, Kim SH, Park JY, Chung YG: Risk of stroke with temporary arterial occlusion in patients undergoing craniotomy for cerebral aneurysm. **J Korean Neurosurg Soc 46:**31–37, 2009
17. Harari OA, Liao JK: NF-κB and innate immunity in ischemic stroke. **Ann N Y Acad Sci 1207:**32–40, 2010
18. Hasselblatt M, Ehrenreich H, Sirén AL: The brain erythropoietin system and its potential for therapeutic exploitation in brain disease. **J Neurosurg Anesthesiol 18:**132–138, 2006
19. Jerndal M, Forsberg K, Sena ES, Macleod MR, O'Collins VE, Linden T, et al: A systematic review and meta-analysis of erythropoietin in experimental stroke. **J Cereb Blood Flow Metab 30:**961–968, 2010
20. Justicia C, Martín A, Rojas S, Gironella M, Cervera A, Panés J, et al: Anti-VCAM-1 antibodies did not protect against ischemic damage either in rats or in mice. **J Cereb Blood Flow Metab 26:**421–432, 2006
21. Juul SE, McPherson RJ, Farrell FX, Jolliffe L, Ness DJ, Gleason CA: Erytropoietin concentrations in cerebrospinal fluid of nonhuman primates and fetal sheep following high-dose recombinant erythropoietin. **Biol Neonate 85:**138–144, 2004
22. Khatri R, McKinney AM, Swenson B, Janardhan V: Blood-brain barrier, reperfusion injury, and hemorrhagic transformation in acute ischemic stroke. **Neurology 79 (13 Suppl 1):**S52–S57, 2012
23. Liu K, Sun T, Wang P, Liu YH, Zhang LW, Xue YX: Effects of erythropoietin on blood-brain barrier tight junctions in ischemia-reperfusion rats. **J Mol Neurosci 49:**369–379, 2013
24. Lourbopoulos A, Karacostas D, Artemis N, Milonas I, Grigoriadis N: Effectiveness of a new modified intraluminal suture for temporary middle cerebral artery occlusion in rats of various weight. **J Neurosci Methods 173:**225–234, 2008
25. Maio R, Sepodes B, Patel NS, Thiemermann C, Mota-Filipe H, Costa P: Erythropoietin preserves the integrity and quality of organs for transplantation after cardiac death. **Shock 35:**126–133, 2011
26. Martínez-Estrada OM, Rodríguez-Millán E, González-De Vicente E, Reina M, Vilaró S, Fabre M: Erythropoietin protects the in vitro blood-brain barrier against VEGF-induced permeability. **Eur J Neurosci 18:**2538–2544, 2003
27. Masuda S, Okano M, Yamagishi K, Nagao M, Ueda M, Sasaki R: A novel site of erythropoietin production. Oxygen-dependent production in cultured rat astrocytes. **J Biol Chem 269:**19488–19493, 1994
28. Minnerup J, Heidrich J, Rogalewski A, Schäbitz WR, Wellmann J: The efficacy of erythropoietin and its analogues in animal stroke models: a meta-analysis. **Stroke 40:**3113–3120, 2009
29. Prunier F, Bière L, Gilard M, Boschat J, Mouquet F, Bauchart JJ, et al: Single high-dose erythropoietin administration immediately after reperfusion in patients with ST-segment elevation myocardial infarction: results of the erythropoietin in myocardial infarction trial. **Am Heart J 163:**200–207.e1, 2012
30. Sepodes B, Maio R, Pinto R, Sharples E, Oliveira P, McDonald M, et al: Recombinant human erythropoietin protects the liver from hepatic ischemia-reperfusion injury in the rat. **Transpl Int 19:**919–926, 2006
31. Shang Y, Wu Y, Yao S, Wang X, Feng D, Yang W: Protective effect of erythropoietin against ketamine-induced apoptosis in cultured rat cortical neurons: involvement of PI3K/Akt and GSK-3 beta pathway. **Apoptosis 12:**2187–2195, 2007
32. Shen J, Wu Y, Xu JY, Zhang J, Sinclair SH, Yanoff M, et al: ERK- and Akt-dependent neuroprotection by erythropoietin (EPO) against glyoxal-AGEs via modulation of Bcl-xL, Bax, and BAD. **Invest Ophthalmol Vis Sci 51:**35–46, 2010
33. Signore AP, Weng Z, Hastings T, Van Laar AD, Liang Q, Lee YJ, et al: Erythropoietin protects against 6-hydroxydopamine-induced dopaminergic cell death. **J Neurochem 96:**428–443, 2006
34. Silasi G, MacLellan CL, Colbourne F: Use of telemetry blood pressure transmitters to measure intracranial pressure (ICP) in freely moving rats. **Curr Neurovasc Res 6:**62–69, 2009
35. Sirén AL, Fasshauer T, Bartels C, Ehrenreich H: Therapeutic potential of erythropoietin and its structural or functional variants in the nervous system. **Neurotherapeutics 6:**108–127, 2009
36. Sirén AL, Knerlich F, Poser W, Gleiter CH, Brück W, Ehrenreich H: Erythropoietin and erythropoietin receptor in human ischemic/hypoxic brain. **Acta Neuropathol 101:**271–276, 2001
37. Spatz M: Past and recent BBB studies with particular emphasis on changes in ischemic brain edema: dedicated to the memory of Dr. Igor Klatzo. **Acta Neurochir Suppl 106:**21–27, 2010
38. Swanson RA, Morton MT, Tsao-Wu G, Savalos RA, Davidson C, Sharp FR: A semiautomated method for measuring brain infarct volume. **J Cereb Blood Flow Metab 10:**290–293, 1990
39. Utepbergenov DI, Mertsch K, Sporbert A, Tenz K, Paul M, Haseloff RF, et al: Nitric oxide protects blood-brain barrier in vitro from hypoxia/reoxygenation-mediated injury. **FEBS Lett 424:**197–201, 1998
40. Velly L, Pellegrini L, Guillet B, Bruder N, Pisano P: Erythropoietin 2nd cerebral protection after acute injuries: a double-edged sword? **Pharmacol Ther 128:**445–459, 2010
41. Vogel J, Gassmann M: Erythropoietic and non-erythropoietic functions of erythropoietin in mouse models. **J Physiol 589:**1259–1264, 2011
42. Walberer M, Ritschel N, Nedelmann M, Volk K, Mueller C, Tschernatsch M, et al: Aggravation of infarct formation by brain swelling in a large territorial stroke: a target for neuroprotection? Laboratory investigation. **J Neurosurg 109:**287–293, 2008
43. Xiong Y, Mahmood A, Qu C, Kazmi H, Zhang ZG, Noguchi CT, et al: Erythropoietin improves histological and functional outcomes after traumatic brain injury in mice in the absence of the neural erythropoietin receptor. **J Neurotrauma 27:**205–215, 2010

Manuscript submitted October 8, 2013.
Accepted February 27, 2014.
Please include this information when citing this paper: published online April 4, 2014; DOI: 10.3171/2014.2.JNS132197.

*Address correspondence to:* Bernardo Oliveira Ratilal, M.Sc., Department of Neurosurgery, Hospital São José—Centro Hospitalar de Lisboa Central, Rua José António Serrano, 1150-199 Lisboa, Portugal. email: bratilal@yahoo.com.

Biomedicine & Aging Pathology 4 (2014) 361–367

Available online at
ScienceDirect
www.sciencedirect.com

Elsevier Masson France
EM|consulte
www.em-consulte.com/en

Original article

# TDZD-8 pre-treatment in transient middle cerebral artery occlusion

Bernardo Oliveira Ratilal[a,*], João Pedro Fidalgo Rocha[b], Adelaide Maria Afonso Fernandes[c], Mariana Moreira Coutinho Arroja[b], Andreia Pereira Barateiro[c], Dora Maria Tuna Oliveira Brites[c], Rui Manuel Amaro Pinto[b], Bruno Miguel Nogueira Sepodes[b], Helder Dias Mota-Filipe[b]

[a] Department of Neurosurgery, Hospital de São José, Centro Hospitalar de Lisboa Central, Lisboa, Portugal
[b] Pharmacology and Translational Research, Faculdade de Farmácia, Universidade de Lisboa, Lisboa, Portugal
[c] Department of Biochemistry and Human Biology, Faculdade de Farmácia, Universidade de Lisboa, Lisboa, Portugal

ARTICLE INFO

*Article history:*
Received 13 June 2014
Accepted 10 July 2014
Available online 15 August 2014

*Keywords:*
GSK-3β inhibitor
Intracranial aneurysm surgery
Ischemia-reperfusion
Neuroprotection
Transient focal cerebral ischemia

ABSTRACT

There is an unmet clinical need to develop neuroprotective agents for cerebrovascular procedures requiring transient cerebral artery occlusion. This study aims to investigate the effects of a single pre-treatment dose of 4-benzyl-2-methyl-1,2,4-thiadiazolidine-3,5-dione (TDZD-8), a glycogen synthase kinase-3β (GSK-3β) inhibitor, in a transient focal cerebral ischemia model. Twenty-eight male adult Wistar rats were subjected to right middle cerebral artery (MCA) occlusion via intraluminal thread technique for 60 min under continuously cortical perfusion monitoring by laser-Doppler flowmetry. Rats were divided into two groups: control or treatment groups. In the treated group, TDZD-8 (5 mg/kg; intravenously) was administered 10 min before the onset of the MCA ischemia. At 24-h reperfusion, the following parameters were evaluated: neurological deficits, brain infarct volume, ipsilateral hemispheric oedema, neuron specific enolase (NSE) plasma levels, parenchyma histology (H–E staining), Fluoro-Jade positive neurons, p-Akt and total Akt expression by western blot analysis and p-Akt-positive nuclei by immunohistochemistry. Infarct volume ($P < 0.001$) and neurological deficits severity ($P < 0.001$) were reduced in TDZD-8 treated group. TDZD-8 attenuated hemispheric oedema ($P < 0.001$), prevented the NSE plasma level increase ($P < 0.001$) and diminished the number of degenerated neurons in the infarct area ($P < 0.001$), as shown by Fluoro-Jade staining. TDZD-8 treated rats showed few signs of perivascular oedema when compared to control group. No variations in total Akt and p-Akt expression were observed; instead immunohistochemistry showed increased p-Akt nucleus translocation in TDZD-8 treated rats ($P < 0.05$). TDZD-8 is a potential pre-treatment intraoperative drug to prevent neuronal injury induced by transitory artery occlusion during cerebrovascular procedures.



## 1. Introduction

The use of elective transient artery occlusion in intracranial aneurysm surgery is widely accepted and it is sometimes an essential approach to decrease the risk of intraoperative rupture, facilitate safer dissection of the aneurysm neck and perforators, allow precise clip placement, and open the aneurysm for thrombus or atheroma removal. Generally, it is recommended to limit the duration of temporary occlusion to brief periods, restricting to less than 10 min to avoid ischemic damage and neurologic complications [1,2]. Still, up to 45% of patients undergoing clipping surgery with transient vessel occlusion experience brain infarct [2].

Brain ischemia leads to cell mitochondrial dysfunction that result in a rapid loss of high-energy phosphate compounds and generalized cell depolarization. Nevertheless, when ischemia is induced for a short period of time, the recovery of energy metabolism during reperfusion can restore ionic imbalance. Reperfusion itself may, however, lead to brain damage due to numerous events, including inflammatory response, oxidative stress, blood-brain barrier (BBB) disruption, cerebral oedema and haemorrhagic transformation. The paradox of reperfusion injury can be understood in terms of counter-adaptive changes occurring during

*Abbreviations:* BBB, Blood-brain barrier; CBF, Cerebral blood flow; CCA, Common carotid artery; ECA, External carotid artery; GSK, Glycogen synthase kinase; H–E, Hematoxilin–Eosin; ICA, Internal carotid artery; MCA, Middle cerebral artery; NSE, Neuron specific enolase; TDZD-8, 4-Benzyl-2-methyl-1,2,4-thiadiazolidine-3,5-dione, thiadiazolidinone-8; TTC, Triphenyltetrazolium chloride.

* Corresponding author. Department of Neurosurgery, Hospital de São José – Centro Hospitalar de Lisboa Central, Rua José António Serrano, 1150-199 Lisboa, Portugal Tel.: +351218841479; fax: +351218841052.
*E-mail address:* bratilal@yahoo.com (B.O. Ratilal).

http://dx.doi.org/10.1016/j.biomag.2014.07.005
2210-5220/

cerebral ischemia that predispose the tissues to cellular dysfunction, apoptosis, and necrosis during the reperfusion phase. Although extensive research has been made exploring these molecular pathways, so far, there are no effective neuroprotective drugs for patients undergoing transient cerebral artery occlusion [3]. Also, the enthusiasm regarding the use of intraoperative hypothermia as a neuroprotective adjunct has decreased in latest years, highlighting the need for the development of novel neuroprotective agents and strategies [4–6].

Glycogen synthase kinase-3 (GSK-3), a cytoplasmic serine/threonine protein kinase, was originally described as a component of the metabolic pathway of glycogen metabolism and has been involved in a wide range of cellular functions, including metabolism, cytoskeletal integrity, gene expression, cell division, and apoptosis [7]. Several studies have implicated GSK-3 signalling transduction pathway in multiple central nervous system diseases, particularly stroke, traumatic brain injury and neurodegenerative conditions, such as Alzheimer's disease, Parkinson's disease and amyotrophic lateral sclerosis [8,9]. GSK-3β, one of the two isoforms of GSK-3, is widespread both in developing and adult mammalian nervous system and its overexpression induces intrinsic apoptotic signalling pathway in neuronal cells following hypoxia/ischemia stimulus [10]. The acknowledgement of a potential involvement of GSK-3β in neuronal apoptosis, lead to the development of specific antagonists. Martinez et al. described small heterocyclic thiadiazolidinones (TDZDs) and their structure–activity relationships as the first non-ATP competitive selective GSK-3β inhibitors [11]. TDZDs are small molecules with favourable absorption, distribution, metabolism, excretion and toxicity properties [12]. TDZD-8 is a BBB permeable compound and appears to be one the most effective anti-inflammatory and tissue-protective thiadiazolidinones in conditions, such as stroke, spinal cord injury, kidney injury, arthritis, or colitis [12–18]. Furthermore, phase IIb and phase III clinical trials suggest that TDZDs have a favourable safety profile and may become valuable for the treatment of some neurological diseases in the near future [19,20].

The aim of this study was to investigate the effects of a single dose of TDZD-8 (5 mg/kg) as a possible pre-treatment against neuronal damage in intraoperative transient cerebral artery clipping during intracranial aneurysm surgery. TDZD-8 doses were determined in accordance with previous effective studies in central nervous system and administered with the established therapeutic time window in the clinical setting [15,21]. To better reproduce the surgical procedure, we performed a rodent model of focal cerebral ischemia-reperfusion (I/R).

## 2. Materials and methods

A total of 28 adult male Wistar rats (240–340 g) housed under diurnal light conditions with unlimited access to food and water were used ($n = 14$ per group). Animal care followed the recommendations of European Convention for the Protection of Vertebrate Animals Used for Experimental and Other Scientific Purposes (Council Directive 2010/63/EU) and National Law 1005/92 (rules for protection of experimental animals). The Institutional Animal Care and Use Committee approved all animal procedures. All efforts were made to minimize animal suffering and to reduce the number of animals used.

### 2.1. Intervention

Animals were randomly assigned in two different groups: TDZD-8 (4-benzyl-2-methyl-1,2,4-thiadiazolidine-3,5-dione, Sigma-Aldrich, St. Louis, MO, USA) treatment group in which a dose of 5 mg/kg was administered in the tail vein intravenously (i.v.) 10 min previous to ischemia onset or; control group, in which animals had administered saline i.v. according to protocol. Allocation concealment was attained by having drug or saline individually prepared and labelled for each animal according to randomization by an independent investigator. A single investigator blinded to treatment carried out the surgical procedures.

### 2.2. Middle cerebral artery ischemia-reperfusion

Rats were food deprived 12 h prior to surgery. Anaesthesia was induced by intraperitoneal administration of ketamine (80 mg/kg) and xylazine (8 mg/kg) mixture, supplemented as needed. Anesthetized rats were placed onto a thermostatically controlled heating pad, a rectal probe was inserted, and body temperature was monitored and maintained between 36.5 °C and 37.5 °C. Transient focal cerebral ischemia was induced by 60-min right MCA occlusion followed by 24-h reperfusion, as previously reported by our group [22].

Briefly, under the operating microscope, the right common carotid artery (CCA), internal carotid artery (ICA) and external carotid artery (ECA) were exposed and isolated from branches through a midline neck incision. The ECA was tied and cut at approximately 5 mm from the bifurcation and a loose 6-0 silk knot was placed around the ECA origin. After, microvascular clips were placed on the CCA and ICA, an ECA stump arteriotomy distal to the loose knot was performed and a 4-0 nylon silicone rubber-coated tip monofilament (Doccol Corporation, Sharon, MA, USA) was inserted. The suture around the ECA stump and the intraluminal nylon filament was tightened to prevent bleeding and the clips were removed. The filament was gently introduced (19–21 mm) into the ICA to the level where the MCA branches out, until laser-Doppler signal decreased to less than 30% of baseline values, occluding the right MCA at its origin at the circle of Willis. After a 60-min period of ischemia, the thread was cautiously removed re-establishing the blood flow in the MCA. The ECA was permanently ligated at the level of bifurcation. Animals were allowed to recover and euthanized with anaesthetic overdose at 24 h into reperfusion.

### 2.3. Blood flow measurements

Cortical cerebral blood flow (CBF) was monitored by laser-Doppler flowmetry (Periflux System 4000, Probe 407, Perimed-Instruments, Stockholm, Sweden) in the supply territory of the right MCA where transient ischemia was to be done, before, during occlusion and within 1 h of reperfusion. A small burr hole was drilled 2 mm posterior to the bregma and 3.5 mm lateral to the midline and the micro-Doppler probe positioned above the dura in a holder glued to the bone. Steady-state baseline values were recorded before occlusion, and the CBF measured during occlusion and reperfusion was expressed as a percentage of the baseline values. Rats with CBF patterns suggesting subarachnoid haemorrhage, incomplete ischemia (CBF does not decrease to a maximum of 30% of baseline) or incomplete reperfusion (CBF does not recover to over 80% of baseline within 30 min of filament withdrawal) were excluded and replaced.

### 2.4. Neurological examination

At 24-h, a nine-point scale neurological test (0 = normal to 9 = highest handicap) was performed, as previously described [23]. Four tests were performed by an observer blinded to the treatment groups in order to assess:

- spontaneous activity (moving/exploring = 0, moving without exploration = 1, no displacement = 2);

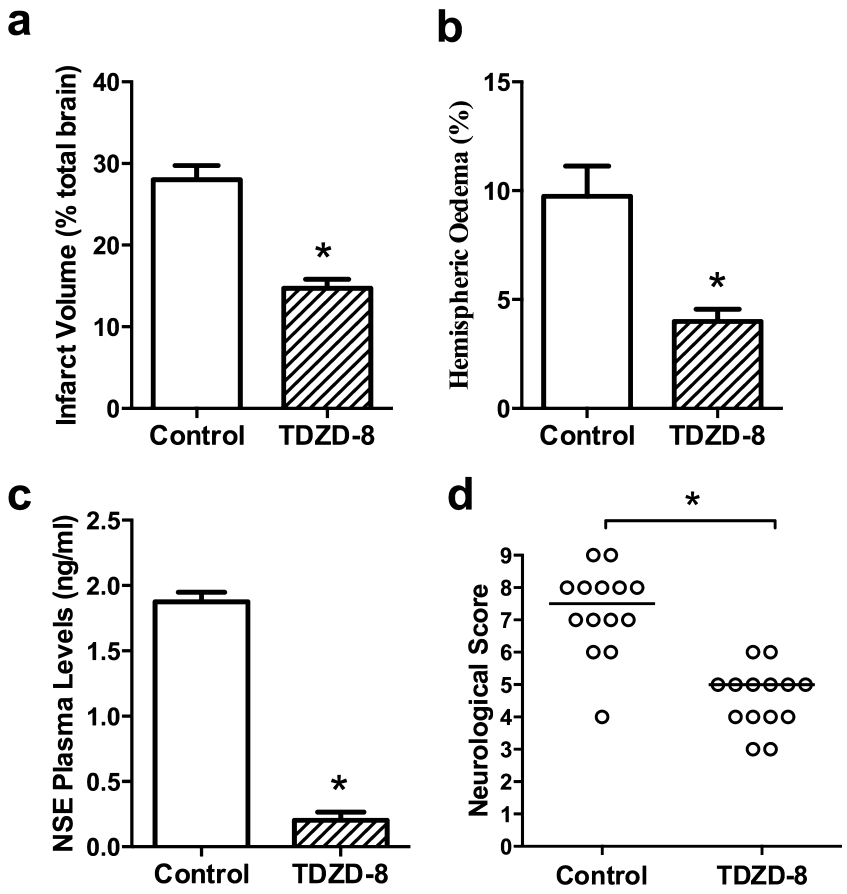


**Fig. 1.** a–c: bar graphs comparing groups for several endpoints: total infarct volume (a), percentage of hemispheric oedema (b) and NSE plasma levels at 24 h of reperfusion (c). Infarct volumes are presented as percentages of the contralateral hemisphere (28.02 ± 1.73% in control group compared to 14.70 ± 1.12% in treatment group). Data are means ± SEM. Asterisks (*) depicts differences with $P < 0.001$; d: scatter plot showing the effects of TDZD-8 at 24 h on a 9-point neurologic score. Open circles indicate values for individual animals. Horizontal bars indicate group median values. TDZD-8 significantly reduced neurologic deficits. Asterisk (*) depicts differences with $P < 0.001$, Mann–Whitney test.

- laterality in movement (symmetrical = 0, left drifting when elevated by the tail = 1, spontaneous left drifting = 2, circling to the left without displacement or spinning = 3);
- resistance to left forepaw stretching (no stretching allowed = 0, stretching allowed = 1, no resistance = 2);
- parachute reflex (symmetrical = 0, asymmetrical = 1, contralateral forelimb retracted = 2).

Scores obtained for each test were added to obtain the final neurological score.

### 2.5. Infarct volume and brain oedema assessment

The brains were removed, placed in a brain matrix (World Precision Instrument, Hertfordshire, UK) and sliced in 2-mm thick coronal sections, beginning 2 mm from the frontal pole and ending rostral to the cortico-cerebellar junction, resulting in 6 slices per animal ($n = 8$ per group). The sections were stained in 2% 2,3,5-triphenyltetrazolium chloride (TTC) (Sigma-Aldrich, St. Louis, MO, USA) saline solution for 10 min at 37 °C in the dark and fixed in 4% paraformaldehyde at 4 °C overnight. Sections were scanned and analyzed using ImageJ software version 1.45. Brain infarction was visualized as areas of unstained (white) tissue, which contrasted from brick stained areas of viable tissue. Summing the infarct area of each coronal slice and multiplying that number by the thickness of the sections allowed the calculation of the total infarct volume. Right and left hemispheric volumes were calculated similarly. The amount of infarction was expressed in absolute term in cubic millimetres and as a percentage of the contralateral hemisphere adjusted for brain oedema [24]. An index of brain oedema was assessed by calculating the percentage increase of size of the ipsilateral (injured) hemisphere compared with the contralateral (uninjured) hemisphere. A single observer, blinded to the individual treatment, performed the described analysis.

### 2.6. Determination of neuron specific enolase (NSE) plasma levels

Blood samples were taken by puncture of the left cardiac ventricle prior to sacrifice. Blood was centrifuged at 10,000 rpm for 10 min and the isolated serum was frozen and stored until time of assay. Serum NSE measurements were performed with an electrochemiluminescence immunoassay, using a sandwich technique with double monoclonal antibodies directed against NSE (Roche Diagnostics, Mannheim, Germany) and an Elecsys 2010 analyser (Roche Diagnostics, Mannheim, Germany). Data were normalized to nanograms per millilitre of plasma.

### 2.7. Histology and immunohistochemistry procedures

Rat brains were removed, fixed in 4% paraformaldehyde in PBS for 72 h at room temperature, dehydrated through a graded ethanol series and embedded in paraffin ($n = 3$ per group). Hematoxilin–Eosin (H–E) staining was performed as previously described [25]. Images were acquired using a bright field Axioscop microscope (Zeiss, Göttingen, Germany).

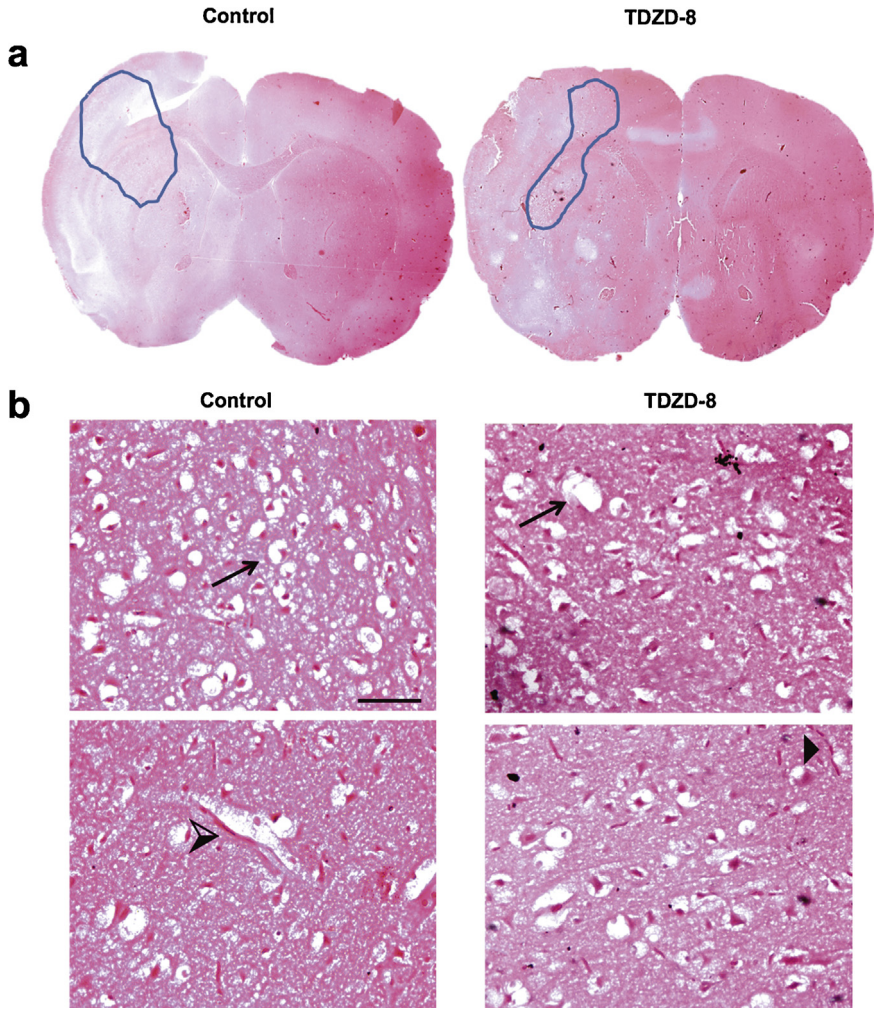


**Fig. 2.** Cerebral vascular and parenchyma alterations. a: representative whole brain section with delineated infarct area of control and TDZD-8-treated rats, H–E staining; b: representative photomicrographs of cerebrovascular changes in the infarct area: neuropil spongiosis (arrows) and perivascular oedema (➢) in control animals or its absence in TDZD-8-treated ones, H–E staining (▶). Scale bar equals 200 μm.

For Fluoro-Jade staining, 6 μm thick coronal sections were deparaffinised and rehydrated. Slides were first immersed in 100% alcohol for 3 min followed by 1 min in 70% alcohol and 1 min in distilled water. The slides were then transferred to a solution of 0.06% potassium permanganate for 15 min on a shaker table and protected from light. The slides were after rinsed in distilled water for 1 min and immersed in Fluoro-Jade B (Chemicon, Temecula, CA, USA) staining solution 0.001% for 30 min with moderate agitation. Slides were rinsed for one min in each of three distilled water washes and dried at room temperature. The dry slides were cleared by immersion in xylene for at least a minute before cover slipping with DPX (Sigma-Aldrich, St. Louis, MO, USA). The tissue was then examined using an epifluorescent AxioScope microscope (Zeiss, Göttingen, Germany) with blue (450–490 nm) excitation light. The number of positive Fluoro-Jade B neurons were counted in 4 sections of 0.16 $\mu m^2$ ($n = 3$ per group) within the region of interest using ImageJ software version 1.45 and expressed as positive cells/section.

For immunostaining, 6 μm thick coronal sections were submitted to antigen retrieval in 20 mM citrate buffer with 1.5% $H_2O_2$ for 15 min at room temperature in the dark, incubated for 10 min in Tris–EDTA buffer at 84 °C and blocked for 1 h at room temperature in 1% bovine serum albumin (BSA) in phosphate buffered saline (PBS). Primary antibody, rabbit anti-p-Akt (1:100, CellSignaling Technology, Beverly, MA, USA) was used in 0.5% BSA in PBS overnight at 4 °C. After washing in PBS, sections were incubated for 1 h at room temperature with antibodies anti-rabbit coupled to AlexaFluor 568 (#A11077, 1:1000, Invitrogen, Carlsbad, CA, USA) in 0.5% BSA in PBS, incubated for 20 min in 4,6-diamidino-2-phenylindole (DAPI) and mounted with Shandon Immu-Mount™ Aqueous Non-fluorescing Mounting Medium (Thermo Scientific, Rockford, IL, USA). Tissue sections were visualized with a epifluorescent AxioScope microscope (Zeiss, Göttingen, Germany) and the number of total nuclei (DAPI staining) and the ones positive for p-Akt counted to present the results as percentage of p-Akt-positive nuclei (2 sections within the region of interest, $n = 3$ per group).

### 2.8. Western blot analysis

For western blot analysis ($n = 3$ per group), frozen tissue samples cells were lysed in RIPA buffer containing Tris 50 mM (pH 8.0), 5 mM EDTA (pH 8.0), 150 mM NaCl, 1% NP-40, 10% glycerol and 0.1% SDS, and sonicated for 20 s. The lysate was centrifuged at 14,000 *g* for 10 min at 4 °C and the supernatants were collected and stored at −80 °C. Protein concentrations were determined using Nanodrop ND-1000. Cell extracts containing equal amounts of protein (100–150 μg) were separated on sodium dodecyl sulphate–polyacrylamide gel electrophoresis and transferred to a nitrocellulose membrane. The membranes were blocked with 5% non-fat milk, incubated with the primary antibody overnight at 4 °C anti-rabbit p-Akt (1:1000) (#12178, Cell Signaling, Danvers, MA, USA), anti-rabbit Akt (1:1000) (#4691, Cell Signaling, Danvers,

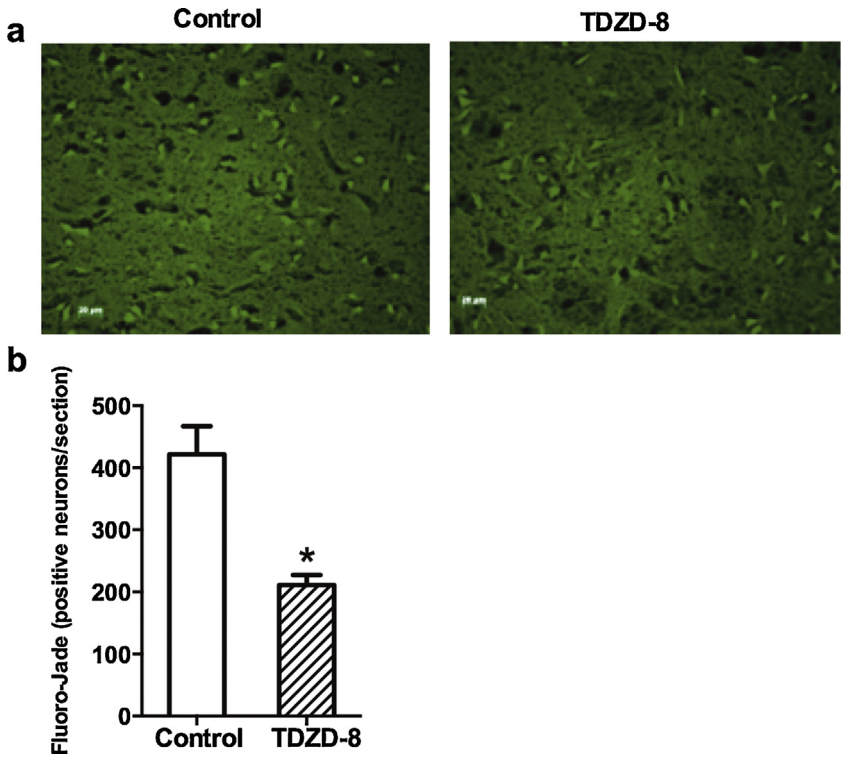


**Fig. 3.** Comparison of degenerating neurons in both control and TDZD-8-treated groups. a: representative images of brain section stained for degenerating neurons using Fluoro-Jade. Scale bar equals 20 μm; b: bar graph comparing the number of positive Fluoro-Jade staining neurons per 0.16 $\mu m^2$ in 4 sections for each rat of the infarcted area. Data are means ± SEM (4 sections for each individual, $n = 3$ per group). Asterisk (*) depicts differences with $P < 0.001$.

MA, USA), and then with a horseradish peroxidase-labelled secondary antibody for 1 h at room temperature. After extensive washes, immunoreactive bands were detected by LumiGLO® (Cell Signaling, Danvers, MA, USA) and visualized by autoradiography with Hyperfilm ECL. Phosphorylation levels of Akt were analysed by the ratio of p-Akt to total Akt levels and expressed as fold compared to contralateral MCA occlusion hemisphere.

### 2.9. Statistical analysis

Statistical analysis was performed using GraphPad Prism software version 6.0. Parametric data were analysed using Student's *t*-test for single comparisons between groups and non-parametric data (neurologic scores) were subjected to the two-tailed Mann–Whitney test. Data are presented as means ± SEM (standard error of the mean) for *n* observations, where *n* represents the number of animals studied. For histological scoring and western blot analysis, each data point represents analyses of brain sections taken from 3 individual rats. A *P* value of less than or equal to 0.05 was the threshold considered for a statistically significant difference or association.

## 3. Results

All animals lost between 10 to 18% of body weight during the 24-h recovery period with no significant differences between groups. Normothermia was maintained in all animals. There were no significant differences between groups with respect to CBF pattern and glycaemia values during the procedure.

Prophylactic administration of TDZD-8 resulted in significant differences between groups for most outcomes and endpoints evaluated (Fig. 1). The whole brain infarct volume was significantly different between groups (265.46 ± 13.88 $mm^3$ for control group and 125.99 ± 11.26 $mm^3$ for treatment group, $n = 8$ per group) and treatment group had a significant decrease in the ipsilateral hemispheric oedema (9.74 ± 1.39% compared to 3.99 ± 0.56%, $n = 8$ per group). TDZD-8 administration also prevented the rise of NSE plasma levels (0.20 ± 0.06 ng/mL in treatment group, compared to 1.88 ± 0.07 ng/mL in control group, $n = 13$ for treatment group and $n = 8$ for control group). Consistently, rats treated with TDZD-8 presented significantly less neurological deficits compared to the control group ($n = 14$ per group). Neuropathological examination corroborated these findings: H–E staining performed in the ischemic area showed less neuropil spongiosis and less perivascular oedema on TDZD-8-treated group (Fig. 2) and there was a 50% reduction in the number of degenerating Fluoro-Jade positive neurons in TDZD-8 treatment group (421.3 ± 45.61 compared to 210.8 ± 16.14 positive cells per section) (Fig. 3). Western blot analysis revealed that p-Akt and total Akt expression levels exhibited no significant changes between groups (data not shown); instead immunostaining techniques revealed that TDZD-8 significantly increased p-Akt nucleus translocation (22.7 ± 3.44% of positive p-Akt nuclei in control group compared to 34.3 ± 3.61% in treatment group) (Figs. 4 and 5).

## 4. Discussion

To our knowledge, this study provides first evidence that a single TDZD-8 pre-treatment dose protects rat brain against injury following 60-min transient MCA ischemia. Our data demonstrates that for cerebral I/R injury, TDZD-8:

- reduced brain damage extent – 48% reduction on the infarct volume and 59% reduction of the hemispheric oedema;
- diminished the number of apoptotic/degenerating neurons;
- improved neurological performance at 24 h;
- prevented plasma rise of NSE.

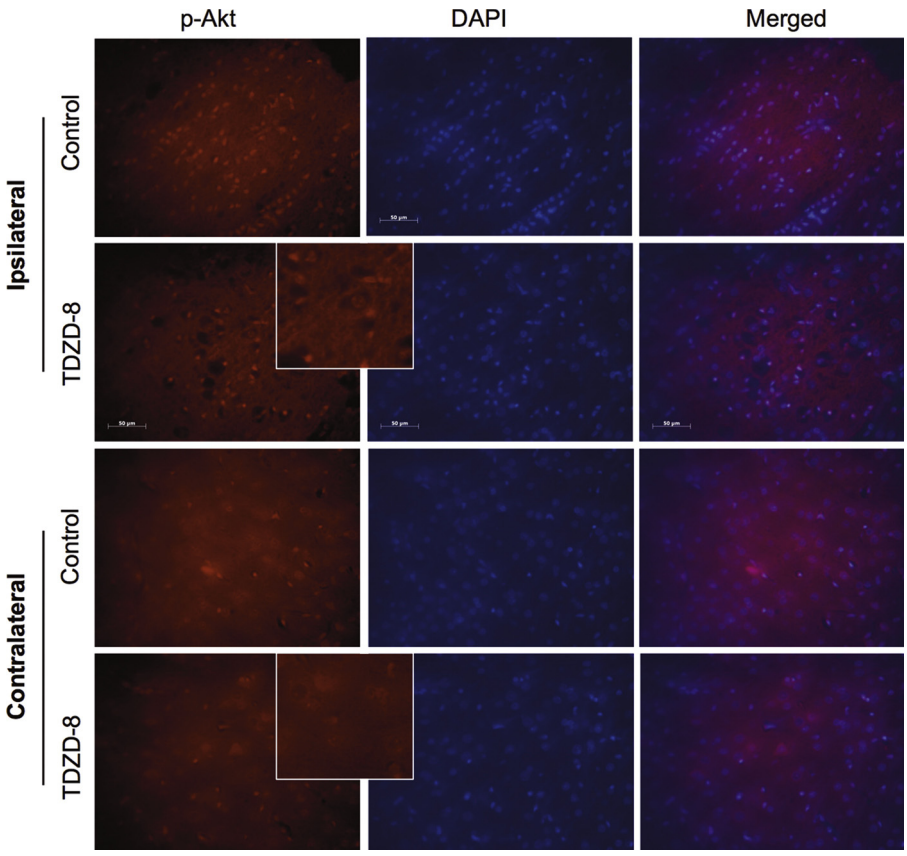


**Fig. 4.** Akt phosphorylation in control and TDZD-8-treated groups. Representative images of the infarcted area of the I/R injured and contralateral hemispheres after double staining for p-Akt and nuclear DAPI. Insert shows p-Akt zoom-in images. Merged images are also presented. Scale bar equals 50 μm.

NSE is rapidly released by injured neurons, reaching its maximum at 24 h, and is assumed to be a reliable marker to follow-up neuronal damage since the plasma levels of NSE correlate with the extent of cerebral infarction [26].

Blood glucose levels during ischemia or reperfusion were not different between groups, indicating that the effects induced by TDZD-8 are independent from this variable.

GSK-3β inhibition has been shown to induce neuroprotective effects in cerebral ischemia by suppressing neuronal apoptosis and protecting against the loss of barrier integrity due to a decrease in the generation of several pro-inflammatory mediators and preventing leukocyte adhesion and migration into the brain [14,27]. Furthermore, GSK-3β inhibition is thought to promote autophagy activation in ischemic injury, an intracellular catabolic process by which cells remove their damaged organelles for the maintenance of cellular homeostasis, and to induce astrocyte sensitization and tolerance to inflammatory molecules [28,29]. These neuronal pro-survival effects are consistent with the fewer positive degenerating/necrotic neurons stained with Fluoro-Jade and lower plasma levels of NSE seen in the treatment group. GSK-3β inhibition has been proposed to be a potent and effective therapeutic approach for attenuating inflammatory response associated to brain microvascular endothelial cells dysfunction, which includes preservation of BBB tightness by promoting tight junction protein stability [27,30]. It is possible that TDZD-8 attenuates BBB disruption and consequential secondary brain injury.

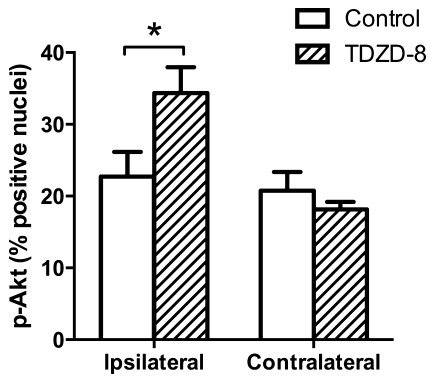


**Fig. 5.** Bar graph representing the percentage of positive p-Akt nuclei in the infarct area, comparing ipsilateral to contralateral hemispheres. Data are means ± SEM (2 sections for each individual, $n = 3$ per group). Asterisk (*) depicts differences with $P < 0.05$.

The Akt/GSK-3β pathway is a central mediator in signal transduction pathways that help to regulate cell growth, metabolism, inflammation and cell survival. Following cerebral ischemia, activated phosphorylated-Akt (p-Akt) levels transiently increase in neurons, and this elevation is believed to be a neuroprotective response [31]. Activated protein kinase p-Akt phosphorylates a number of downstream cytosolic and nuclear proteins that regulate mitochondrial activity, cell growth, and cell survival. The cytosolic modulation includes the inhibition of Bcl-2-associated death promoter (BAD) protein, caspases and GSK-3β itself [31]. Phosphorylated-Akt has been shown to translocate to the nucleus where it phosphorylates several other targets, such as p53 tumour suppressor, Forkhead box transcription factors, nuclear S6-kinase-related kinase (SRK), and Nur77, therefore inhibiting their activity and ability to induce the expression of death genes [32,33]. We found that TDZD-8 did not affect total p-Akt expression in our I/R experiment, which is explained by the fact that GSK-3β inhibition occurs downstream to the phosphorylation site of Akt and its potential targets. Interestingly, an increased translocation of

p-Akt into the nucleus was observed following TDZD-8 treatment, suggesting Akt signalling pathway activation. Accordingly, phosphorylation of Akt appears to be essential for its intranuclear permanence and recent evidence indicates that Akt plays its roles by regulating its phosphorylation state, rather than its protein expression [32,34,35].

We recognize some caveats in our study. The mechanism of action by which TDZD-8 acts in focal cerebral I/R is lacking and requires further investigation. Also, it would be interesting to perform dose-response and time course experiments. This dynamics would be of both experimental and clinical relevance.

## 5. Conclusions

The efficacy of intraoperative drugs most commonly used during aneurismal clipping surgery offer limited neuroprotection. It has been recently described that thiadiazolidinones compounds have potent anti-inflammatory and tissue-protective effects. Our study reveals that it is likely that the neuroprotective effects induced by TDZD-8 are due to a complex and mixed synergic interaction between GSK-3β inhibition and Akt modulation. In conclusion, TDZD-8 is neuroprotective *in vivo* and may have a role in the clinical setting as a pre-treatment against neuronal damage induced by transient cerebral artery occlusion during cerebrovascular procedures.

## Disclosure of interest

The authors declare that they have no conflicts of interest concerning this article.

## Author contributions

Conception and design: Ratilal, Rocha, Fernandes, Sepodes, Mota-Filipe. Acquisition of data: Ratilal, Rocha, Fernandes, Barateiro, Pinto. Analysis and interpretation of data: Ratilal, Rocha, Sepodes. Drafting the article: Ratilal, Rocha, Arroja, Sepodes. Statistical analysis: Ratilal, Rocha. Study supervision: Brites, Mota-Filipe. Critically revising the article: all authors.

## Acknowledgments

We acknowledge Prof. Anna Planas and her group for their help and advice on setting the animal model. We are grateful to Prof. Cristina Sampaio and to Prof. João Lobo Antunes for their support.

## References

[1] Lavine SD, Masri LS, Levy ML, Giannotta SL. Temporary occlusion of the middle cerebral artery in intracranial aneurysm surgery: time limitation and advantage of brain protection. J Neurosurg 1997;87:817–24.
[2] Ha SK, Lim DJ, Seok BG, Kim SH, Park JY, Chung YG. Risk of stroke with temporary arterial occlusion in patients undergoing craniotomy for cerebral aneurysm. J Korean Neurosurg Soc 2009;46:31–7.
[3] O'Collins VE, Macleod MR, Donnan GA, Horky LL, van der Worp BH, owells HDW. 1026 experimental treatments in acute stroke. Ann Neurol 2006;59:467–77.
[4] Hindman BJ, Bayman EO, Pfisterer WK, Torner JC, Todd MM, IHAST Investigators. No association between intraoperative hypothermia or supplemental protective drug and neurologic outcomes in patients undergoing temporary clipping during cerebral aneurysm surgery: findings from the Intraoperative Hypothermia for Aneurysm Surgery Trial. Anesthesiology 2010;112:86–101.
[5] Li LR, You C, Chaudhary B. Intraoperative mild hypothermia for postoperative neurological deficits in intracranial aneurysm patients. Cochrane Database Syst Rev 2012, http://dx.doi.org/10.1002/14651858.CD008445.pub2.
[6] Zhao ZX, Wu C, He M. A systematic review of clinical outcomes, perioperative data and selective adverse events related to mild hypothermia in intracranial aneurysm surgery. Clin Neurol Neurosurg 2012;114:827–32.
[7] Dugo L, Collin M, Thiemermann C. Glycogen synthase kinase 3beta as a target for the therapy of shock and inflammation. Shock 2007;27:113–23.
[8] Lei P, Ayton S, Bush AI, Adlard PA. GSK-3 in neurodegenerative diseases. Int J Alzheimers Dis 2011;2011:189246.
[9] Ren M, Senatorov VV, Chen RW, Chuang DM. Postinsult treatment with lithium reduces brain damage and facilitates neurological recovery in a rat ischemia/reperfusion model. Proc Natl Acad Sci U S A 2003;100:6210–5.
[10] Sasaki C, Hayashi T, Zhang WR, Warita H, Manabe Y, Sakai K, et al. Different expression of glycogen synthase kinase-3beta between young and old rat brains after transient middle cerebral artery occlusion. Neurol Res 2001;23:588–92.
[11] Martinez A, Alonso M, Castro A, Pérez C, Moreno FJ. First non-ATP competitive glycogen synthase kinase 3 beta (GSK-3beta) inhibitors: thiadiazolidinones (TDZD) as potential drugs for the treatment of Alzheimer's disease. J Med Chem 2002;45:1292–9.
[12] Saitoh M, Kunitomo J, Kimura E, Iwashita H, Uno Y, Onishi T, et al. 2-{3-[4-(Alkylsulfinyl)phenyl]-1-benzofuran-5-yl}-5-methyl-1,3,4-oxadiazole derivatives as novel inhibitors of glycogen synthase kinase-3beta with good brain permeability. J Med Chem 2009;52:6270–86.
[13] Martinez A, Castro A, Dorronsoro I, Alonso M. Glycogen synthase kinase 3 (GSK-3) inhibitors as new promising drugs for diabetes, neurodegeneration, cancer, and inflammation. Med Res Rev 2002;22:373–84.
[14] Collino M, Thiemermann C, Mastrocola R, Gallicchio M, Benetti E, Miglio G, et al. Treatment with the glycogen synthase kinase-3beta inhibitor, TDZD-8, affects transient cerebral ischemia/reperfusion injury in the rat hippocampus. Shock 2008;30:299–307.
[15] Cuzzocrea S, Genovese T, Mazzon E, Crisafulli C, Di Paola R, Muià C, et al. Glycogen synthase kinase-3 beta inhibition reduces secondary damage in experimental spinal cord trauma. J Pharmacol Exp Ther 2006;318:79–89.
[16] Cuzzocrea S, Mazzon E, Di Paola R, Muià C, Crisafulli C, Dugo L, et al. Glycogen synthase kinase-3beta inhibition attenuates the degree of arthritis caused by type II collagen in the mouse. Clin Immunol 2006;120:57–67.
[17] Bao H, Ge Y, Zhuang S, Dworkin LD, Liu Z, Gong R. Inhibition of glycogen synthase kinase-3β prevents NSAID-induced acute kidney injury. Kidney Int 2012;81:662–73.
[18] Whittle BJ, Varga C, Posa A, Molnar A, Collin M, Thiemermann C. Reduction of experimental colitis in the rat by inhibitors of glycogen synthase kinase-3beta. Br J Pharmacol 2006;147:575–82.
[19] www.clinicaltrials.gov [cited 2014 April 4]. Available from http://www.clinicaltrials.gov/ct2/show/NCT01049399?term=NP031112&rank=1
[20] Del Ser T, Steinwachs KC, Gertz HJ, Andrés MV, Gómez-Carrillo B, Medina M, et al. Treatment of Alzheimer's disease with the GSK-3 inhibitor tideglusib: a pilot study. J Alzheimers Dis 2013;33:205–15.
[21] Aguilar-Morante D, Morales-Garcia JA, Sanz-SanCristobal M, Garcia-Cabezas MA, Santos A, Perez-Castillo A. Inhibition of glioblastoma growth by the thiadiazolidinone compound TDZD-8. PLoS One 2010;5:e13879.
[22] Ratilal BO, Arroja MM, Rocha JP, Fernandes AM, Barateiro AP, Brites DM, et al. Neuroprotective effects of erythropoietin pretreatment in a rodent model of transient middle cerebral artery occlusion. J Neurosurg 2014;121:55–62.
[23] Justicia C, Martín A, Rojas S, Gironella M, Cervera A, Panés J, et al. Anti-VCAM-1 antibodies did not protect against ischemic damage either in rats or in mice. J Cereb Blood Flow Metab 2006;26:421–32.
[24] Swanson RA, Morton MT, Tsao-Wu G, Savalos RA, Davidson C, Sharp FR. A semi-automated method for measuring brain infarct volume. J Cereb Blood Flow Metab 1990;10:290–3.
[25] Fischer AH, Jacobson KA, Rose J, Zeller R. Hematoxylin and eosin staining of tissue and cell sections. CSH Protoc 2008, http://dx.doi.org/10.1101/pdb.prot4986.
[26] Ahmad O, Wardlaw J, Whiteley WN. Correlation of levels of neuronal and glial markers with radiological measures of infarct volume in ischaemic stroke: a systematic review. Cerebrovasc Dis 2012;33:47–54.
[27] Ramirez SH, Fan S, Zhang M, Papugani A, Reichenbach N, Dykstra H, et al. Inhibition of glycogen synthase kinase 3beta (GSK3beta) decreases inflammatory responses in brain endothelial cells. Am J Pathol 2010;176:881–92.
[28] Zhou X, Zhou J, Li X, Guo C, Fang T, Chen Z. GSK-3β inhibitors suppressed neuroinflammation in rat cortex by activating autophagy in ischemic brain injury. Biochem Biophys Res Commun 2011;411:271–5.
[29] Beurel E, Jope RS. Glycogen synthase kinase-3 regulates inflammatory tolerance in astrocytes. Neuroscience 2010;169:1063–70.
[30] Ramirez SH, Fan S, Dykstra H, Rom S, Mercer A, Reichenbach NL, et al. Inhibition of glycogen synthase kinase 3 promotes tight junction stability in brain endothelial cells by half-life extension of occludin and claudin-5. PLoS One 2013;8:e55972.
[31] Zhao H, Sapolsky RM, Steinberg GK. Phosphoinositide-3-kinase/akt survival signal pathways are implicated in neuronal survival after stroke. Mol Neurobiol 2006;34:249–70.
[32] Xuan Nguyen TL, Choi JW, Lee SB, Ye K, Woo SD, Lee KH, et al. Akt phosphorylation is essential for nuclear translocation and retention in NGF-stimulated PC12 cells. Biochem Biophys Res Commun 2006;349:789–98.
[33] Masuyama N, Oishi K, Mori Y, Ueno T, Takahama Y, Gotoh Y. Akt inhibits the orphan nuclear receptor Nur77 and T-cell apoptosis. J Biol Chem 2001;276:32799–805.
[34] Lan R, Xiang J, Zhang Y, Wang GH, Bao J, Li WW, et al. PI3K/Akt pathway contributes to neurovascular unit protection of Xiao-Xu-Ming decoction against focal cerebral ischemia and reperfusion injury in rats. Evid Based Complement Alternat Med 2013:459467.
[35] Xie R, Cheng M, Li M, Xiong X, Daadi M, Sapolsky RM, et al. Akt isoforms differentially protect against stroke-induced neuronal injury by regulating mTOR activities. J Cereb Blood Flow Metab 2013;33:1875–85.